Fungible Simple Slopes in Moderated Regression

Zane Blanton

A thesis submitted to the faculty of the University of North Carolina at Chapel Hill in partial fulfillment of the requirements for the degree of Master of Arts in the Department of Psychology (Quantitative).

Chapel Hill
2012

Approved by

Dr. Robert MacCallum, Ph.D.

Dr. David Thissen, Ph.D.

Dr. Abigail Panter, Ph.D.

ABSTRACT

ZANE BLANTON: Fungible Simple Slopes in Moderated Regression
(Under the direction of Dr. Robert MacCallum)

This thesis concerns an application of fungible weights methodology to the question of moderation in least squares (LS) regression. Fungible weights are weights that produce predictions correlated to a given degree with the LS predictions and scaled so that they produce minimal sum of squared errors. Waller (2008) proposes that fungible weights be used to determine if LS weights should be interpreted as representing relative contributions of predictors or only as a composite effect. In this project, data were simulated from regression models with a variety of structures and fungible weights were generated for each dataset. For each set of fungible weights, corresponding simple slopes were computed. The variability of fungible weights and simple slopes across samples was examined, as well as the conditions under which fungible solutions suggest a qualitatively different regression model. Factors that were varied include the R^2 of the model, the correlation of the predictors, the relative weights of predictors, the presence of the interaction, and the sample size. Tentative recommendations of conditions for which sample fungible solutions give good approximations of population fungible solutions are made, and a simple bootstrapping method for generating confidence sets around fungible weights is proposed.

ACKNOWLEDGEMENTS

I would like to thank all of the members of my committee for their advice, recommendations, and their patience. Particularly, I would like to thank my advisor, Dr. Robert MacCallum, who has been a great help to me in this process, tirelessly continuing to offer advice even after his official retirement. In addition, I would like to thank Dr. Sy-Miin Chow, who was on an earlier version of my committee but is not on the current one due to accepting an appointment at Pennsylvania State University.

TABLE OF CONTENTS

LIST OF TABLES

LIST OF FIGURES

CHAPTER 1

Introduction

1.1 Proposal Overview

Recent research in regression has demonstrated the existence of an infinite class of alternative weights that are correlated with the least-squares weights at a given level (Waller, 2008; Waller, 2009). Waller calls these alternative weights "fungible" in reference to their common correlation with the least squares weights and their identically equal sum of squared error (SSE) when predicting the dependent variable. In fact, each correlation that defines a set of fungible weights is also associated with a fixed decrement in R^2, the proportion of the predicted variance that is explained by the weighted combination of the predictors. By setting a sufficiently large correlation between the fungible and optimal weights, one can obtain a set of fungible weights that yield predictions virtually equivalent in accuracy to predictions produced from the optimal weights.

Examining this set of fungible weights can help researchers understand the conclusions that should be drawn from the regression model; large variability of fungible weights suggests that the optimal regression weights should not be interpreted as reflective of the relative predictive contributions of variables. This use of fungible weights could be considered as a type of sensitivity analysis. If regression weights change a great deal in response to a small perturbation in R^2, this implies that optimal weights should not be interpreted except as a composite. Small changes of weights in response to small changes in R^2 imply that least-squares weights can be interpreted.

Fungible weights could be particularly useful when applied to regression models that include interaction terms, because in the social sciences, significant interaction coefficients are often interpreted as evidence for a substantively important interaction. When a significant interaction is found, it is often probed by calculating simple slopes. To perform this procedure, one of the variables is assigned the role of moderator, usually decided by substantive theories about the process involved. Several values of the moderator are chosen to represent its distribution in the sample, and the conditional slope of the other predictor in the interaction is examined. In addition to interpreting these conditional slopes, they can also be tested for significance to determine whether there is a significant effect at a given value of the moderator.

By generating fungible weights for a data set, one could examine how the corresponding fungible simple slopes vary. If fungible simple slopes are found to show a wide variety of effects, it would be sensible to refrain from making statements about the nature of the interaction. If fungible simple slopes do not markedly vary, this would be evidence that the interaction is integral to the explanatory power of the model. Fungible weights allow one to examine the meaningfulness of interactions from a different perspective than significance tests, because fungible weights give information about the specificity of the model's parameters rather than giving confidence intervals for them.

In this thesis, I will review Waller's research on fungible weights as well as past research on cross-validity and alternative weights in linear regression. I will then link these concepts to simple slopes in moderated regression and propose a method to use fungible simple slopes to evaluate interactions. Afterwards, I will discuss factors that may affect the distribution of fungible simple slopes, including the size of the class of fungible weights, its orientation, and its variability across samples, to justify a simulation study that varies the correlation between the predictors, the R^2 of the model, the number of data points, and the relative explanatory power of the interaction term compared with the unmodified predictors. I will propose a simple bootstrap estimate of the confidence

set of fungible weights based upon case-resampling. Lastly, I will discuss the results of the study, including the distribution of fungible weights and fungible simple slopes across samples and the performance of the bootstrap estimator in simulated data.

1.2 Statistical Concepts Related to Fungible Weights

To understand the characteristics of fungible weights and their utility, one must first have a motivation and a definition. The motivation for fungible weights comes from the observation that it is possible to specify alternative combinations of predictors that yield slightly suboptimal predictions of the dependent variable. If these alternative weights differ substantially from the optimal weights, a skeptical researcher could use this observation as evidence that the optimal weights should not be given substantial substantive interpretation. This observation addresses the flexibility of a model in representing predicted values that are close to the least squares values.

Flexibility of parameter estimates is taken to the extreme for models with exact linear dependence among variables, for which there is a an infinite class of solutions that yield equivalent R^2 and SSE. This is not an exact analogy for shifting parameter estimates in a well-defined model; however, statistical intuition suggests that fungible weights might be related to multicollinearity, since a greater amount of common variance might allow parameters to compensate for one another. Even without complete linear dependence, though, multicollinearity can still cause problems with estimation and prediction.

It is widely known that multicollinearity can make estimation unstable. Statistical remedies include ridge regression, where the conditioning of a near-singular predictor covariance matrix is improved by adding a constant to its diagonal. There is some evidence that ridge regression improves cross-validation, suggesting that least-squares (LS) estimates are not ideal in these cases (Obenchain, 1979). Principal components regression, which uses orthogonal components of the predictors, also eliminates problems with multicollinearity by creating orthogonal composites of the predictors. Lastly, generalized ridge regression, which uses attenuated weights from principal components, shows im-

provement in prediction in cases with many predictors and high noise. These approaches reduce variability in parameter estimation by combining predictors together and biasing estimates towards an equally-weighted model.

A related topic in psychological methodology is cross-validation. Since data sets often have idiosyncratic characteristics, a model from a particular data set often does not perform well when predicting other data. In fact, Wainer (1976) suggested that regression weights "don't make no never mind," showing analytically that, given moderately correlated predictors, using equal weights results in only a small decrement in R^2. Using multiple empirical datasets, Dana and Dawes (2004) showed a general crossover pattern in both empirical and simulated datasets, where unit-weights performed best at low n, correlation weights performed best at moderate n, and regression weights performed best at high n.

The common thread through these approaches is modifying optimal regression weights in order to improve prediction, a similar problem in spirit to modifying weights without greatly decreasing predictive accuracy. The difference is that the previous methods are focused on prediction of future datasets, whereas fungible weights focus on alternative models within a single observed dataset.

CHAPTER 2

Equations and Derivations

2.1 Green's Indifference Region

Green (1977) provides foundational work for Waller's conception of fungible weights. He defines parameter sensitivity as the loss in explained variance when parameters are shifted from their LS weights. Using this definition of sensitivity, he defines an indifference region **S** for each regression dataset, the set of alternative parameter estimates **a** that satisfy $R^2_{\mathbf{a}} \geq pR^2_{\mathbf{b}}$, where p is the minimum proportion of the least squares coefficient of determination, $R^2_{\mathbf{b}}$, that the alternative weights must explain. Green shows that the size of this indifference region is not dependent upon N, α, or R^2, but only upon σ^2_y and the characteristics of the sample predictor correlation matrix, **R**. Thus, the eigenvalues and eigenvectors of **R** determine how much estimates can be perturbed while still giving predictions that still explain a given amount of variance in **y**. Although this region varies across samples and is more stable with higher N, it is fixed for any given sample and approaches the indifference region of the population asymptotically. This is in contrast to the behavior of simultaneous confidence sets, whose size is based upon N and α.

2.2 Koopman's Maximally Dissimilar Weights

Koopman (1988) continued to investigate fungible weights by creating an analytical method for maximizing the angle between the LS weights and a set of alternative weights; however, Koopman defines his alternative weights differently than Green. Koopman's

alternative weights $\mathbf{a}$ satisfy

$$r_{\hat{y}_{\mathbf{a}}\hat{y}_{\mathbf{b}}} = \frac{\mathbf{a}'\mathbf{R}\mathbf{b}}{(\mathbf{a}'\mathbf{R}\mathbf{a}\mathbf{b}'\mathbf{R}\mathbf{b})^{1/2}}, \tag{2.1}$$

where $r_{\hat{y}_{\mathbf{a}}\hat{y}_{\mathbf{b}}}$ is the correlation between the predicted y values produced by $\mathbf{a}$, the alternative weights, and $\mathbf{b}$, the LS weights. The function

$$s = \frac{\mathbf{a}'\mathbf{b}}{(\mathbf{a}'\mathbf{a}\mathbf{b}'\mathbf{b})^{1/2}}, \tag{2.2}$$

equivalent to the cosine of the angle between the two sets of weights, is then maximized for a given $r_{\hat{y}_{\mathbf{a}}\hat{y}_{\mathbf{b}}}$. It should be noted, however, that these criteria do not specify the length of $\mathbf{a}$ since angles and correlations are invariant to scale. Koopman does suggest examining vectors scaled to minimize SSE, an idea that Waller carries further in his work.

2.3 Waller's Fungible Weights

Waller (2008) initially defines fungible weights as Koopman does, as in (2.1). However, he adds the additional criterion that all fungible weights should be scaled to minimize SSE. This means that he does not consider a scaled version of the LS weights to be a set of fungible weights, in contrast to MacCallum, Lee, and Browne (in press).

A summary of Waller's derivation appears here. It uses standardized variables and correlations, but the method could be generalized to unstandardized predictors. Waller first decomposes the correlation matrix of the predictors into its eigenvectors and eigenvalues, $\mathbf{R} = \mathbf{V}\mathbf{\Lambda}\mathbf{V}'$. Then, the correlation defined by (2.1) is written as the product of two unit-length vectors $\mathbf{u}$ and $\mathbf{v}$ so that

$$r_{\hat{y}_{\mathbf{a}}\hat{y}_{\mathbf{b}}} = \mathbf{v}'\mathbf{u}, \tag{2.3}$$

$$\text{where } \mathbf{v} = \frac{\mathbf{\Lambda}^{1/2}\mathbf{V}'\mathbf{a}}{(\mathbf{a}'\mathbf{R}\mathbf{a})^{1/2}}, \mathbf{u} = \frac{\mathbf{\Lambda}^{1/2}\mathbf{V}'\mathbf{b}}{(\mathbf{b}'\mathbf{R}\mathbf{b})^{1/2}}.$$

The second vector, $\mathbf{u}$, is constant because it depends only on the optimal weights $\mathbf{b}$. All valid fungible weights $\mathbf{a}$ generate $\mathbf{v}$ that satisfy (2.3). However, one can also work backwards, generating $\mathbf{v}$ that satisfy (2.3) and using them to find valid $\mathbf{a}$. To find acceptable $\mathbf{v}$, we can use the formula

$$\mathbf{v} = r\mathbf{u} + (1 - r^2_{\hat{y}_\mathbf{a}\hat{y}_\mathbf{b}})^{1/2}\mathbf{l} \tag{2.4}$$

where $\mathbf{l}$ is any unit-length vector that is orthogonal to $\mathbf{u}$. The complete set of valid $\mathbf{v}$ can be written as $\mathbf{z}'\mathbf{U}$, where $\mathbf{z}$ is any $p-1$ component unit vector, and $\mathbf{U}$ is an orthonormal basis for the subspace of $\mathbb{R}^p$ orthogonal to $\mathbf{b}$. These $\mathbf{v}$ can then be converted into fungible weights that satisfy the correlation condition using the expression

$$\mathbf{v} = \frac{\mathbf{\Lambda}^{1/2}\mathbf{V}'\mathbf{a}}{(\mathbf{a}'\mathbf{R}\mathbf{a})^{1/2}}. \tag{2.5}$$

By ignoring the denominator, a scalar, we can obtain an unscaled version of $\mathbf{a}$, $\tilde{\mathbf{a}} = \mathbf{V}\mathbf{\Lambda}^{-1/2}\mathbf{v}$.

These weight vectors $\tilde{\mathbf{a}}$ can then be rescaled to minimize their SSE. We accomplish this using the fact that a weight vector has its SSE minimized when its predicted variance, $\sigma^2_{\hat{y}_\mathbf{a}}$, is equal to its coefficient of prediction, $R^2_\mathbf{a}$. In this case,

$$\sigma^2_{\hat{y}_\mathbf{a}} = \mathbf{a}'\mathbf{R}\mathbf{a} \text{ and } R^2_\mathbf{a} = \frac{(\mathbf{a}'\mathbf{r}_{Xy})^2}{(\mathbf{a}'\mathbf{R}\mathbf{a})^2},$$

where $\mathbf{r}_{Xy}$ is the vector of correlations of the predictors X with the outcome y (Green, 1977). So, we multiply $\tilde{\mathbf{a}}$ by $s = \frac{\tilde{\mathbf{a}}'\mathbf{r}_{Xy}}{\tilde{\mathbf{a}}'\mathbf{R}\tilde{\mathbf{a}}}$. The quantity s is equal to $\tilde{\mathbf{a}}'\mathbf{r}_{Xy}$, since

$$\tilde{\mathbf{a}}'\mathbf{R}\tilde{\mathbf{a}} = (\mathbf{V}\mathbf{\Lambda}^{-1/2}\mathbf{v})'\mathbf{R}\mathbf{V}\mathbf{\Lambda}^{-1/2}\mathbf{v} = \mathbf{v}'\mathbf{v} = 1.$$

The minimum SSE weight vector $\mathbf{a}$ is then

$$\mathbf{a} = (\mathbf{r}_{Xy}{}'\mathbf{V}\mathbf{\Lambda}^{-1/2}\mathbf{k})\mathbf{V}\mathbf{\Lambda}^{-1/2}\mathbf{k}. \tag{2.6}$$

By the manipulations performed to scale the fungible weights $\mathbf{a}$ to their minimum SSE, the expression $r_{y\hat{y}_\mathbf{a}} = \mathbf{a}'\mathbf{R}\mathbf{a}$ is constant for all $\mathbf{a}$. Using the equation

$$r_{y\hat{y}_\mathbf{a}} = r_{y\hat{y}_\mathbf{b}} r_{\hat{y}_\mathbf{a}\hat{y}_\mathbf{b}}, \tag{2.7}$$

one can equate $r_{\hat{y}_\mathbf{a}\hat{y}_\mathbf{b}}$ with a decrement in R^2, $\theta = R^2_\mathbf{a} - R^2_\mathbf{b}$ so that

$$r_{y\hat{y}_\mathbf{a}} = (1 - \frac{\theta}{R^2_\mathbf{b}})^{1/2}. \tag{2.8}$$

Thus, Waller's fungible weights can be equivalently defined with either a correlation (2.1) or a decrement in R^2. In addition, this derivation shows that one can generate an infinite number of fungible weights for any $0 < r_{\hat{y}_\mathbf{a}\hat{y}_\mathbf{b}} < 1$ if there are at least three lianerly independent predictors.

Additionally, if the $\mathbf{z}$ used to generate fungible weights are considered random unit-length vectors generated from a uniform distribution, the covariance matrix of the fungible weights can be expressed as

$$\text{cov}(\mathbf{a}) = \frac{1}{p-1} R^2_\mathbf{b} r_{\hat{y}_\mathbf{a}\hat{y}_\mathbf{b}} (1 - r^2_{\hat{y}_\mathbf{a}\hat{y}_\mathbf{b}}) \mathbf{G}\mathbf{G}', \tag{2.9}$$

where $\mathbf{G} = \mathbf{V}\mathbf{\Lambda}^{-1/2}\mathbf{U}$ and its center, $r^2_{\hat{y}_\mathbf{a}\hat{y}_\mathbf{b}}\mathbf{b}$.

2.4 Geometry of Fungible Weights

The resulting class of fungible weights is shaped as an ellipsoid of $p-1$ dimensions. The reason for this is that the fungible weights satisfy two constraints that can be thought

of geometrically as the intersection of an ellipsoid

$$\mathbf{a}'\mathbf{R}\mathbf{a} = r^2_{y\hat{y}_\mathbf{a}} \tag{2.10}$$

and a hyperplane

$$\mathbf{a}'\mathbf{R}\mathbf{b} = r^2_{y\hat{y}_\mathbf{a}}. \tag{2.11}$$

Although the intersection of these two constraints is the same as the intersection of the minimum SSE and correlation constraints, these two pairs of constraints are not equivalent. The ellipsoid represents the constraint that the optimal scaling of any weight is the one that sets its variance to its R^2. The hyperplane is the set of weights such that the covariance of the fungible predictions and the LS predictions is equal to $r^2_{y\hat{y}_\mathbf{a}}$. The SSE constraint, by contrast, is associated with Green's indifference region, an ellipsoid around the optimal weights.

Figure 2.1, copied from Waller (2009) helps give an understanding of how the eigenstructure of the fungible weights and the optimal weights define a fungible ellipse.

We can analyze both of these constraints separately to understand the geometry of the fungible ellipsoid. The eigenvectors of $\mathbf{R}$ determine the ellipsoid's axes, with the length of each axis inversely proportional to the square root its associated eigenvalue. Thus, the ellipsoid is narrow in directions associated with large components of the variance and wide in directions with little variance. Intuitively, this means that there is less flexibility in parameter estimates that are associated with large components of the variance.

The other shape that defines the fungible weights is a hyperplane orthogonal to $\mathbf{r}_{Xy}$ that passes through the point $r^2_{y\hat{y}_\mathbf{a}}\mathbf{b}$. This hyperplane can be thought of as determining what part of the predictor correlation matrix will define the fungible weights. If the correlations point towards a short axis of the predictor ellipsoid, then the fungible ellipsoid will be larger. If the correlations point in a direction associated with little variance, then

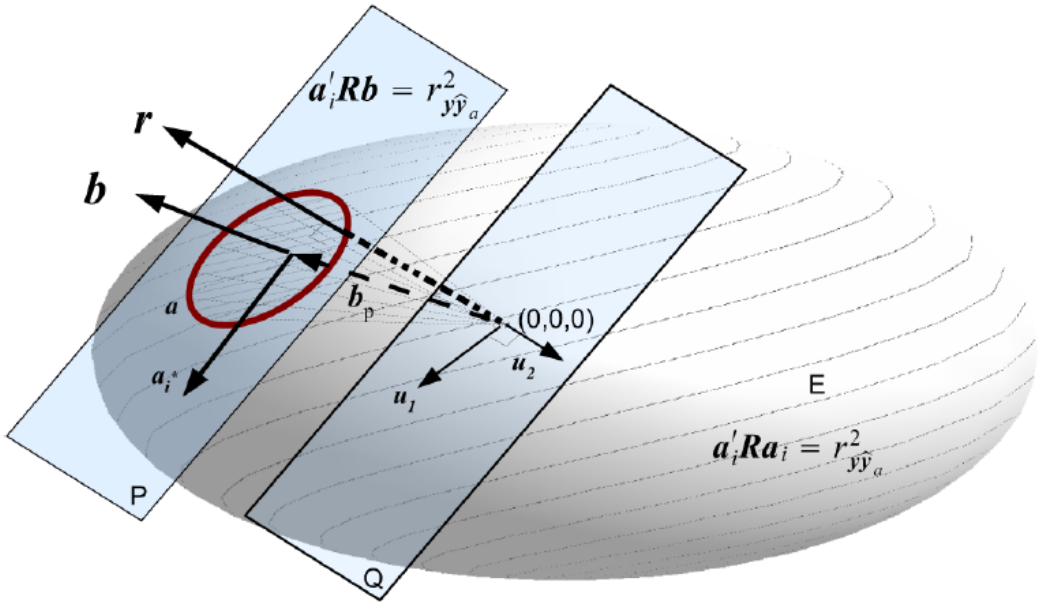

Figure 2.1: Geometry of fungible weights, from Waller, 2009.

this long axis will not play a part in generating the fungible ellipsoid.

2.5 Finding Fungible Extrema Using LaGrange Maximization

Waller (2009) has also devised a method for maximizing and minimizing the angle between the optimal weights and a defined class of fungible weights, similar to the method that Koopman developed. However, Waller can find both maximally different and minimally different weights, and the resulting weights are scaled to minimize SSE. He accomplishes this through numerical LaGrange Maximization of the cosine of the weights over the fungible constraints. However, this method is computationally intensive, and in the context of this study, unnecessary.

CHAPTER 3

Waller's Examples

Waller has applied his methods to two separate data sets. The application in his 2008 paper uses a set of GRE data (Kuncel et al., 2001). An ordinary regression analysis was run regressing graduate school GPA on verbal, quantitative, and analytic GRE scores for 82,659 students. The correlations among thepredictors ($\mathbf{R}$) and correlations of predictors with the dependent variable ($\mathbf{r}_{Xy}$) were

$$\mathbf{R} = \begin{pmatrix} 1.00 & 0.56 & 0.77 \\ 0.56 & 1.00 & 0.73 \\ 0.77 & 0.73 & 1.00 \end{pmatrix}, \mathbf{r}_{Xy} = \begin{pmatrix} 0.39 \\ 0.34 \\ 0.38 \end{pmatrix}.$$

The standardized LS weights were $(0.24, 0.14, 0.10)$ with an R^2 of 0.176. A decrement of .005 in R^2 was judged to be close enough for practical purposes, so 20,000 fungible weight vectors with $R^2 = .171$ were generated using the R code from Waller's 2008 paper. Weights selected to show the breadth of fungible solutions in Table 3.1. Both the second and third predictors can have relatively high weights or weights close to 0. Thus, a qualitative interpretation that emphasized the importance of verbal skills in predicting GPA would not be tenable, as other distinct combinations of predictors could perform indistinguishably well from a practical perspective.

Table 3.1: GRE fungible weights

	a_1	a_2	a_3
$\mathbf{a_1}$ high	**0.33**	0.12	0.00
$\mathbf{a_2}$ high	0.22	**0.23**	0.01
$\mathbf{a_3}$ high	0.16	0.07	**0.23**
$\mathbf{a_1}$ low	**0.13**	0.14	0.19
$\mathbf{a_2}$ low	0.24	**0.03**	0.17
$\mathbf{a_3}$ low	0.31	0.19	**−0.04**

Waller generated fungible weights for another empirical dataset in his 2009 paper to demonstrate the use of his algorithm to find maximally similar and dissimilar weights. In this example, fungible weights are generated for an executive compensation dataset, predicting 33 executive salaries based upon the sales, profits, and employment of their respective firms. Correlations appear below:

$$\mathbf{R} = \begin{pmatrix} 1.00 & 0.9202 & 0.9228 \\ 0.9202 & 1.00 & 0.8622 \\ 0.9228 & 0.8622 & 1.00 \end{pmatrix}, \mathbf{r}_{Xy} = \begin{pmatrix} 0.6758 \\ 0.6979 \\ 0.6823 \end{pmatrix}$$

The optimal weights were $(-0.080, 0.466, 0.354)$ with $R^2 = 0.513$, which, if interpreted, would suggest a negative effect of sales on compensation. However, the maximally dissimilar weights for a decrement in R^2 of .005 were $(0.132, 0.373, 0.234)$, which shows a positive effect for all predictors. The maximally similar weights at an R^2 decrement of 0.005 were $(-0.228, 0.618, 0.340)$, which shows an even greater negative effect of sales. The conflicting fungible weights, together with the substantive idea that sales should not decrease compensation, suggest that in this dataset, it is not individual predictor weights that should be considered but their composite effect.

CHAPTER 4

Moderators, Interactions, and Simple Slopes

Moderators in multiple regression are continuous predictors that affect the regression weight of another variable (Cohen & Cohen, 1983). Usually, the moderator is uncorrelated with the outcome, but this is not necessarily the case. In addition, in the absence of strong substantive knowledge, it is also possible to reverse the conception of the moderation relationship.

Simple slopes are often used in the social sciences to investigate the nature of a moderation relationship. By specifying values of the moderator across the range it takes across the population, one can examine and test the significance of the moderated slope at each of these values. This allows one to determine if there is a significant effect of an index variable depending on the level of the moderator. Also, simple slopes can be used to determine if the moderator makes a practical difference in the slope of the variable of interest. By evaluating across the meaningful range of both the predictors, one can see if predicted values would be reasonably affected in the population of interest.

In the case of two predictors and one interaction term, the equation for moderated regression is

$$\hat{Y} = b_1 X_1 + b_2 X_2 + b_3 X_1 X_2 + b_0 \tag{4.1}$$

If X_2 is the moderator and X_1 is the moderated variable, then for $X_2 = x_2$, the equation

representing the simple slope for X_1 is

$$\hat{Y} = (b_1 + b_3 x_2)X_1 + (b_0 + b_2 x_2) \tag{4.2}$$

The standard error of the simple slope of X_1 is

$$s_b = \sqrt{s_{11} + 2x_2 s_{13} + x_2^2 s_{33}}, \tag{4.3}$$

where s_{ij} designates the covariance of b_i with b_j. The significance of a given simple slope can be tested using the test statistic

$$\frac{b_1 + b_3 x_2}{s_b} \sim t_{N-3-1}. \tag{4.4}$$

For any set of fungible weights computed as alternative values to the LS weights (b_1, b_2, b_3), one can compute corresponding fungible simple slopes using (4.2). In the present study, we explore the behavior of fungible simple slopes under various conditions.

CHAPTER 5

Design

5.1 Motivating Factors for Design

There were two major goals for this study. The first was to combine fungible weights with simple slopes methodology to investigate the sensitivity of observed interactions to perturbations in R^2. The second was to investigate when fungible weights calculated from sample covariances yield results similar to fungible weights calculated from population covariances.

To investigate simple slopes with fungible weights, simple slopes were generated for each weight in the class of fungible weights. This was accomplished by simulating data from a moderated regression model with given properties and computing fungible simple slopes from the simulated dataset. Simple slopes were then generated from the resulting fungible vectors of fungible weights.

The second goal of this simulation was to look at the sampling distribution of fungible weights. This was accomplished by repeatedly drawing samples from a given distribution, calculating correlations, and generating the fungible ellipse associated with the sample. These ellipses were compared to the fungible ellipse generated from the population parameters in order to better understand how fungible ellipses vary across samples under varying conditions. In addition, an ancillary goal was to devise a method to generate a confidence set for the fungible weights from a sample of data.

5.2 Design Factors

The simulation had both a $2 \times 2 \times 2 \times 2$ factorial condition and a 2×2 factorial condition. The factors varied in the simulation were R^2, N, ρ_{12} (the correlation between X_1 and X_2), $\frac{\beta_1}{\beta_2}$ (the relative weight of X_1 compared to X_2) , and the proportion of the variance of y accounted for by the interaction term.

In the first factorial condition, the levels of the factors were 0.3 and 0.7 for R^2, 40 and 400 for N, 0.4 and 0.8 for ρ_{12}, and 1 and 3 for the ratio of the X_1 to the X_2 weights. β_3 was set so that X_3 explains 1/3 of the explained variance. This design permitted the investigation of fungible weights and simple slopes when an interaction was present in the population. Of particular interest was if fungible simple slopes from samples implied different conclusions about the presence of an interaction as compared to fungible weights generated using population parameters. In the second set of conditions, the interaction weight, β_3, was set to 0. The other parameters were $R^2 = 0.7$, $N = 400$, $rho = 0.4$ and 0.8, and a ratio of X_1 to X_2 of 1 and 3. This part was designed to investigate the behavior of simple slopes when no interaction was present in the population. Specifically of interest was if fungible simple slopes implied the presence of an interaction even when there was no interaction present in the population. There were 10,000 simulations performed in each condition in order to obtain detailed information about the distribution of fungible ellipses across samples. One would imagine that the addition of a fungible ellipse would decrease the Type I error since it makes it more difficult to detect an interaction and that the Type II error would be increased.

According to Waller's results, these factors should affect the fungible ellipses in predictable ways. Increasing R^2 will increase the size of the fungible ellipse, a result that can be seen by examining Waller's covariance equation (2.9). By looking at Figure 2.1, we can also see that increasing R^2 will increase the $r_{\hat{y}_\mathbf{a}\hat{y}_\mathbf{b}}$, moving the hyperplane closer to the edge of the predictor ellipsoid. The R^2 affects Waller's fungible weights and not Green's indifference region because Green defines his weights as the proportion of the R^2

that the alternative weights explain, effectively scaling the criteria to the R^2 to keep the region constant. Increasing N will make the estimates of the correlations between the variables more stable, which should in turn make the fungible ellipses more stable across samples. The ratio of the population weights of X_1 to X_2 affects the distribution of the fungible weights in a more subtle manner. This ratio does not affect the correlations among predictors, so the ellipsoid constraint is unaffected. However, it does increase the correlation between X_1 and Y, shifting the normal of the plane that is the other constraint. Examining the predictor correlation matrix shows how this will affect the generated fungible ellipses:

$$\text{where } R = \begin{pmatrix} 1 & \rho_{12} & 0 \\ \rho_{12} & 1 & 0 \\ 0 & 0 & 1 \end{pmatrix} \text{ with eigenvectors } \mathbf{U} = \begin{pmatrix} 1 & 1 & 0 \\ 1 & -1 & 0 \\ 0 & 0 & 1 \end{pmatrix}$$

and associated eigenvalues $(1 + \rho_{12}, 1 - \rho_{12}, 1)$.

So, by (2.10), the shortest axis of the ellipsoid constraint is $(1, 1, 0)$. Changing X_1 to have a higher weight than X_2 will cause the outcome correlations to point towards a longer axis, decreasing the size of the fungible ellipse. Increasing the correlation between X_1 and X_2 should in general increase the size of the fungible ellipse by increasing multicollinearity. However, the specific result obtained depends upon $\mathbf{r}_{Xy}$.

CHAPTER 6

Simulation Method

This section describes the simulation method. In each condition, multivariate normal X_1 and X_2 variables as linear combination of pairs of independent normal observations generated using the default "rnorm" function in R. Then, X_1 and X_2 were standardized and multiplied together to generate the interaction term X_3. The variance of this term is $\sigma_{X_3} = 1 + \rho_{12}^2$.

By design, X_3 accounted for either 1/3 or none of the explained variance. The case in which the interaction accounted for 1/3 of the variance is treated first. Since X_3 is uncorrelated with X_1 and X_2, β_3 is

$$\beta_3 = \frac{R^2/3}{(1+\rho_{12}^2)^{1/2}}. \tag{6.1}$$

$\frac{\beta_1}{\beta_2}$ and ρ_{12} are factors set for each cell. To find β_1 and β_2, one needs only to find a scaling constant since their ratio q is already assigned. This can be done by substituting $\beta_1 = q \cdot \beta_2$ into the equation

$$(\beta_1^2 + \beta_2^2 + 2 \cdot \rho_{12} \cdot \beta_1 \cdot \beta_2) = \frac{2}{3}R^2, \tag{6.2}$$

yielding

$$\beta_1 = \sqrt{\frac{\frac{2}{3}R^2}{q^2 + 2\rho_{12}c + 1}}.$$

When β_3 is set to 0,

$$(\beta_1^2 + \beta_2^2 + 2 \cdot \rho_{12} \cdot \beta_1 \cdot \beta_2) = R^2, \tag{6.3}$$

yielding

$$\beta_1 = \sqrt{\frac{R^2}{q^2 + 2\rho_{12}c + 1}}.$$

A weighted composite $\mathbf{y}$ is then created,

$$\mathbf{y} = \beta' \mathbf{X} + k \cdot N(0, 1). \tag{6.4}$$

$$\text{where } k = \sqrt{\frac{R^2 - (R^2)^2}{R^2 - 3/N}}.$$

k is chosen so that the proportion of the variance explained by the predictors is equal to the specified R^2. This choice corrects for the fact that a proportion of the random noise, $\frac{3}{N}$, is collinear with the predictors. This value is obtained by solving the equation

$$R^2 = \frac{R^2 + \frac{3}{N}k}{k + R^2} \tag{6.5}$$

where R^2 is the desired proportion of variance explained and the variance of the predictor composite and k is the variance of the normal noise added to the the composite.

Fungible weights were generated using the algorithm from Waller (2008) with the decrement in R^2 set to .01 and converted to the corresponding $r_{\hat{y}_\mathbf{a}\hat{y}_\mathbf{b}}$ using (2.8). The only change to the algorithm was that that instead of using random $\mathbf{z}$ vectors, 40 vectors of the form $\mathbf{z}_i = (\cos((i/40)2\pi), \sin((i/40)2\pi))$ were used for computational convenience.

Fungible weights were also generated from the population correlations. The correlations among predictors are

$$\mathbf{R} = \begin{pmatrix} 1 & \rho_{12} & 0 \\ \rho_{12} & 1 & 0 \\ 0 & 0 & 1 \end{pmatrix},$$

and $\mathbf{r}_{Xy}$ can be found by multiplying $\mathbf{R}$ by the true LS weights.

Simple slopes were generated both from the population fungible weights and for fungible weights calculated from simulated samples. X_2 was treated as the moderator, with X_1 slopes calculated conditional on x_2 set at 0 and ± 1 (X_1 and X_2 were standardized).

To visualize the sampling distribution of the fungible weights in each condition of the design, 10,000 samples of data were simulated and a fungible ellipse was generated for each one. The maximum distance from the weights in each sample fungible ellipse to the true LS weights was calculated. Then, a convex hull was generated around the 95% of ellipses closest to the true weights. This convex hull represents an approximate 95% containment region, since there is approximately a 95% chance that a fungible ellipse generated from a sample will lie completely within this region. The volumes of these regions were calculated in order to compare the variability of fungible ellipses across the design. For each cell in the design, this 95% containment region was plotted along with 200 sample fungible ellipses and the population fungible weights.

Bootstrapping Confidence Sets for Fungible Weights

A bootstrapping method was devised to create confidence sets for fungible weights from a sample. To do this, 10,000 bootstrap samples were created using case resampling. A fungible ellipse was calculated for each using the correlations found within each sample. A confidence set was calculated by generating a convex hull around the 95% of the bootstrapped fungible ellipses closest to the LS weights obtained from the original sample.

CHAPTER 7

Results

10,000 data sets were generated for each cell in the design. Tables 7.1 and 7.2 give the volume of the convex hull containing the 95% of the ellipses closest to the center of the population fungible ellipse by condition. Larger volumes represent a greater amount of variation across samples. The effect of increasing the R^2 and n was to decrease the size of the containment region, and the effect of increasing the correlation between predictors was to increase the size of the containment region. There did not seem to be any effect of varying $\frac{\beta_1}{\beta_2}$: the difference between conditions was relatively small and was not in any consistent pattern.

Figures showing the 95% containment regions for six conditions from the design are given in the following section. In these figures, the colored region represents the 95% containment region for the simulated fungible ellipses, the red ellipse is the population fungible ellipse, and the black ellipses are 200 randomly selected sample fungible ellipses. The center of the red ellipse is at $r^2_{\hat{y}_\mathbf{a}\hat{y}_\mathbf{b}} b$, where b is the LS weights. The design conditions depicted are thematically centered around the interaction condition with $\rho_{X_1X_2} = 0.4$, $\frac{b_1}{b_2} = 1$, $R^2 = 0.3$, and $n = 40$, which is shown in Figure 7.1. This condition was chosen because it represents a somewhat typical model encountered in the behavioral sciences. Four other conditions were chosen to show the effect of changing each parameter on the containment region: $\rho_{X_1X_2} = 0.8$ in Figure 7.2, $\frac{b_1}{b_2} = 3$ in Figure 7.3, $R^2 = 0.7$ in Figure 7.4, and $n = 400$ in Figure 7.5. Figure 7.6 represents the containment region for a

condition without interactions with parameters of $n = 400$ and $R^2 = 0.7$, chosen because this was condition without an interaction closest to the typical condition. All of the effects that are later discussed can be seen in these plots: the area of the population fungible weights, the volume of the containment region, the average area of sample ellipses, and the average distance of sample fungible ellipses to the center of the population fungible weights.

Simple slopes are also presented for these same conditions. There are four figures for each condition, including the population fungible simple slopes, the sample with least range in simple slopes, the sample with greatest range in simple slopes, and a representation of fungible simple slopes from 120 simulated samples. The typical condition with $\rho_{X_1X_2} = 0.4$, $\frac{b_1}{b_2} = 1$, $R^2 = 0.3$, and $n = 40$ is presented in Figures 7.7 through 7.10. The condition with $\rho_{X_1X_2} = 0.8$ is presented in Figures 7.11 through 7.14, $\frac{b_1}{b_2} = 3$ in Figures 7.15 to 7.18, $R^2 = 0.7$ in Figures 7.19 to 7.22, and $n = 400$ in Figures 7.23 to 7.25 (the population fungible simple slopes for this condition are the same as for the typical condition). Lastly, the no interaction condition is represented in Figures 7.26 to 7.29.

These figures show effects similar to those observed in the containment regions for sample fungible ellipses, that is, the slopes show less variance when the R^2 is lower, when the correlation between predictors is higher, and when there is a lower n. For example, consider the population fungible simple slopes for the typical condition, Figure 7.7. For $n = 40$, the fungible simple slopes with least variation, in Figure 7.9, would be interpreted as showing no interaction, and the simple slopes in Figure 7.8, showing the most variation, would be interpreted as showing a much greater interaction. In contrast, for $n = 400$ there is an interaction present even in the least varying condition, Figure 7.24, and, in the most varying condition, Figure 7.24, the fungible simple slopes do not greatly differ from the population fungible simple slopes.

The area of the population fungible ellipses is given in Tables 7.3 and 7.4. In these tables, larger values represent more flexibility in the population regression model. Sample

size is not a factor in these tables because these fungible ellipses were generated from implied population correlations. Increasing the predictors' correlation increased the area of these ellipses, and changing the ratio of the predictors weights from 1 to 3 slightly decreased the ellipses' area. However, increasing R^2 increased the size of the population fungible ellipse, opposite of the effect it had on the containment regions.

These two effects seem contradictory: Conditions with higher R^2 had smaller containment regions across samples, but the area of their population fungible ellipse was larger. To understand the origins of this effect, descriptive statistics were computed for the areas of the fungible ellipses across samples, as seen in Tables 7.5 and 7.6, and for the distances between the centers of the sample fungible ellipses and the population fungible ellipses, seen in Tables 7.7 and 7.8.

The average distance is proportional to n, with the mean being about $\sqrt{10}$ greater for the $n = 400$ condition compared to the $n = 40$ condition. Since the primary determinant of the center of a fungible ellipse is the estimated LS weights, conditions that increase the variance of LS estimates across samples should result in higher average distance. This observation is also consistent with statistical theory in multiple regression where higher multicollinearity of independent variables is associated with larger standard errors of regression coefficients. The ratio of the weights of the first two predictors does not seem to have any effect on the average distance.

The other major factor contributing to the size of the containment region is the average size of the sample fungible ellipses. Increasing the correlation of the predictors and the ratio of the predictor weights increased the average area of the fungible ellipses, consistent with the effect that these factors have on the area of the population fungible ellipse. In addition, decreasing n increases the average area of the sample fungible ellipses, that is, the fungible ellipses are larger on average when they vary more. The effect of n here is not $\sqrt{10}$ as it is in the distances, because the average size of a fungible ellipse does not correspond to the standard deviation of a distribution. However, it does appear that

increasing the variance of the sample correlations causes the fungible ellipses to spread to areas where their area is larger. This seems to suggest that decreasing R^2 increases the containment region for samples by both increasing the average distance that sample ellipses fall from the true weights and, at smaller n, by increasing the average ellipse size.

Tables 7.9 and 7.10 show the proportion of sample fungible ellipses that contained 0, implying there was no interpretable interaction. The population fungible ellipses for conditions with interactions all implied that an interpretable interaction existed, and the population fungible ellipses for conditions without interactions all implied that no interpretable interaction existed. Thus, Table 7.9 represents the simulated Type II error rate, a failure to detect an interpretable interaction, and Table 7.10 represents Type I error, detection of an interpretable interaction that is not present in the population.

For the conditions in this sample, the simulated Type I Error was near 0, and the simulated Type II error was actually 0 for all interaction conditions with $n = 400$. Simulated Type II error was about 0.08 for $R^2 = 0.3$ and about 0.001 for $R^2 = 0.7$. These results are related to the results for the containment regions, in that n decreased error rate most, higher R^2 decreased it second-most, and decreasing correlation between predictors decreased the error rate slightly. These results show that in some conditions, sample fungible weights can cause inappropriate conclusions to be drawn a non-neglible proportion of the time.

Lastly, the case-resampling bootstrap found 96.7% containment over 1,000 replications for the interaction condition with $\rho_{X_1X_2}$ of 0.4, $\frac{b_1}{b_2}$ of 3, R^2 of .7, and n of 40. This containment rate was significantly greater than the nominal containment rate of 0.95. It is possible, however, that increasing the number of bootstrap samples would improve this confidence set. An example of a bootstrapped confidence set is given in Figure 7.30. Figures from the rest of the design are presented in the appendix.

7.1 Tables

Table 7.1: Volume of 95% Containment Region with Interaction Present

	$n = 40$	$n = 400$	$n = 40$	$n = 400$	
$\beta_1/\beta_2 = 1$	0.4776	0.0325	0.1978	0.01778	$\rho_{X1X2} = 0.4$
$\beta_1/\beta_2 = 3$	0.4806	0.0312	0.1985	0.0179	$\rho_{X1X2} = 0.4$
$\beta_1/\beta_2 = 1$	1.0051	0.0552	0.4027	0.0312	$\rho_{X1X2} = 0.8$
$\beta_1/\beta_2 = 3$	1.0022	0.0553	0.4193	0.0316	$\rho_{X1X2} = 0.8$
	$R^2 = .3$	$R^2 = .3$	$R^2 = .7$	$R^2 = .7$	

Table 7.2: Volume of 95% Containment Region with No Interaction

	$\beta_1/\beta_2 = 1$	$\beta_1/\beta_2 = 3$
$\rho_{X1X2} = 0.4$	0.0118	0.0106
$\rho_{X1X2} = 0.8$	0.0169	0.0175

Table 7.3: Area of Population Fungible Ellipse with Interaction Present

	$R^2 = .3$	$R^2 = .7$	
$\beta_1/\beta_2 = 1$	0.0373	0.0380	$\rho_{X1X2} = 0.4$
$\beta_1/\beta_2 = 3$	0.0365	0.0372	$\rho_{X1X2} = 0.4$
$\beta_1/\beta_2 = 1$	0.0627	0.0639	$\rho_{X1X2} = 0.8$
$\beta_1/\beta_2 = 3$	0.0621	0.0633	$\rho_{X1X2} = 0.8$

Table 7.4: Area of Population Fungible Ellipses with No Interaction

	$\beta_1/\beta_2 = 1$	$\beta_1/\beta_2 = 3$
$\rho_{X1X2} = 0.4$	0.04000	0.0389
$\rho_{X1X2} = 0.8$	0.0692	0.0684

Table 7.5: Average Area of Sample Fungible Ellipse with Interactions

	$n = 40$	$n = 400$	$n = 40$	$n = 400$	
$\beta_1/\beta_2 = 1$	0.04551	0.03795	0.04149	0.03835	$\rho_{X1X2} = 0.4$
$\beta_1/\beta_2 = 3$	0.04431	0.03732	0.04075	0.03759	$\rho_{X1X2} = 0.4$
$\beta_1/\beta_2 = 1$	0.07506	0.06417	0.07012	0.0647	$\rho_{X1X2} = 0.8$
$\beta_1/\beta_2 = 3$	0.07428	0.0634	0.06903	0.06405	$\rho_{X1X2} = 0.8$
	$R^2 = .3$	$R^2 = .3$	$R^2 = .7$	$R^2 = .7$	

Table 7.6: Average Area of Sample Fungible Ellipse with no Interaction

	$\beta_1/\beta_2 = 1$	$\beta_1/\beta_2 = 3$
$\rho_{X1X2} = 0.4$	0.04046	0.03928
$\rho_{X1X2} = 0.8$	0.07027	0.06942

Table 7.7: Average Distance of Sample Ellipse to Population Center with Interaction

	$n = 40$	$n = 400$	$n = 40$	$n = 400$	
$\beta_1/\beta_2 = 1$	0.2212	0.0663	0.1610	0.0492	$\rho_{X1X2} = 0.4$
$\beta_1/\beta_2 = 3$	0.2222	0.0669	0.1598	0.0486	$\rho_{X1X2} = 0.4$
$\beta_1/\beta_2 = 1$	0.3051	0.0900	0.2185	0.0650	$\rho_{X1X2} = 0.8$
$\beta_1/\beta_2 = 3$	0.3064	0.0908	0.2158	0.0651	$\rho_{X1X2} = 0.8$
	$R^2 = .3$	$R^2 = .3$	$R^2 = .7$	$R^2 = .7$	

Table 7.8: Average Distance of Sample Ellipse to Population Center with No Interaction

	$\beta_1/\beta_2 = 1$	$\beta_1/\beta_2 = 3$
$\rho_{X1X2} = 0.4$	0.0413	0.0408
$\rho_{X1X2} = 0.8$	0.0579	0.0577

Table 7.9: Proportion of Samples Containing a 0 Interaction Term with Interaction Present

	$n = 40$	$n = 400$	$n = 40$	$n = 400$	
$\beta_1/\beta_2 = 1$	0.0782	0	0.0009	0	$\rho_{X1X2} = 0.4$
$\beta_1/\beta_2 = 3$	0.0789	0	0.0003	0	$\rho_{X1X2} = 0.4$
$\beta_1/\beta_2 = 1$	0.0814	0	0.0005	0	$\rho_{X1X2} = 0.8$
$\beta_1/\beta_2 = 3$	0.0812	0	0.0007	0	$\rho_{X1X2} = 0.8$
	$R^2 = .3$	$R^2 = .3$	$R^2 = .7$	$R^2 = .7$	

Table 7.10: Proportion of Samples Containing a 0 Interaction Term with No Interaction

	$\beta_1/\beta_2 = 1$	$\beta_1/\beta_2 = 3$
$\rho_{X1X2} = 0.4$	0.9996	0.9997
$\rho_{X1X2} = 0.8$	0.9997	1

7.2 Graphs

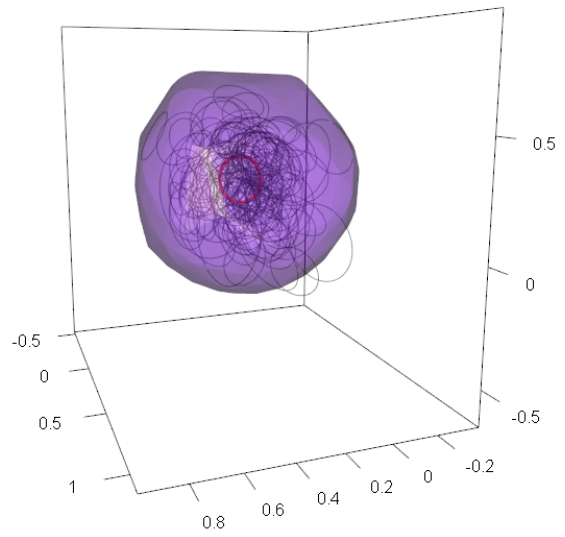

Figure 7.1: Sample Fungible Weights from $n = 40$, $\rho_{X_1X_2} = 0.4$, $R^2 = 0.3$, $\frac{b_1}{b_2} = 1$

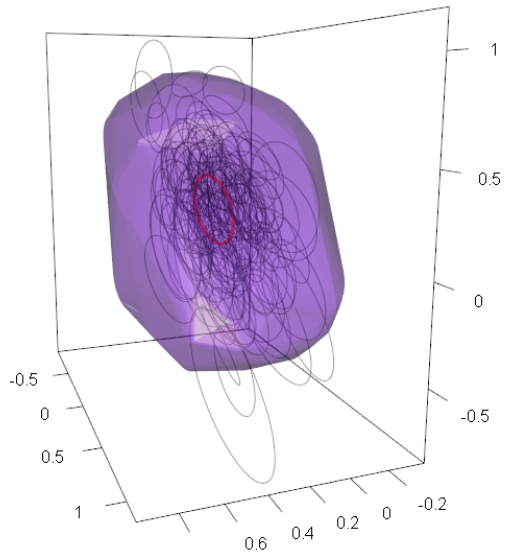

Figure 7.2: Sample Fungible Weights from $n = 40$, $\rho_{X_1X_2} = 0.8$, $R^2 = 0.3$, $\frac{b_1}{b_2} = 1$

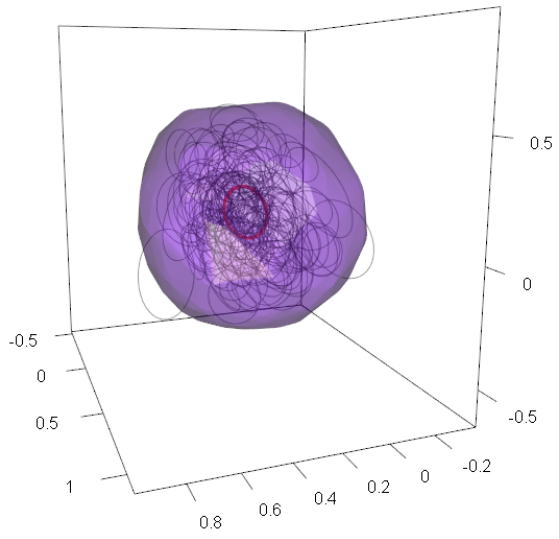

Figure 7.3: Sample Fungible Weights from $n = 40$, $\rho_{X_1X_2} = 0.4$, $R^2 = 0.3$, $\frac{b_1}{b_2} = 3$

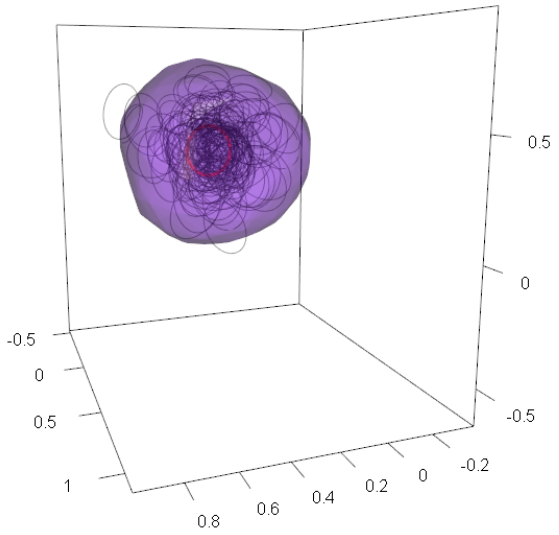

Figure 7.4: Sample Fungible Weights from $n = 40$, $\rho_{X_1X_2} = 0.4$, $R^2 = 0.7$, $\frac{b_1}{b_2} = 1$

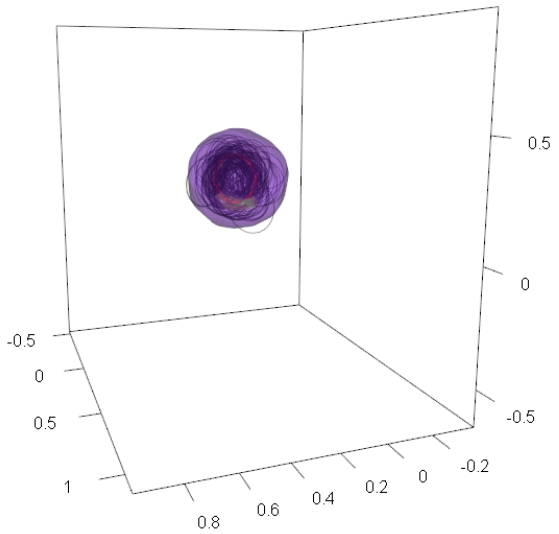

Figure 7.5: Sample Fungible Weights from $n = 400$, $\rho_{X_1X_2} = 0.4$, $R^2 = 0.3$, $\frac{b_1}{b_2} = 1$

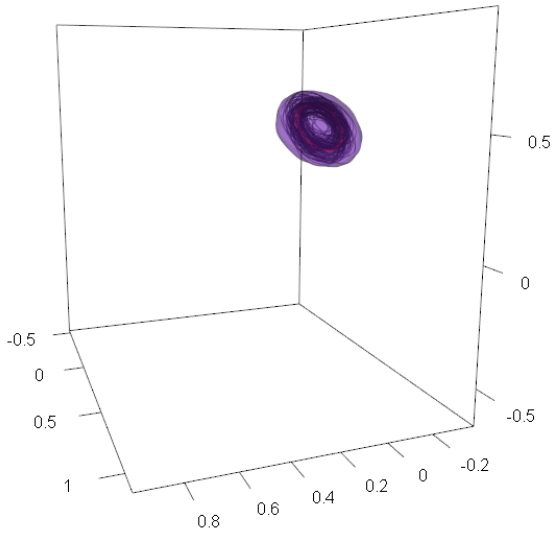

Figure 7.6: Sample Weights from Intx = 0, $n = 400$, $\rho_{X_1X_2} = 0.4$, $R^2 = 0.7$, $\frac{b_1}{b_2} = 1$

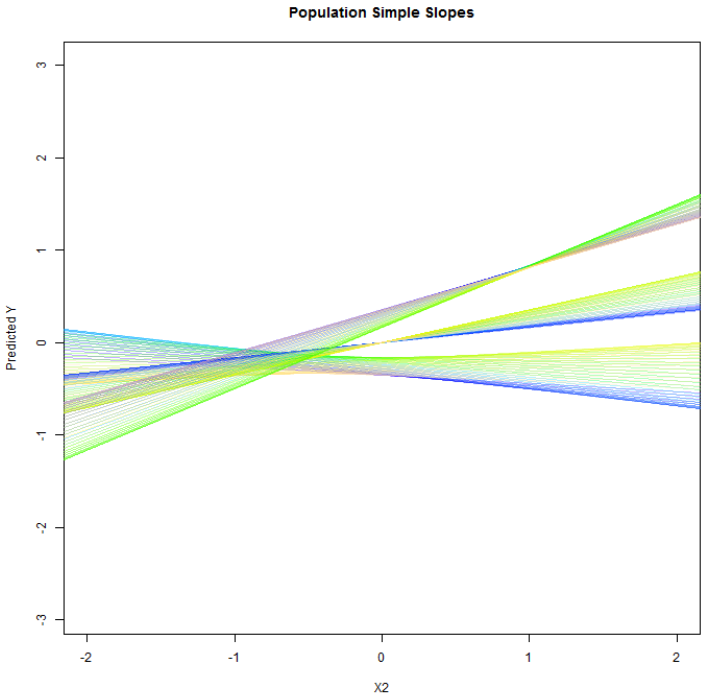

Figure 7.7: Simple Slopes with Intx from $\rho_{X_1X_2} = 0.4$, $R^2 = 0.3$, $\frac{b_1}{b_2} = 1$

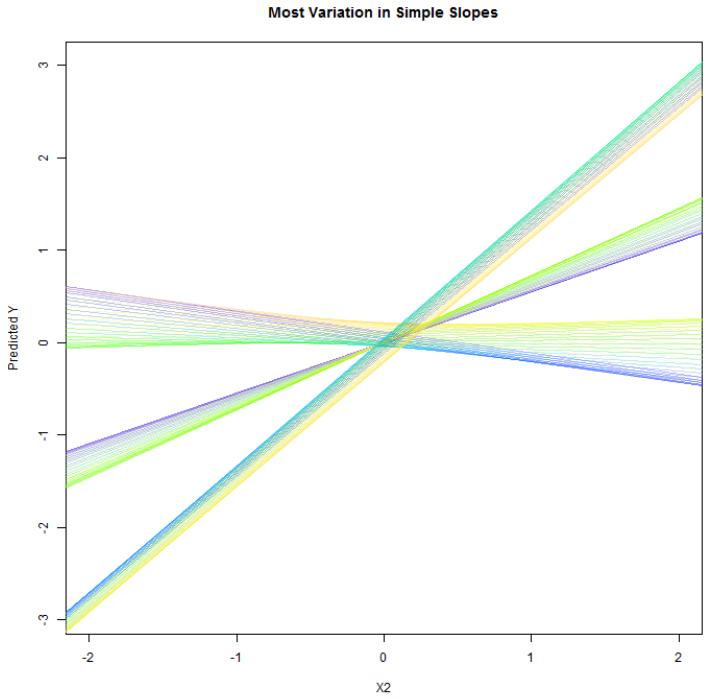

Figure 7.8: Simple Slopes with Intx from $n = 40$, $\rho_{X_1X_2} = 0.4$, $R^2 = 0.3$, $\frac{b_1}{b_2} = 1$

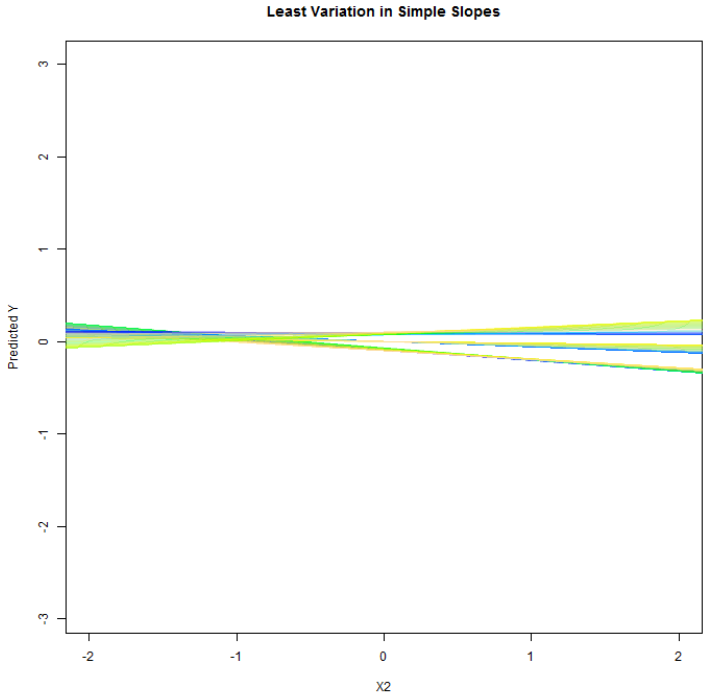

Figure 7.9: Simple Slopes with Intx from $n = 40$, $\rho_{X_1X_2} = 0.4$, $R^2 = 0.3$, $\frac{b_1}{b_2} = 1$

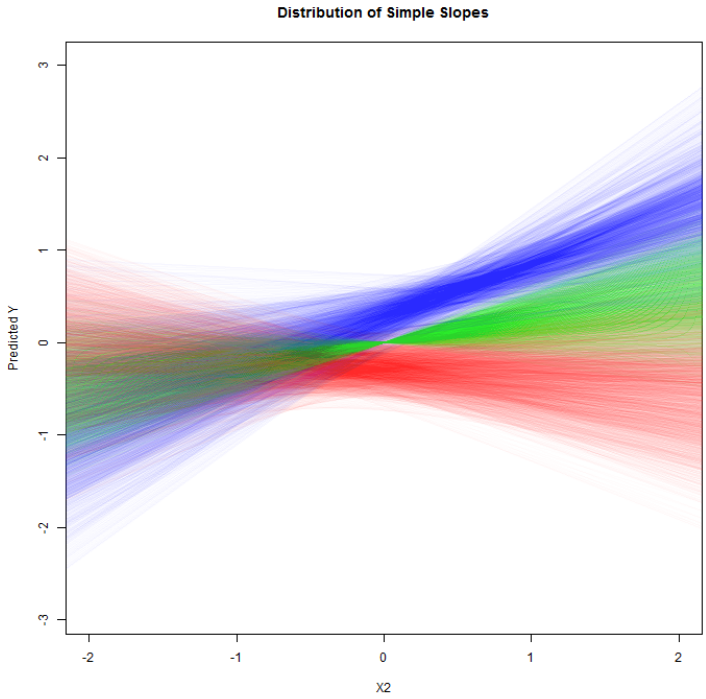

Figure 7.10: Simple Slopes with Intx from $n = 40$, $\rho_{X_1X_2} = 0.4$, $R^2 = 0.3$, $\frac{b_1}{b_2} = 1$

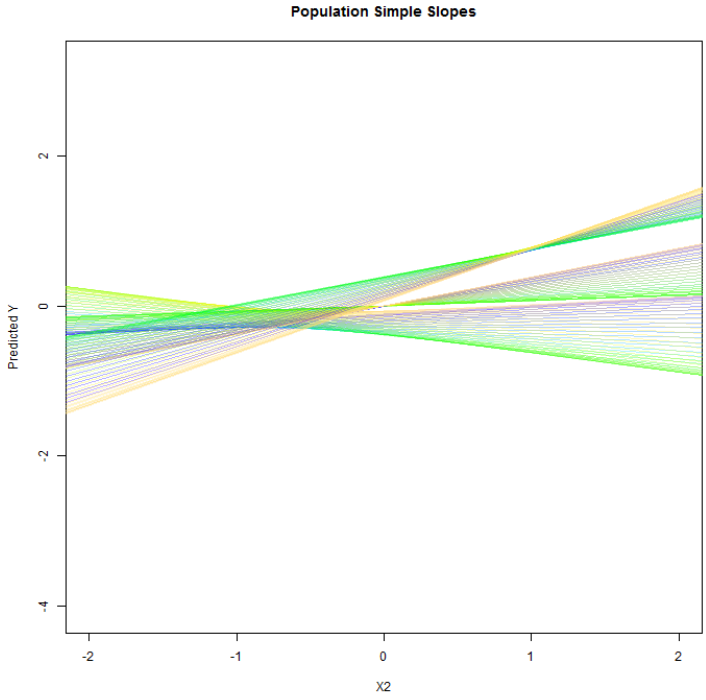

Figure 7.11: Simple Slopes with Intx from $\rho_{X_1X_2} = 0.8$, $R^2 = 0.3$, $\frac{b_1}{b_2} = 1$

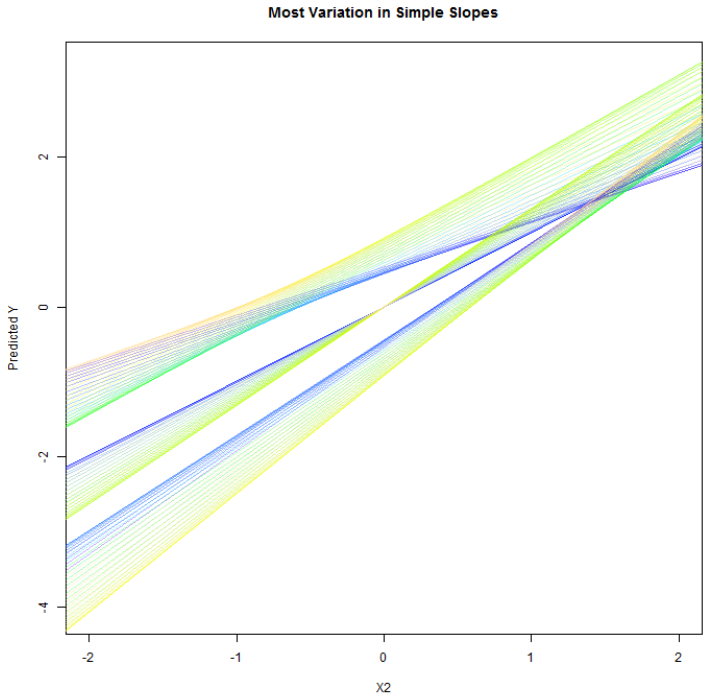

Figure 7.12: Simple Slopes with Intx from $n = 40$, $\rho_{X_1X_2} = 0.8$, $R^2 = 0.3$, $\frac{b_1}{b_2} = 1$

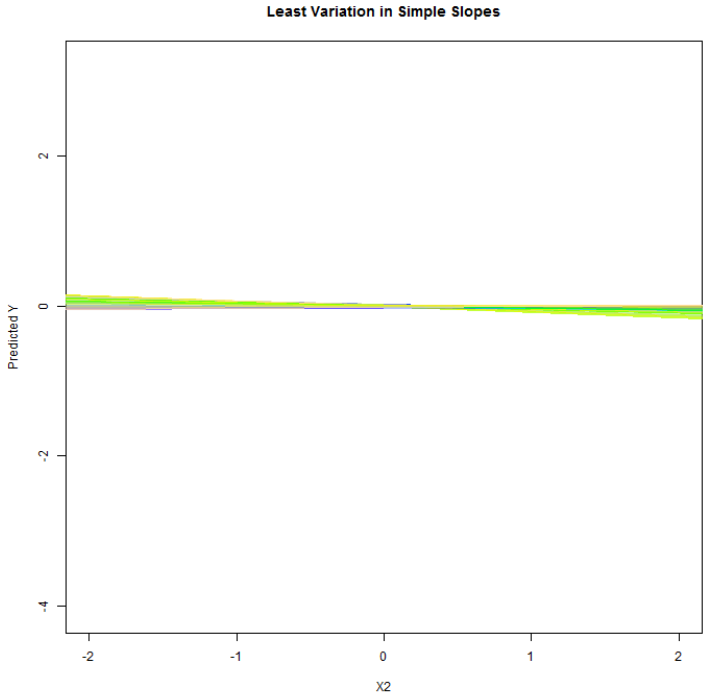

Figure 7.13: Simple Slopes with Intx from $n = 40$, $\rho_{X_1X_2} = 0.8$, $R^2 = 0.3$, $\frac{b_1}{b_2} = 1$

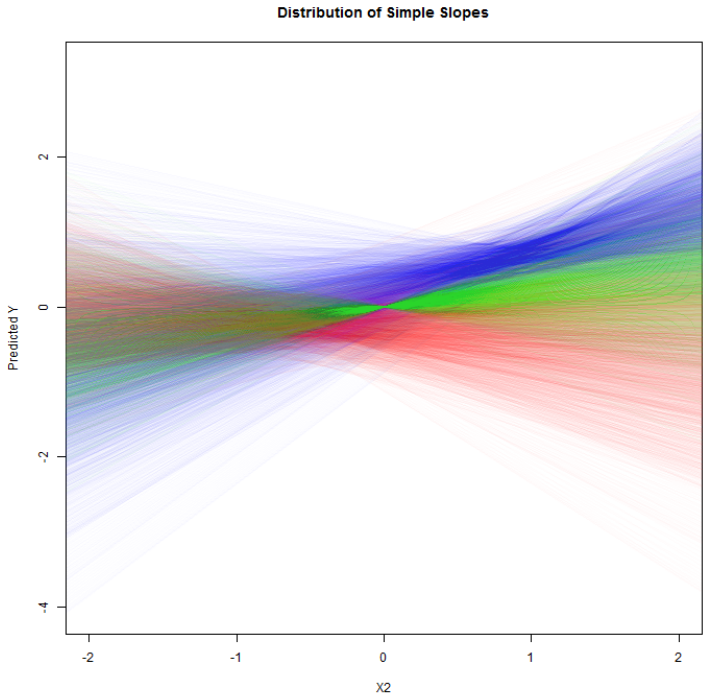

Figure 7.14: Simple Slopes with Intx from $n = 40$, $\rho_{X_1X_2} = 0.8$, $R^2 = 0.3$, $\frac{b_1}{b_2} = 1$

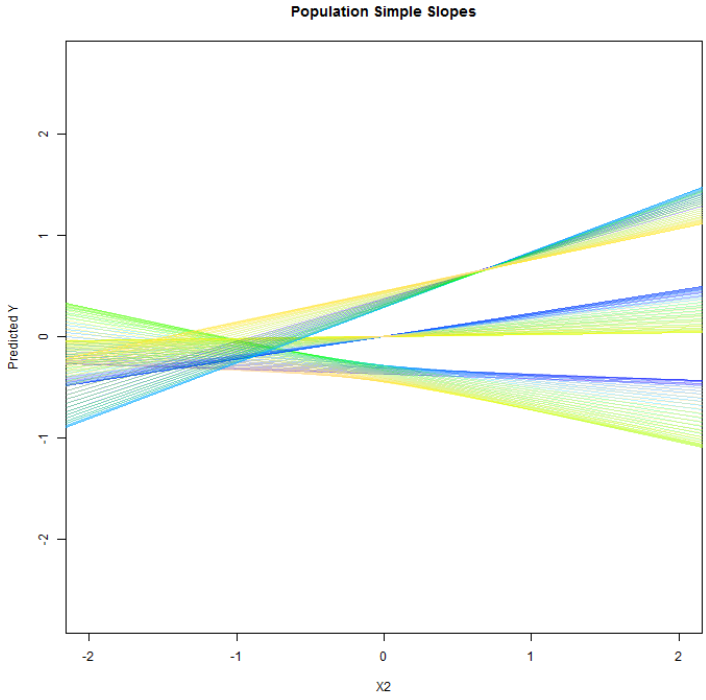

Figure 7.15: Simple Slopes with Intx from $\rho_{X_1X_2} = 0.4$, $R^2 = 0.3$, $\frac{b_1}{b_2} = 3$

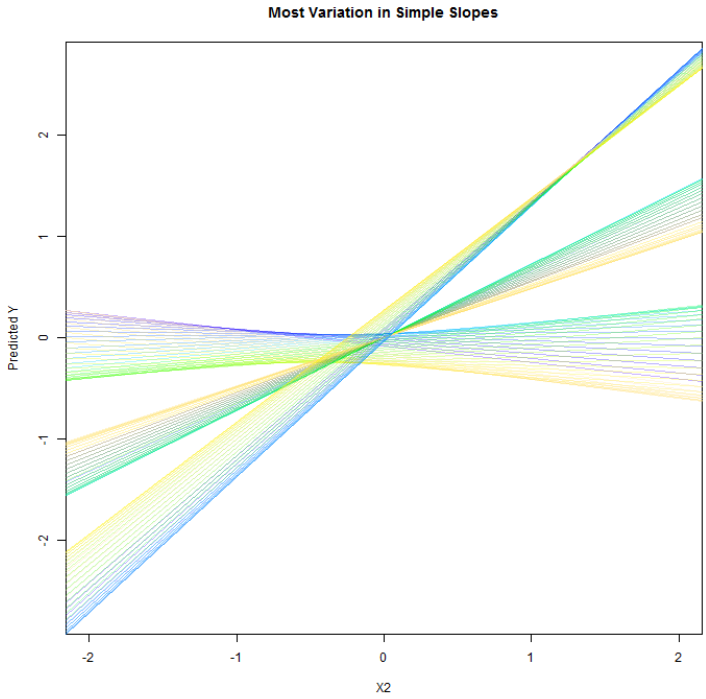

Figure 7.16: Simple Slopes with Intx from $n = 40$, $\rho_{X_1X_2} = 0.4$, $R^2 = 0.3$, $\frac{b_1}{b_2} = 3$

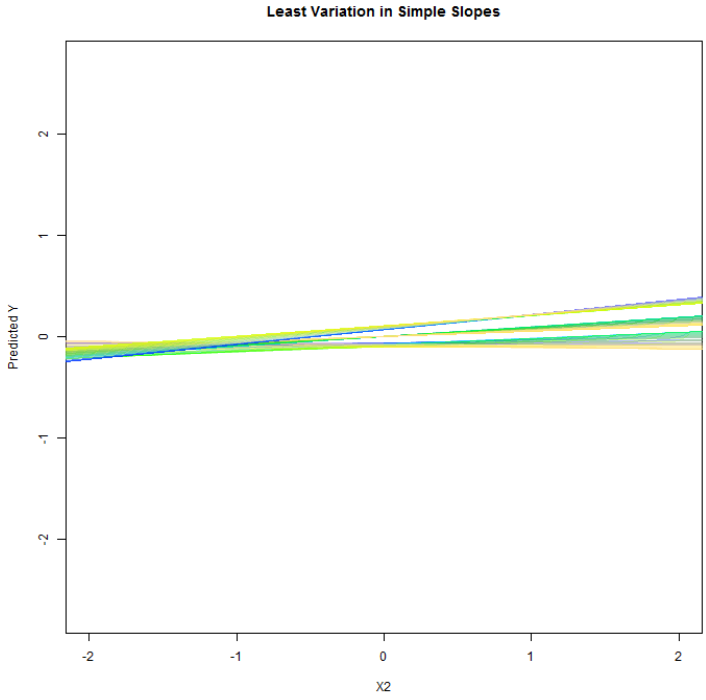

Figure 7.17: Simple Slopes with Intx from $n = 40$, $\rho_{X_1X_2} = 0.4$, $R^2 = 0.3$, $\frac{b_1}{b_2} = 3$

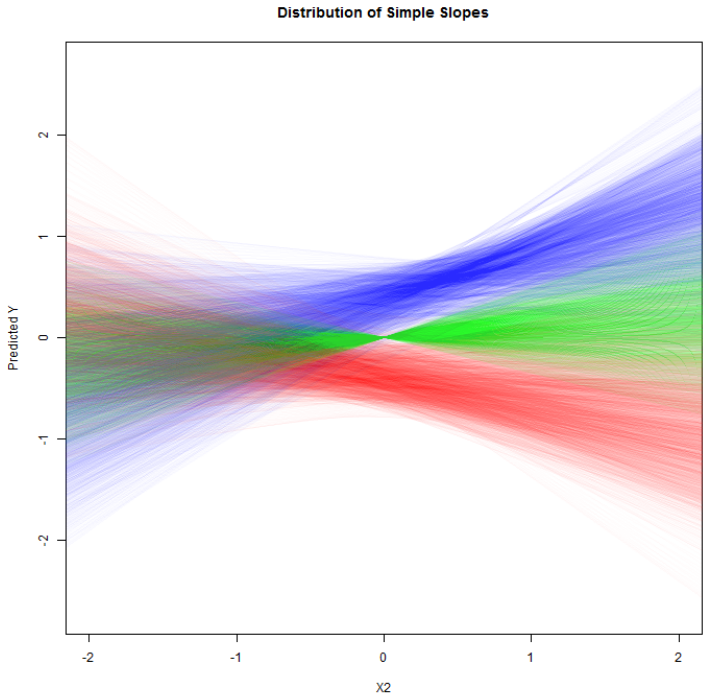

Figure 7.18: Simple Slopes with Intx from $n = 40$, $\rho_{X_1X_2} = 0.4$, $R^2 = 0.3$, $\frac{b_1}{b_2} = 3$

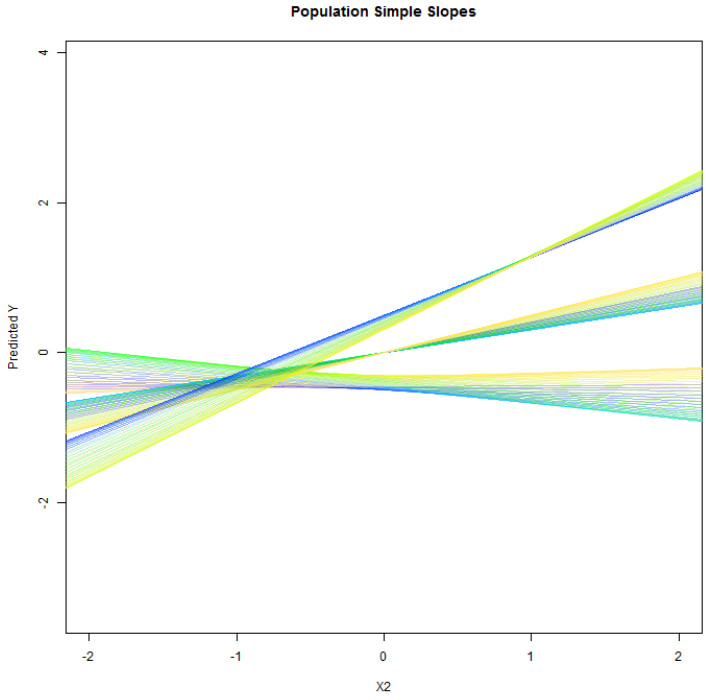

Figure 7.19: Simple Slopes with Intx from $\rho_{X_1X_2} = 0.4$, $R^2 = 0.7$, $\frac{b_1}{b_2} = 1$

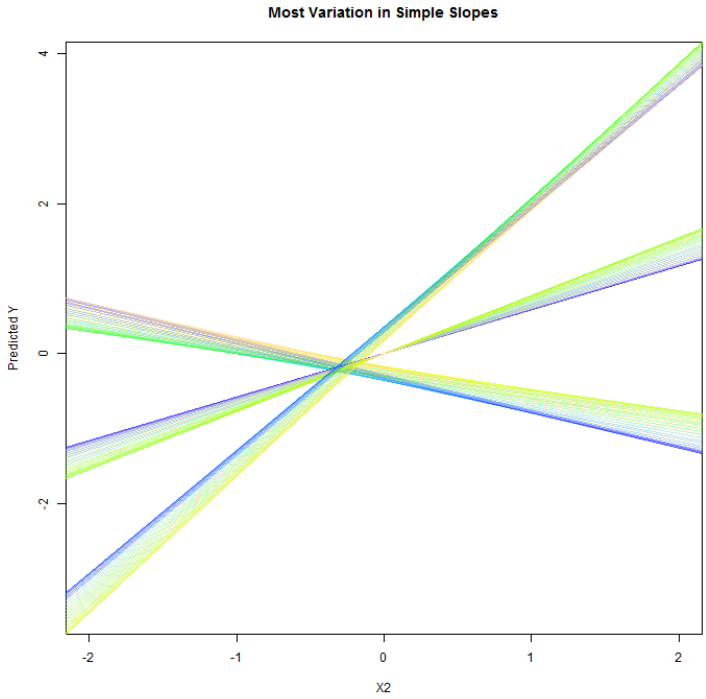

Figure 7.20: Simple Slopes with Intx from $n = 40$, $\rho_{X_1X_2} = 0.4$, $R^2 = 0.7$, $\frac{b_1}{b_2} = 1$

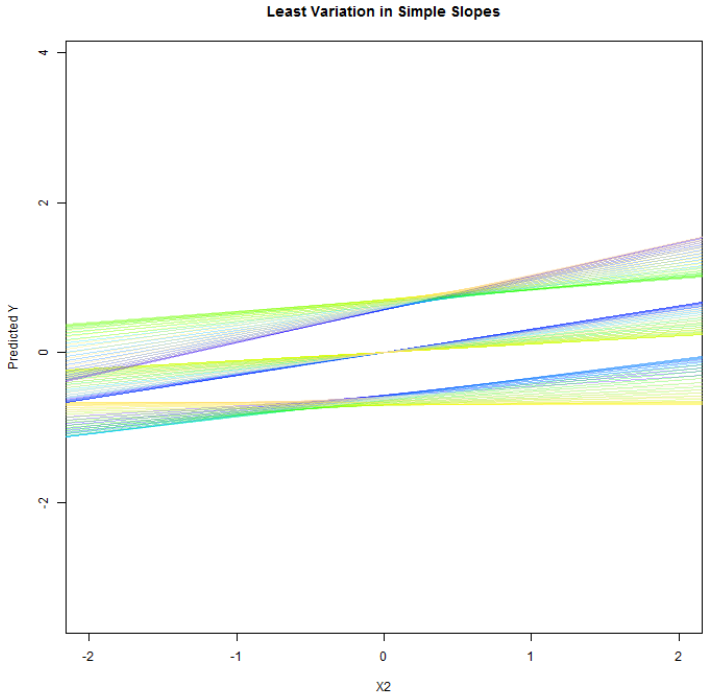

Figure 7.21: Simple Slopes with Intx from $n = 40$, $\rho_{X_1X_2} = 0.4$, $R^2 = 0.7$, $\frac{b_1}{b_2} = 1$

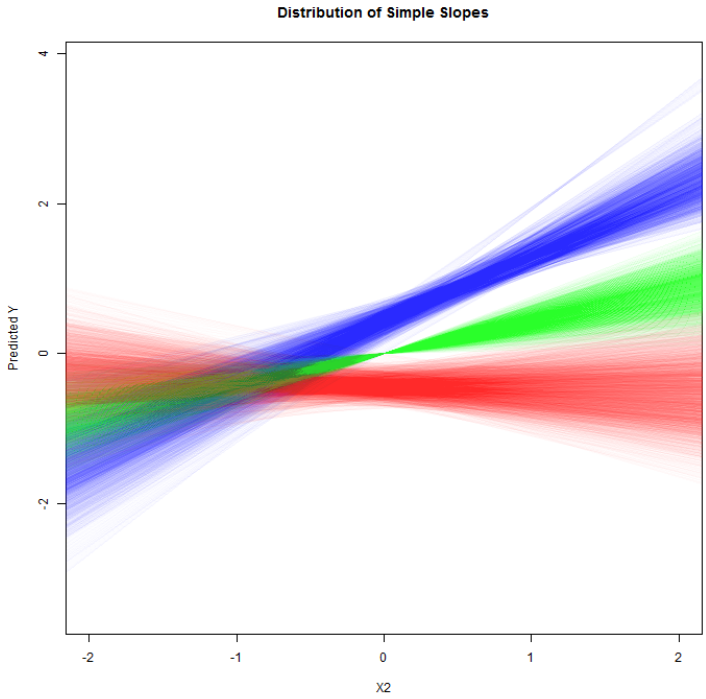

Figure 7.22: Simple Slopes with Intx from $n = 40$, $\rho_{X_1X_2} = 0.4$, $R^2 = 0.7$, $\frac{b_1}{b_2} = 1$

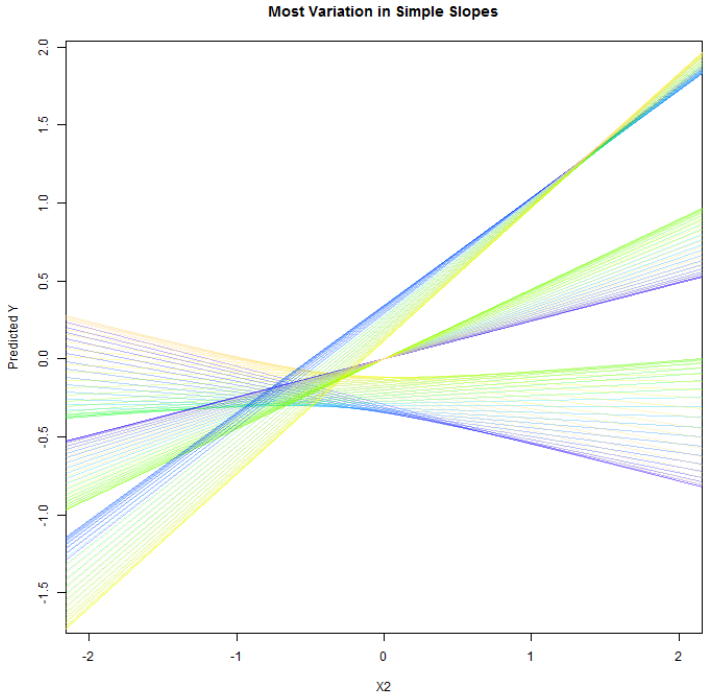

Figure 7.23: Simple Slopes with Intx from $n = 400$, $\rho_{X_1X_2} = 0.4$, $R^2 = 0.3$, $\frac{b_1}{b_2} = 1$

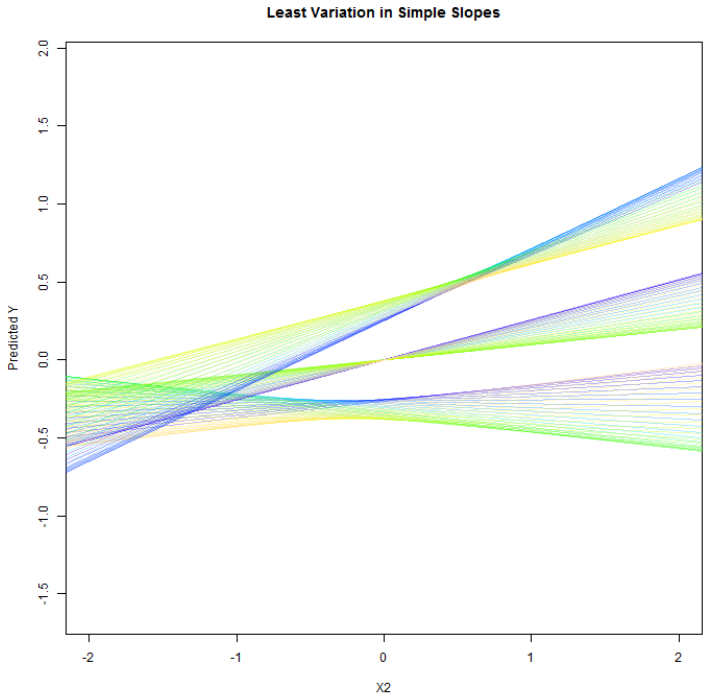

Figure 7.24: Simple Slopes with Intx from $n = 400$, $\rho_{X_1X_2} = 0.4$, $R^2 = 0.3$, $\frac{b_1}{b_2} = 1$

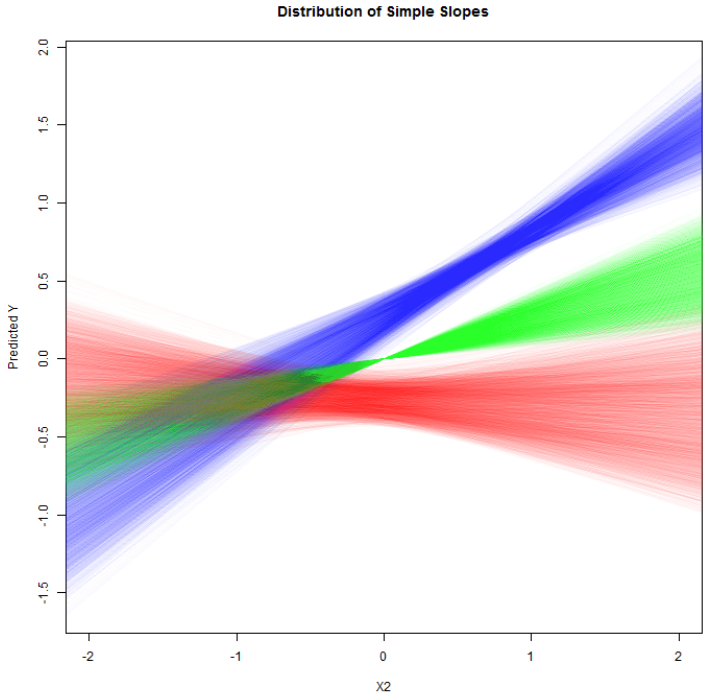

Figure 7.25: Simple Slopes with Intx from $n = 400$, $\rho_{X_1X_2} = 0.4$, $R^2 = 0.3$, $\frac{b_1}{b_2} = 1$

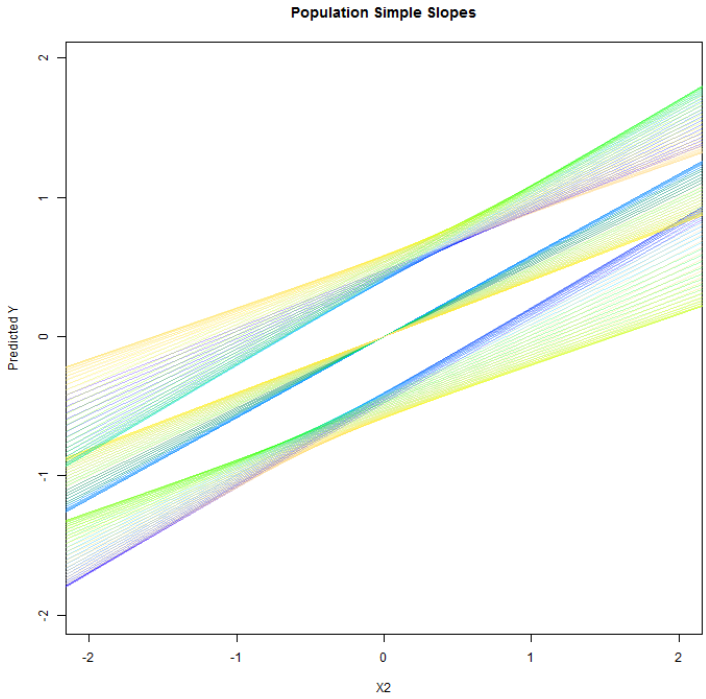

Figure 7.26: Simple Slopes from Intx = 0, $\rho_{X_1X_2} = 0.4$, $R^2 = 0.7$, $\frac{b_1}{b_2} = 1$

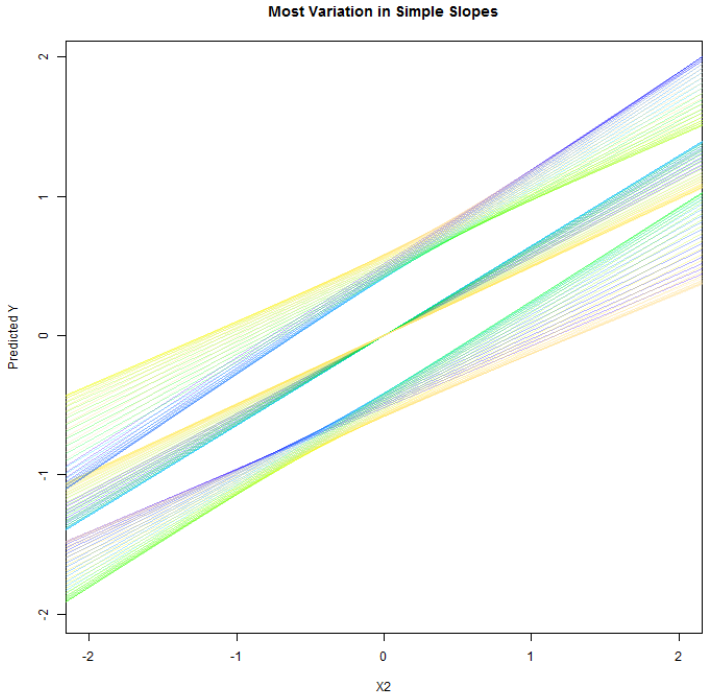

Figure 7.27: Simple Slopes from Intx = 0, $n = 400$, $\rho_{X_1X_2} = 0.4$, $R^2 = 0.7$, $\frac{b_1}{b_2} = 1$

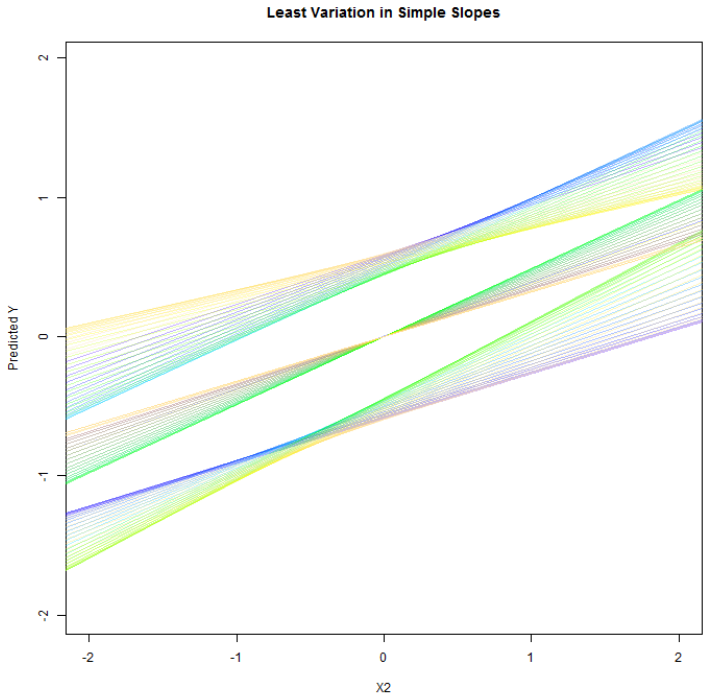

Figure 7.28: Simple Slopes from Intx $= 0$, $n = 400$, $\rho_{X_1X_2} = 0.4$, $R^2 = 0.7$, $\frac{b_1}{b_2} = 1$

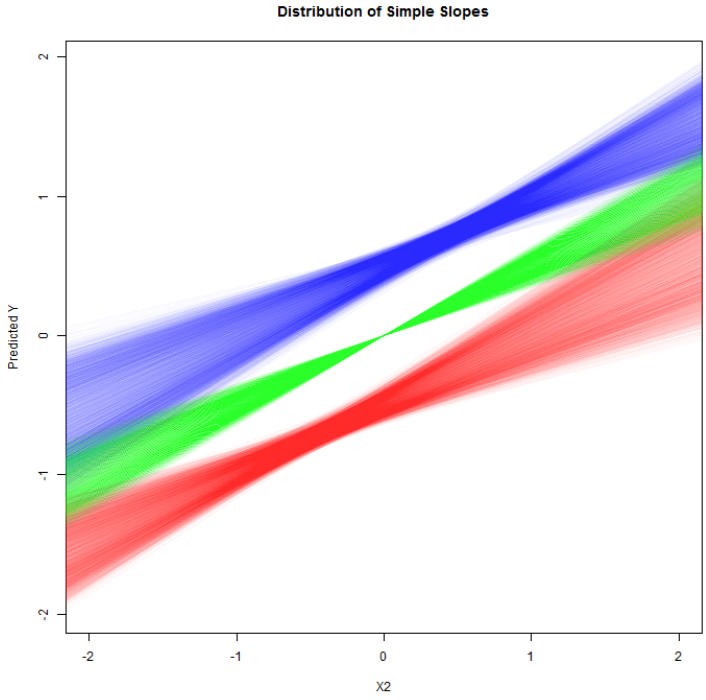

Figure 7.29: Simple Slopes from Intx $= 0$, $n = 400$, $\rho_{X_1X_2} = 0.4$, $R^2 = 0.7$, $\frac{b_1}{b_2} = 1$

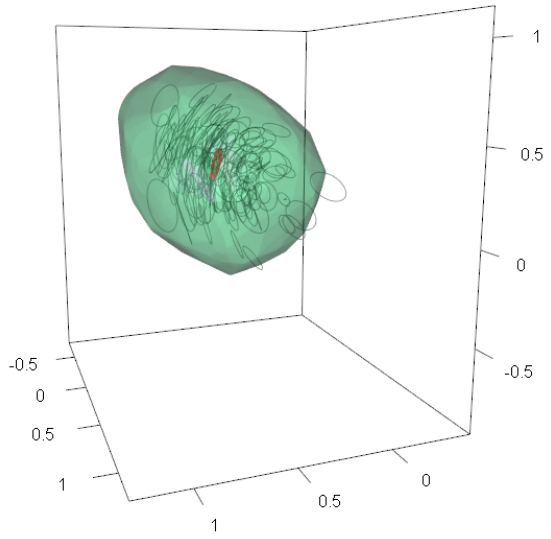

Figure 7.30: Bootstrapped Fungible Weights from $n = 40$, $\rho_{X_1X_2} = 0.4$, $R^2 = 0.7$, $\frac{b_1}{b_2} = 3$

CHAPTER 8

Discussion

The results regarding the area of the population fungible ellipse are consistent with Waller's equations and predictions. In this regard, regression models are less specific when there is a higher level of R^2, when there is a great deal of multicollinearity in the predictors, and when the LS weights are associated with a large component of the predictor variance.

However, these factors do not necessarily affect the sampling variability of fungible weights in a similar way. Higher R^2 actually decreases the variability of fungible weights across samples, leading to a smaller region of containment. Increased correlations between predictors increases both the area of the population fungible ellipse and the containment region, but changing the ratio of the predictor weights did not have a discernible effect on the volume of the containment region despite slightly increasing the area of the population fungible ellipse. For all the models considered here, having a ten-fold increase in sample size was more important in reducing variance of fungible weights than any other factor in the simulation.

These results generalized to simple slopes, where conditions with more variance of fungible ellipses across samples had more variance of simple slopes across samples. If the important criterion was whether or not the fungible ellipse generated from a sample gave evidence of an interaction, then fungible ellipses performed well in all conditions except for those with low R^2 and low sample sizes, where the Type II error was approximately

0.08. Since fungible weights do not take into account sample variance, it is important to know that there are conditions under which fungible weights would occasionally give misleading results. These findings are presented both in tables that show proportion of wrong conclusions, Tables 7.9 and 7.10, and in Figures 7.9, 7.13, 7.17, and 7.21.

The case-resampling bootstrapping method could be helpful in determining risk of drawing an incorrect conclusion due to sampling variation. However, more work will have to be performed to understand the bootstrap's performance across conditions. Even if only a conservative bootstrap estimator can be created, though, this could still be helpful. If the fungible weights calculated directly from sample correlations suggest that no interaction is present, then a bootstrapped confidence set will certainly suggest that there is no interaction. If the sample fungible weights suggest that an interaction is present, then a conservative confidence set suggesting that they are present would give good evidence that they can be trusted. If the bootstrapped set did not confirm an interaction, then there would be doubt as to whether there was or was not an interaction. However, this situation is no worse than if no confidence set had not been generated at all. In addition, this particular method of generating a confidence set would probably not extend to high dimensional data.

The results from this simulation suggest that for this three predictor model an n of 400 will result in sample fungible ellipses that closely resemble the population fungible ellipse. At smaller n, fungible ellipses can vary markedly from the population fungible ellipse. It has also been shown that the factors that cause fungible weights to vary across samples are not always the same factors that make the population fungible ellipse larger. A tentative recommendation is to examine a distribution of fungible ellipses generated using case resampling in order to determine if one is unsure if the fungible weights are a good estimate of the true fungible weights.

CHAPTER 9

Appendix

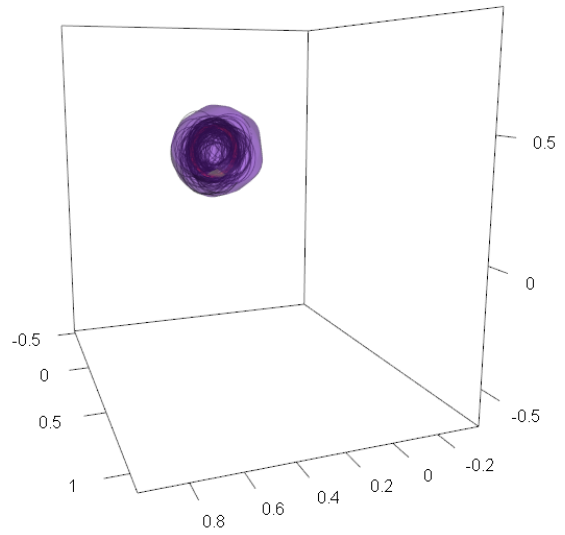

Figure 9.1: Sample Fungible Weights from $n = 400$, $\rho_{X_1X_2} = 0.4$, $R^2 = 0.7$, $\frac{b_1}{b_2} = 1$

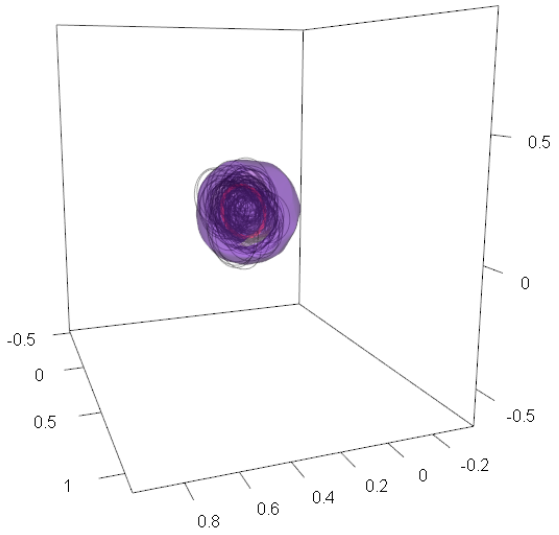

Figure 9.2: Sample Fungible Weights from $n = 400$, $\rho_{X_1X_2} = 0.4$, $R^2 = 0.3$, $\frac{b_1}{b_2} = 3$

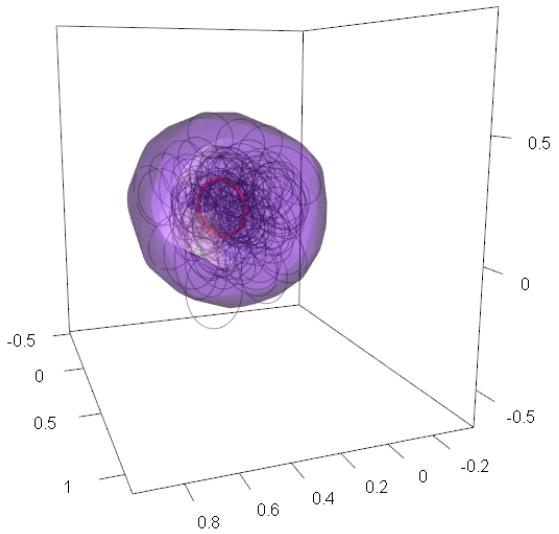

Figure 9.3: Sample Fungible Weights from $n = 40$, $\rho_{X_1X_2} = 0.4$, $R^2 = 0.7$, $\frac{b_1}{b_2} = 3$

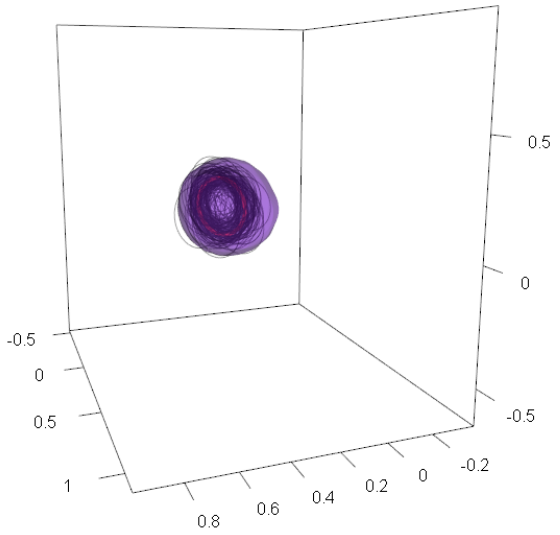

Figure 9.4: Sample Fungible Weights from $n = 400$, $\rho_{X_1X_2} = 0.4$, $R^2 = 0.7$, $\frac{b_1}{b_2} = 3$

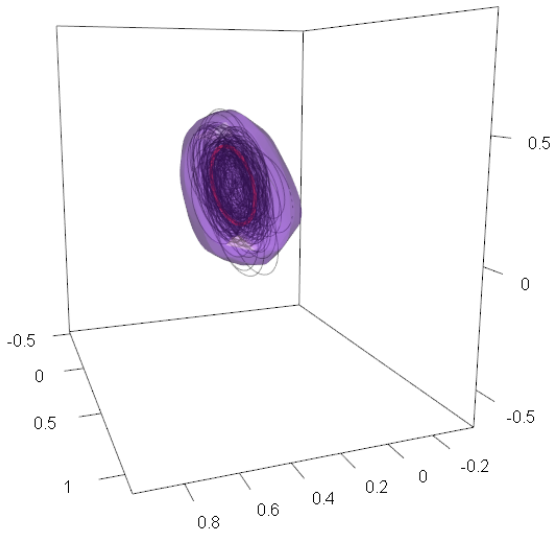

Figure 9.5: Sample Fungible Weights from $n = 400$, $\rho_{X_1X_2} = 0.8$, $R^2 = 0.3$, $\frac{b_1}{b_2} = 1$

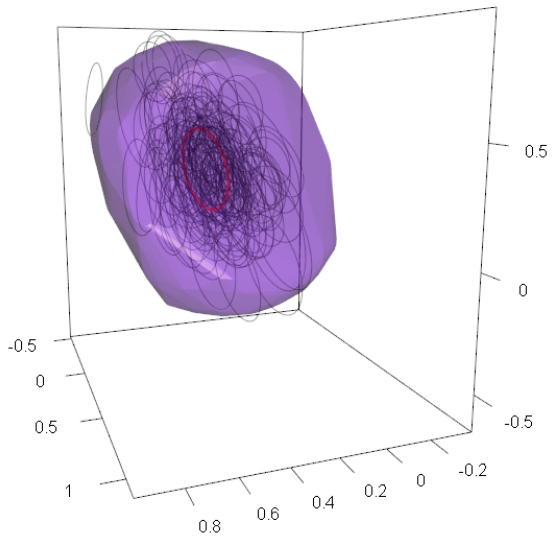

Figure 9.6: Sample Fungible Weights from $n = 40$, $\rho_{X_1X_2} = 0.8$, $R^2 = 0.7$, $\frac{b_1}{b_2} = 1$

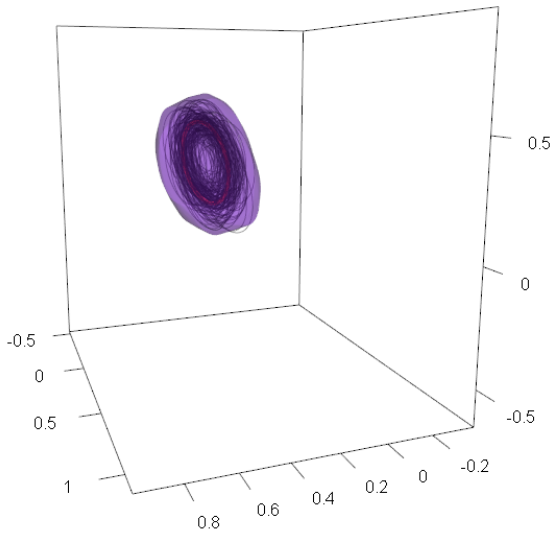

Figure 9.7: Sample Fungible Weights from $n = 400$, $\rho_{X_1X_2} = 0.8$, $R^2 = 0.7$, $\frac{b_1}{b_2} = 1$

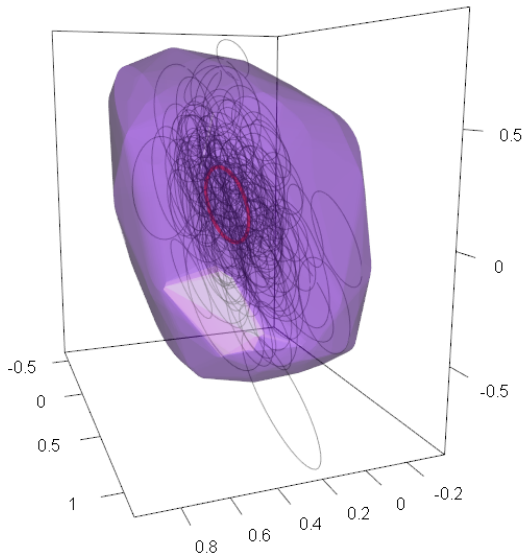

Figure 9.8: Sample Fungible Weights from $n = 40$, $\rho_{X_1X_2} = 0.8$, $R^2 = 0.3$, $\frac{b_1}{b_2} = 3$

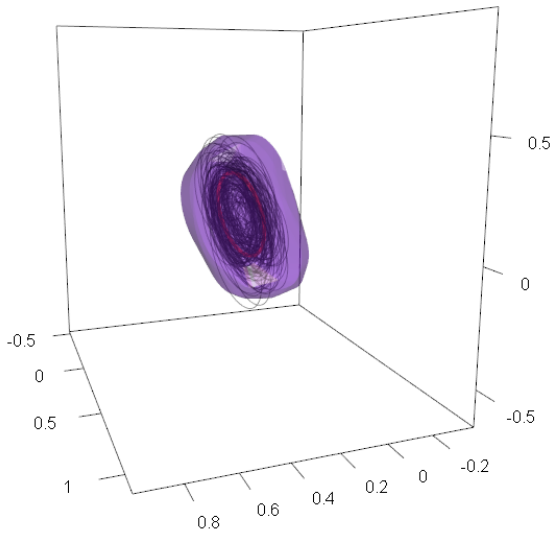

Figure 9.9: Sample Fungible Weights from $n = 400$, $\rho_{X_1X_2} = 0.8$, $R^2 = 0.3$, $\frac{b_1}{b_2} = 3$

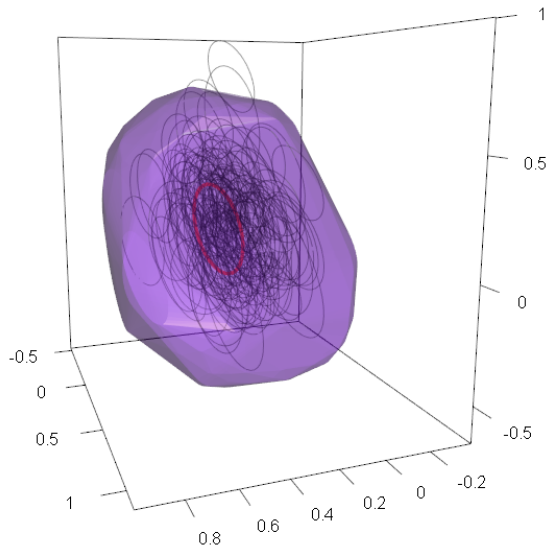

Figure 9.10: Sample Fungible Weights from $n = 40$, $\rho_{X_1X_2} = 0.8$, $R^2 = 0.7$, $\frac{b_1}{b_2} = 3$

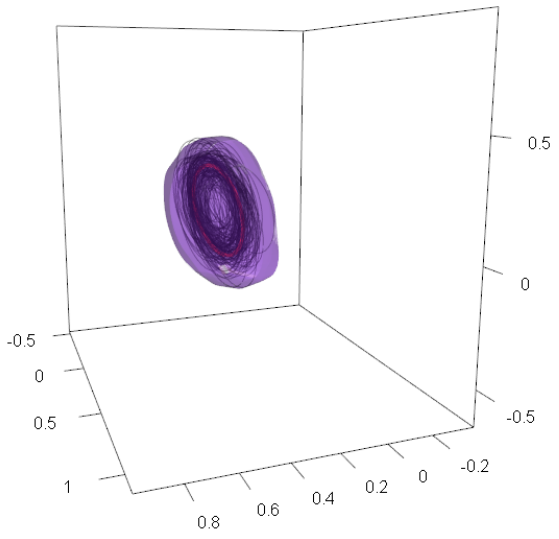

Figure 9.11: Sample Fungible Weights from $n = 400$, $\rho_{X_1X_2} = 0.8$, $R^2 = 0.7$, $\frac{b_1}{b_2} = 3$

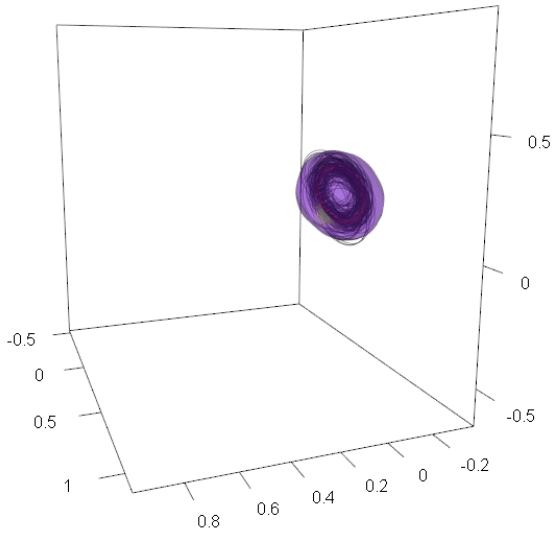

Figure 9.12: Sample Weights from Intx = 0, $n = 400$, $\rho_{X_1X_2} = 0.4$, $R^2 = 0.7$, $\frac{b_1}{b_2} = 3$

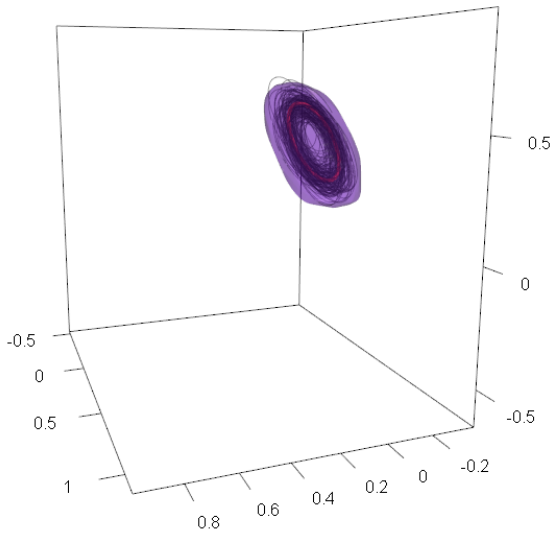

Figure 9.13: Sample Weights from Intx = 0,$n = 400$, $\rho_{X_1X_2} = 0.8$, $R^2 = 0.7$, $\frac{b_1}{b_2} = 1$

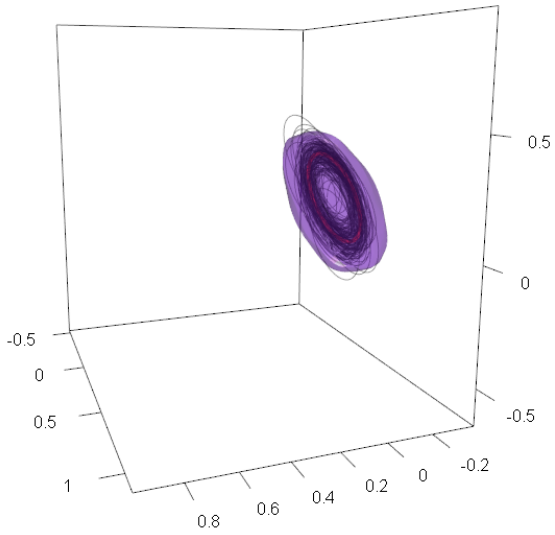

Figure 9.14: Sample Weights from Intx = 0, $n = 400$, $\rho_{X_1X_2} = 0.8$, $R^2 = 0.7$, $\frac{b_1}{b_2} = 3$

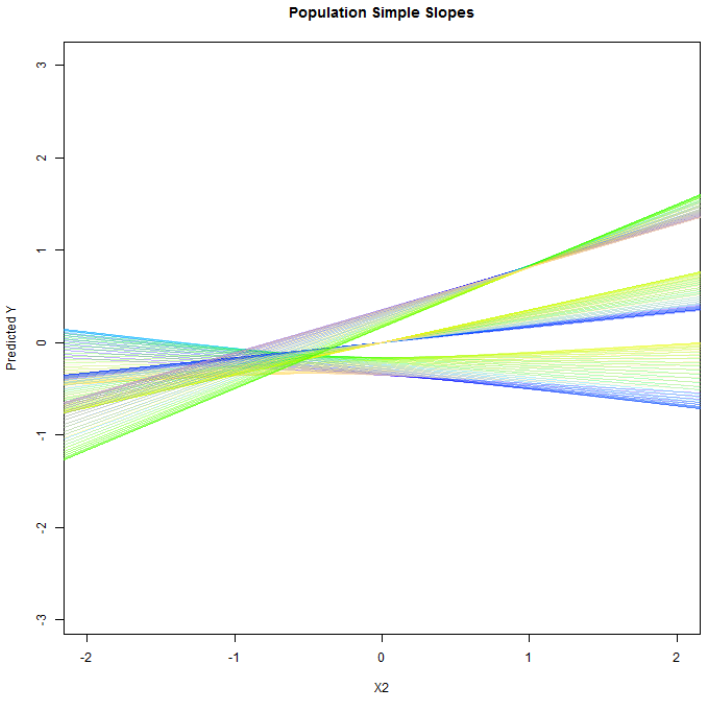

Figure 9.15: Simple Slopes from $\rho_{X_1X_2} = 0.4$, $R^2 = 0.3$, $\frac{b_1}{b_2} = 1$

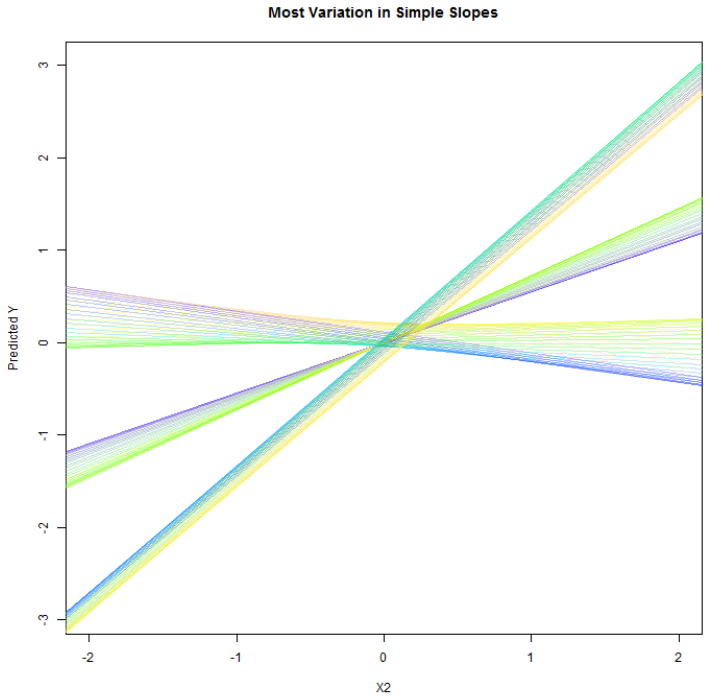

Figure 9.16: Simple Slopes from n = 40, $\rho_{X_1X_2} = 0.4$, $R^2 = 0.3$, $\frac{b_1}{b_2} = 1$

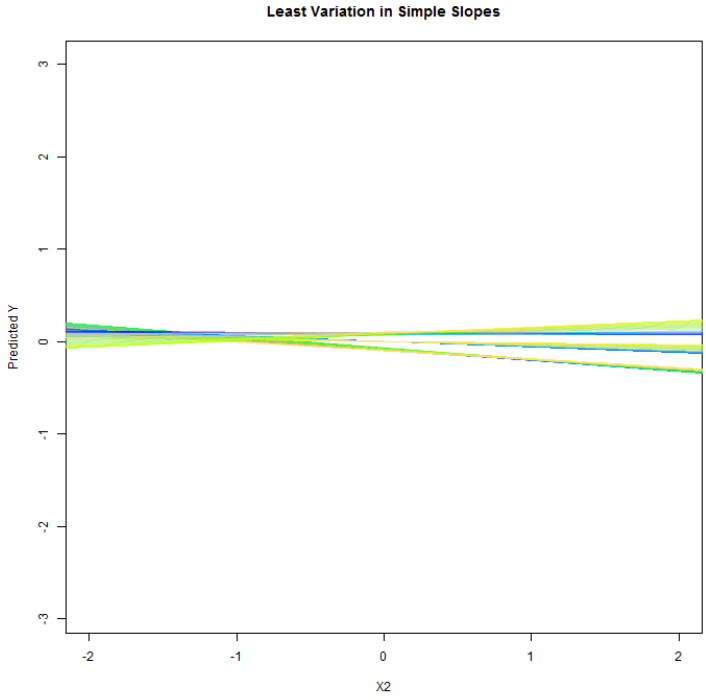

Figure 9.17: Simple Slopes from n = 40, $\rho_{X_1X_2} = 0.4$, $R^2 = 0.3$, $\frac{b_1}{b_2} = 1$

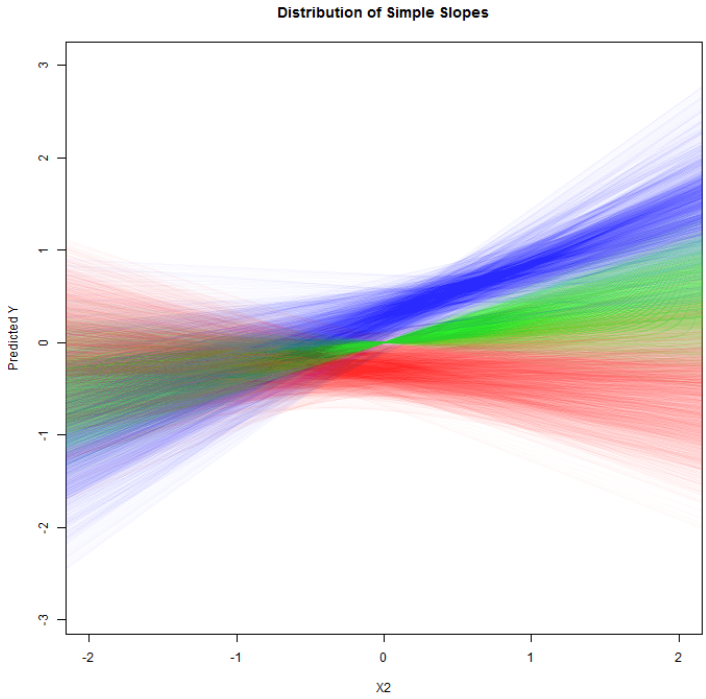

Figure 9.18: Simple Slopes from n = 40, $\rho_{X_1X_2} = 0.4$, $R^2 = 0.3$, $\frac{b_1}{b_2} = 1$

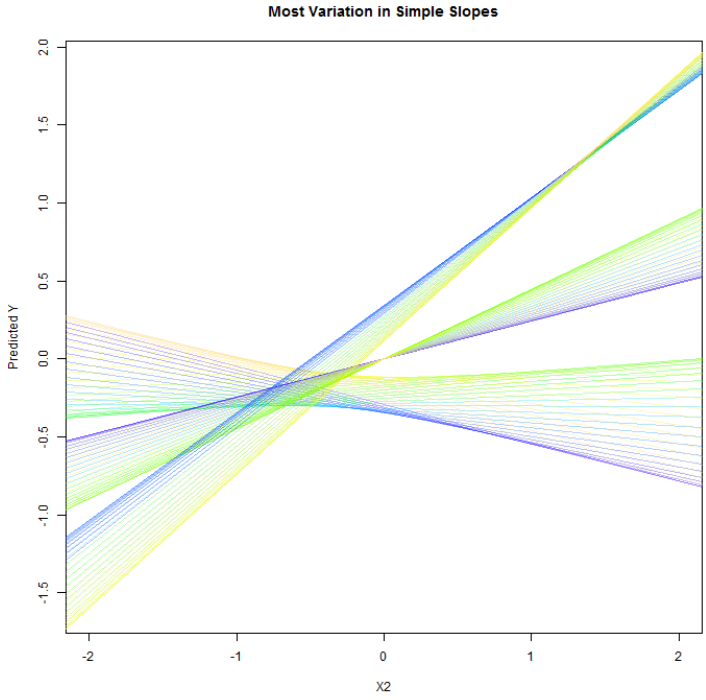

Figure 9.19: Simple Slopes from n = 400, $\rho_{X_1X_2} = 0.4$, $R^2 = 0.3$, $\frac{b_1}{b_2} = 1$

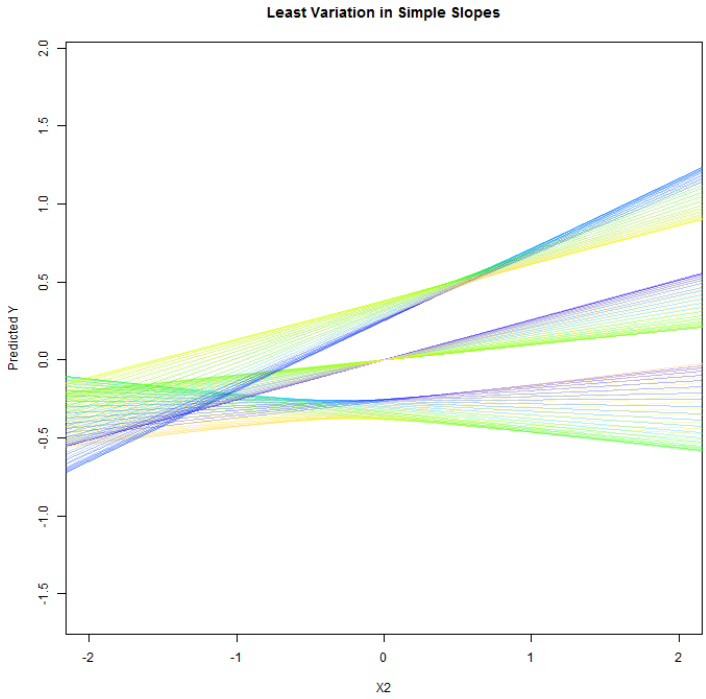

Figure 9.20: Simple Slopes from n = 400, $\rho_{X_1X_2} = 0.4$, $R^2 = 0.3$, $\frac{b_1}{b_2} = 1$

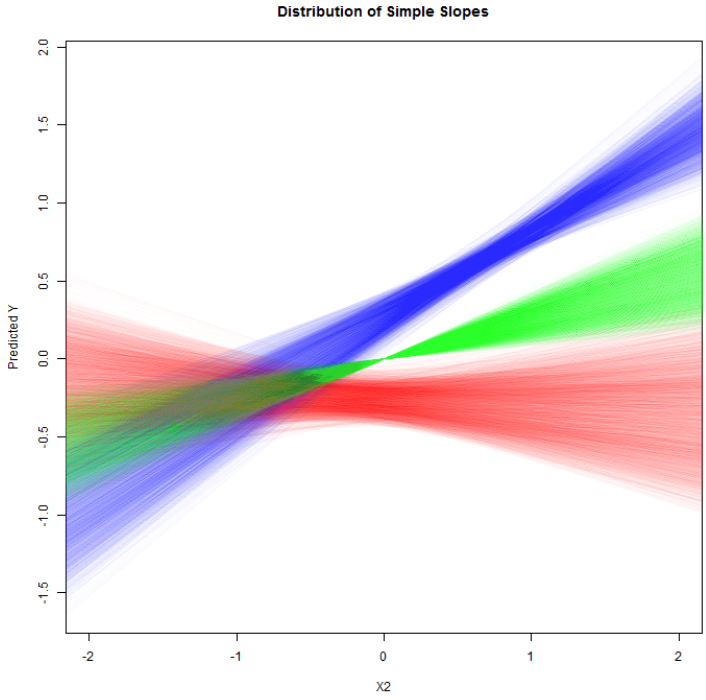

Figure 9.21: Simple Slopes from n = 400, $\rho_{X_1X_2} = 0.4$, $R^2 = 0.3$, $\frac{b_1}{b_2} = 1$

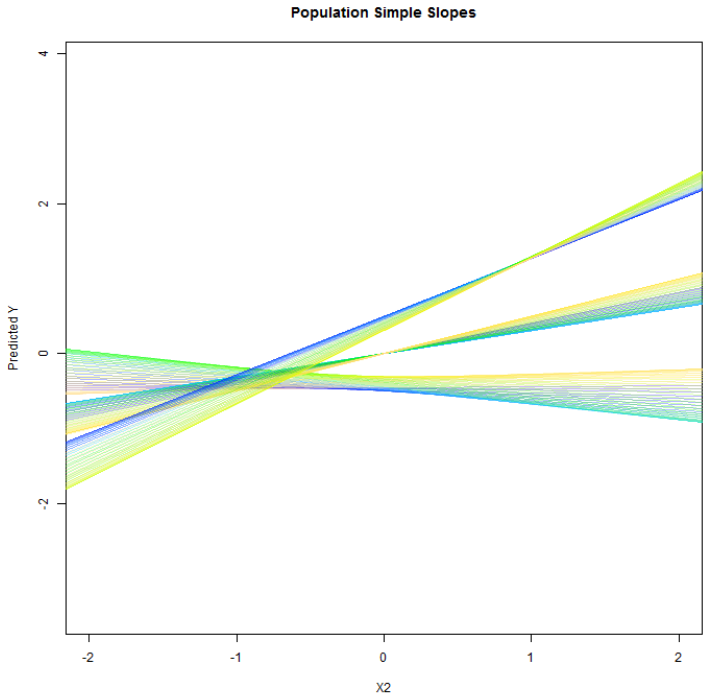

Figure 9.22: Simple Slopes from $\rho_{X_1X_2} = 0.4$, $R^2 = 0.7$, $\frac{b_1}{b_2} = 1$

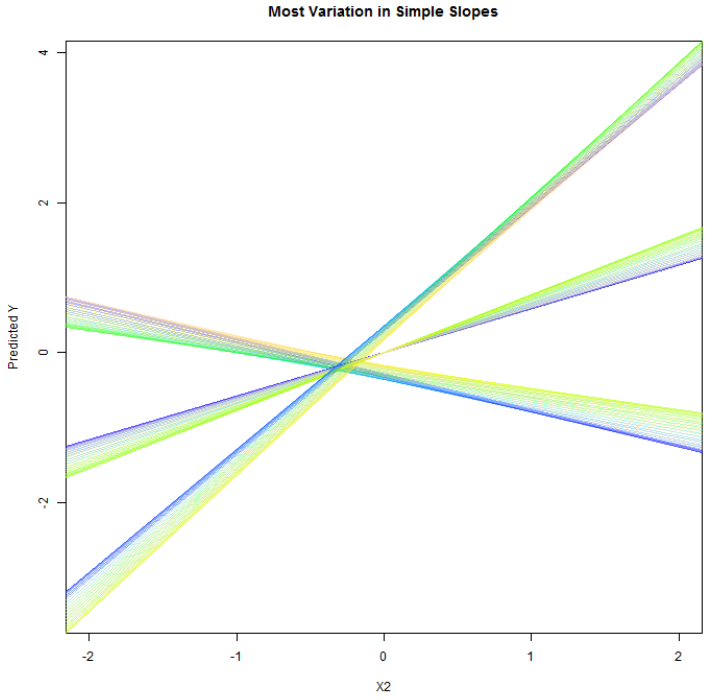

Figure 9.23: Simple Slopes from n = 40, $\rho_{X_1X_2} = 0.4$, $R^2 = 0.7$, $\frac{b_1}{b_2} = 1$

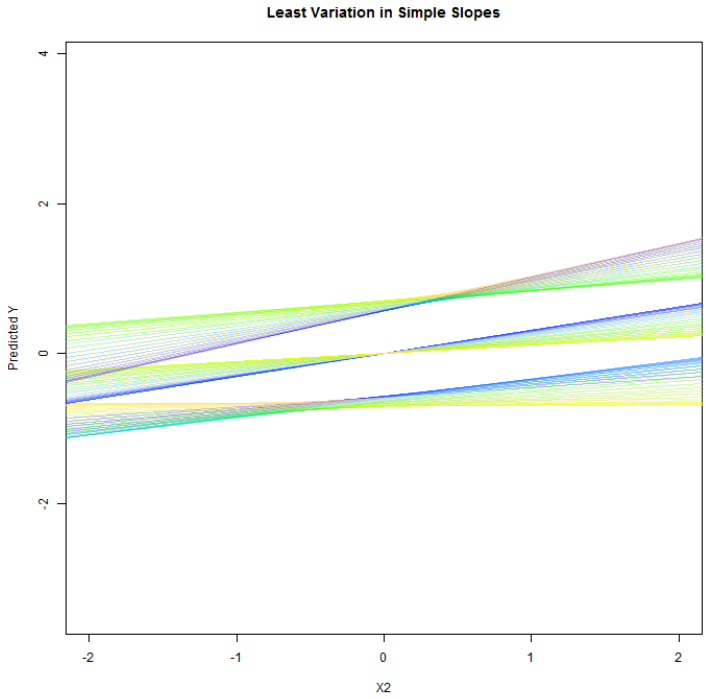

Figure 9.24: Simple Slopes from n = 40, $\rho_{X_1X_2} = 0.4$, $R^2 = 0.7$, $\frac{b_1}{b_2} = 1$

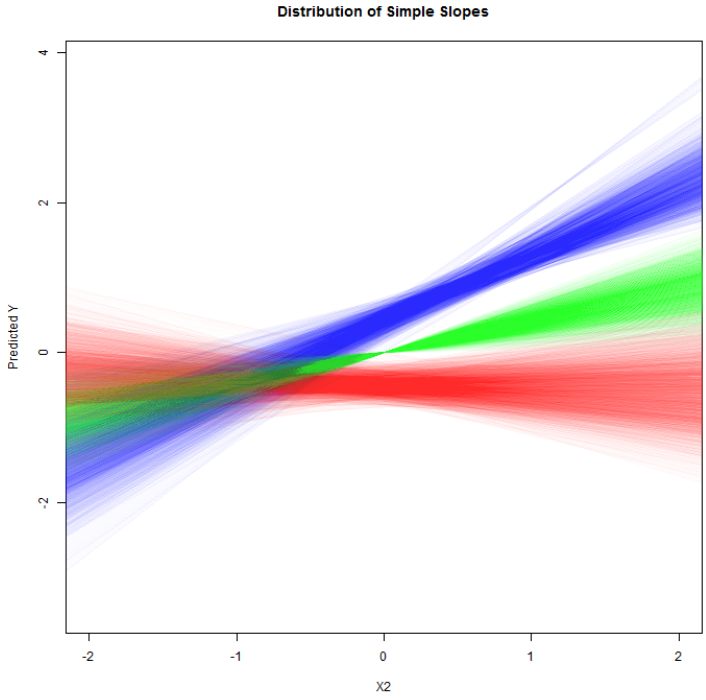

Figure 9.25: Simple Slopes from n = 40, $\rho_{X_1X_2} = 0.4$, $R^2 = 0.7$, $\frac{b_1}{b_2} = 1$

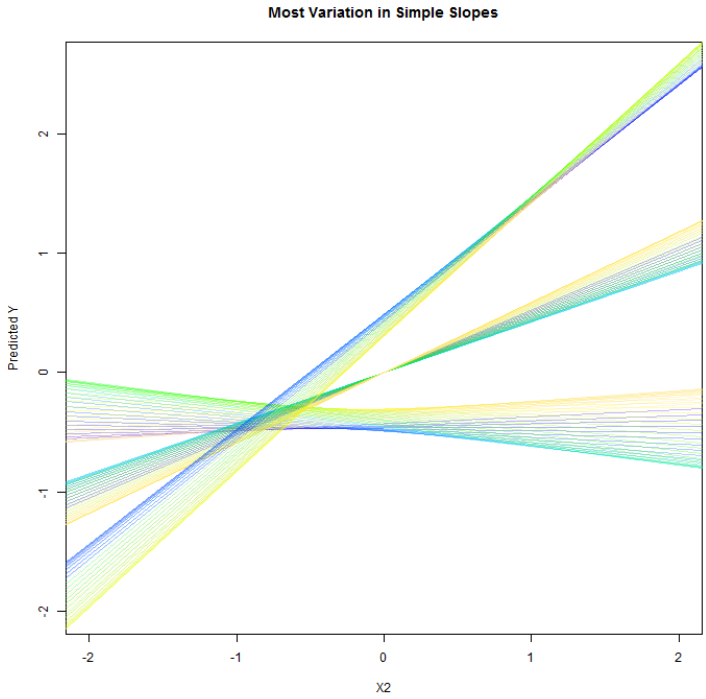

Figure 9.26: Simple Slopes from n = 400, $\rho_{X_1X_2} = 0.4$, $R^2 = 0.7$, $\frac{b_1}{b_2} = 1$

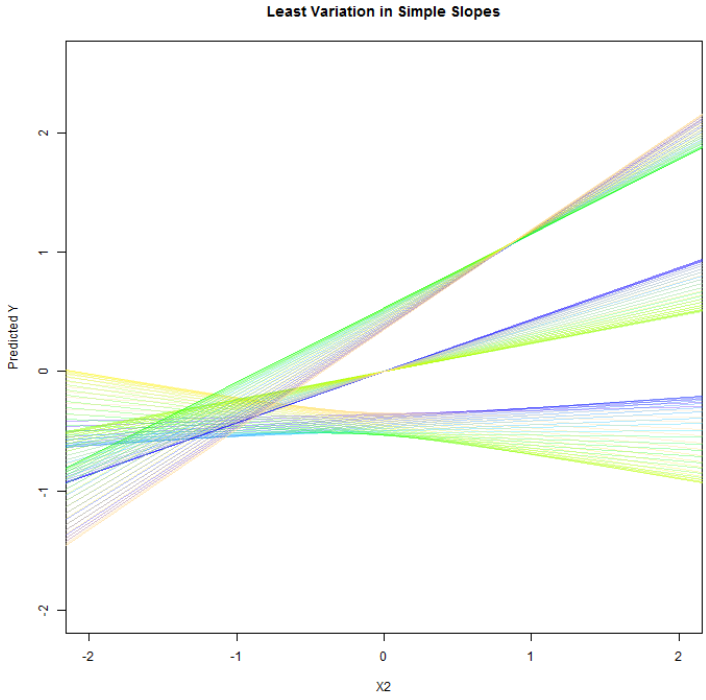

Figure 9.27: Simple Slopes from n = 400, $\rho_{X_1X_2} = 0.4$, $R^2 = 0.7$, $\frac{b_1}{b_2} = 1$

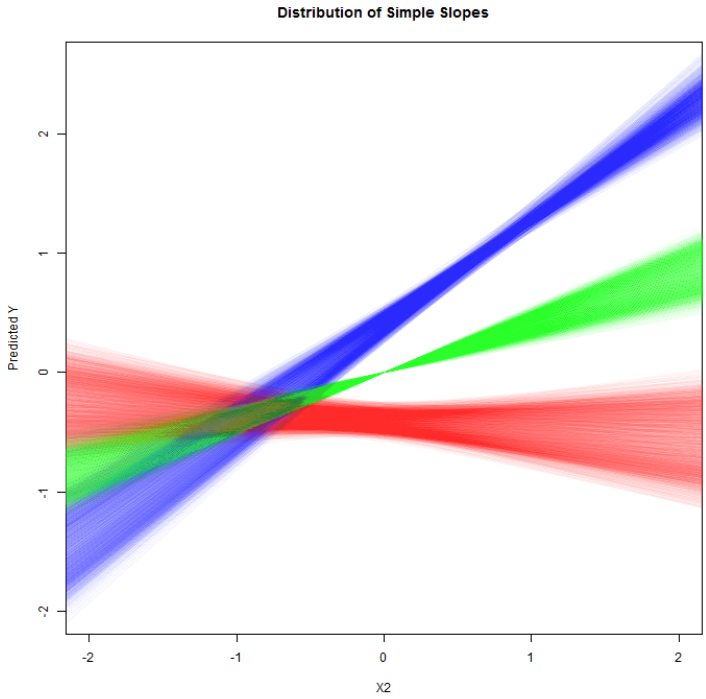

Figure 9.28: Simple Slopes from n = 400, $\rho_{X_1X_2} = 0.4$, $R^2 = 0.7$, $\frac{b_1}{b_2} = 1$

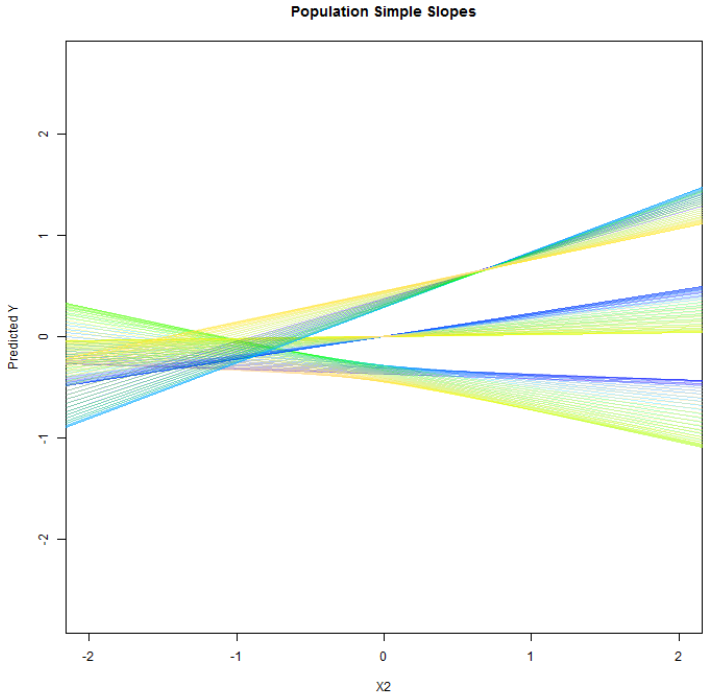

Figure 9.29: Simple Slopes from $\rho_{X_1X_2} = 0.4$, $R^2 = 0.3$, $\frac{b_1}{b_2} = 3$

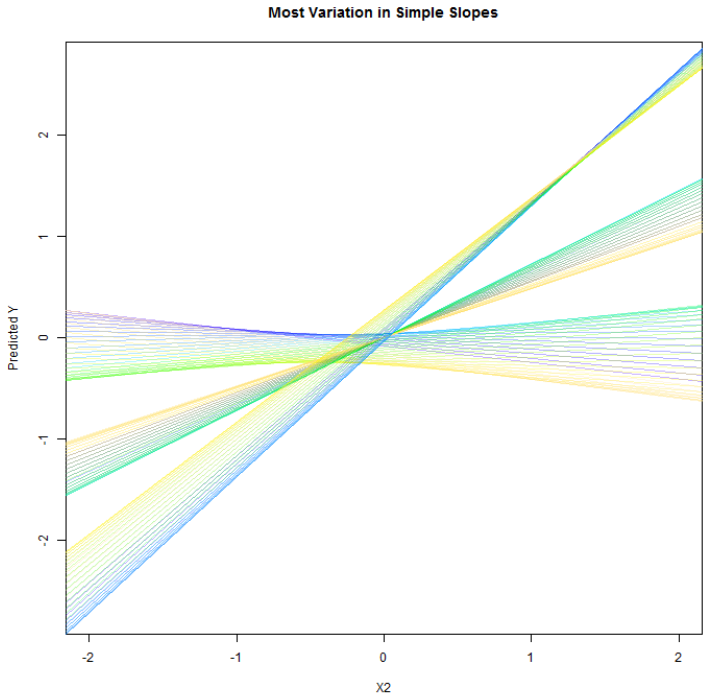

Figure 9.30: Simple Slopes from n = 40, $\rho_{X_1X_2} = 0.4$, $R^2 = 0.3$, $\frac{b_1}{b_2} = 3$

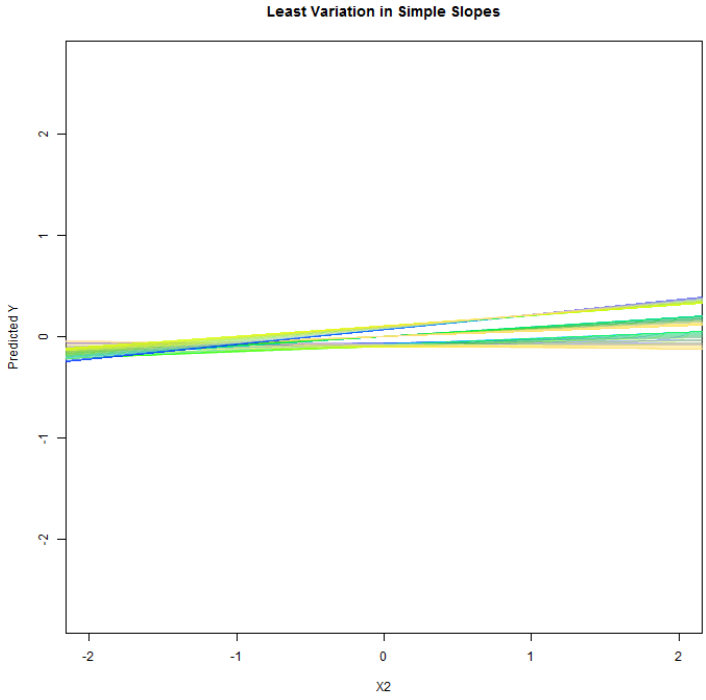

Figure 9.31: Simple Slopes from n = 40, $\rho_{X_1X_2} = 0.4$, $R^2 = 0.3$, $\frac{b_1}{b_2} = 3$

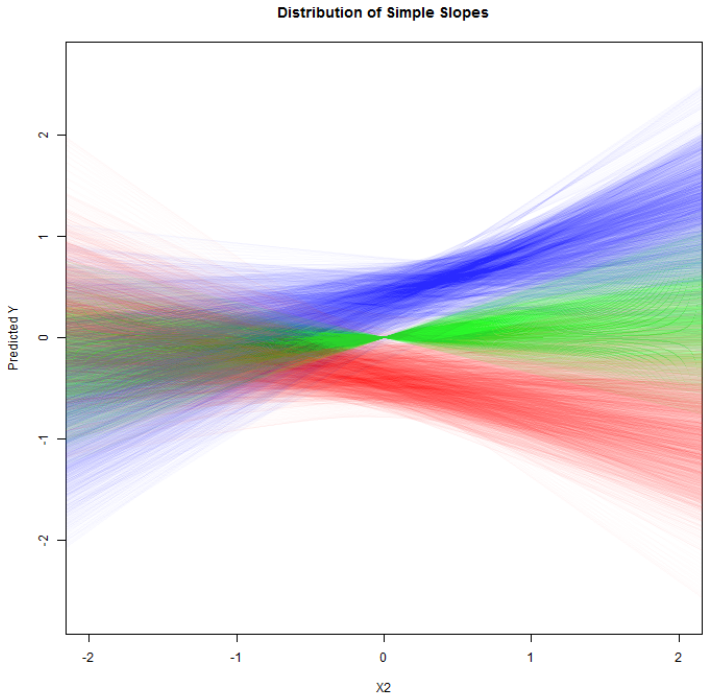

Figure 9.32: Simple Slopes from n = 40, $\rho_{X_1X_2} = 0.4$, $R^2 = 0.3$, $\frac{b_1}{b_2} = 3$

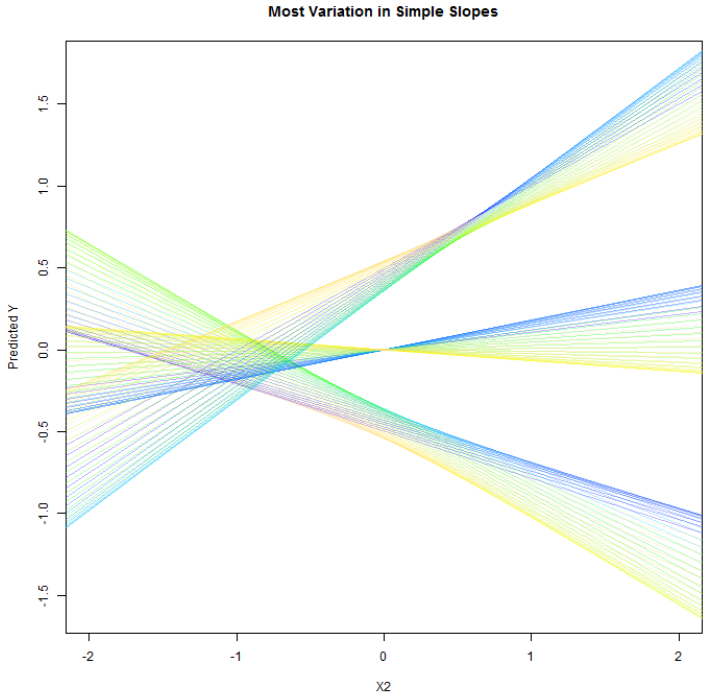

Figure 9.33: Simple Slopes from n = 400, $\rho_{X_1X_2} = 0.4$, $R^2 = 0.3$, $\frac{b_1}{b_2} = 3$

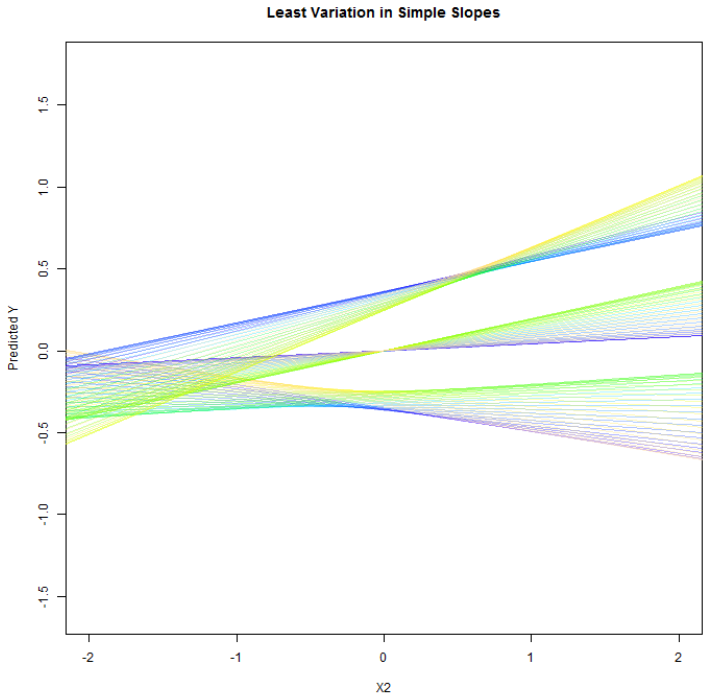

Figure 9.34: Simple Slopes from n = 400, $\rho_{X_1X_2} = 0.4$, $R^2 = 0.3$, $\frac{b_1}{b_2} = 3$

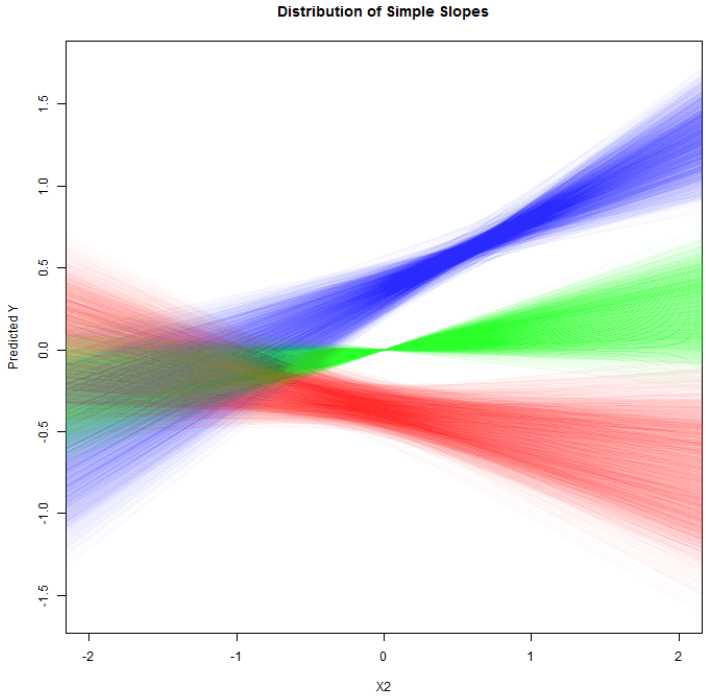

Figure 9.35: Simple Slopes from n = 400, $\rho_{X_1X_2} = 0.4$, $R^2 = 0.3$, $\frac{b_1}{b_2} = 3$

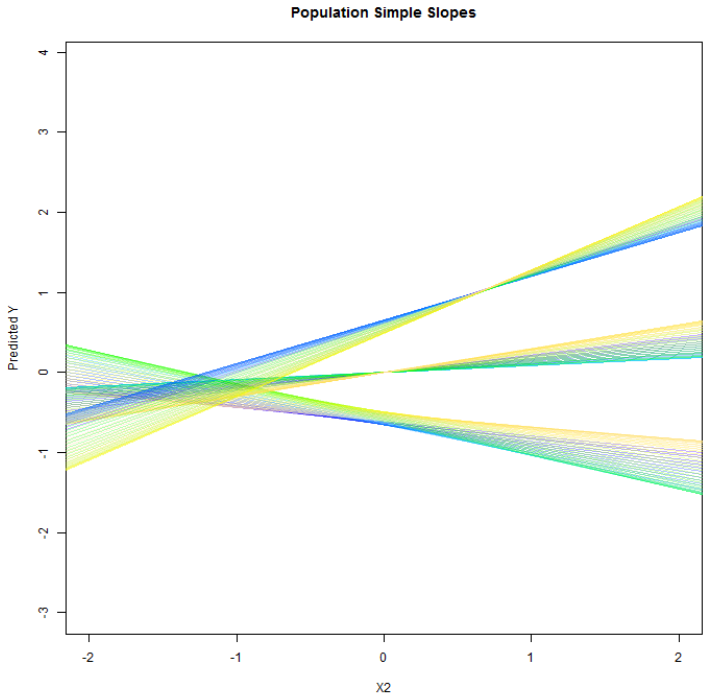

Figure 9.36: Simple Slopes from $\rho_{X_1X_2} = 0.4$, $R^2 = 0.7$, $\frac{b_1}{b_2} = 3$

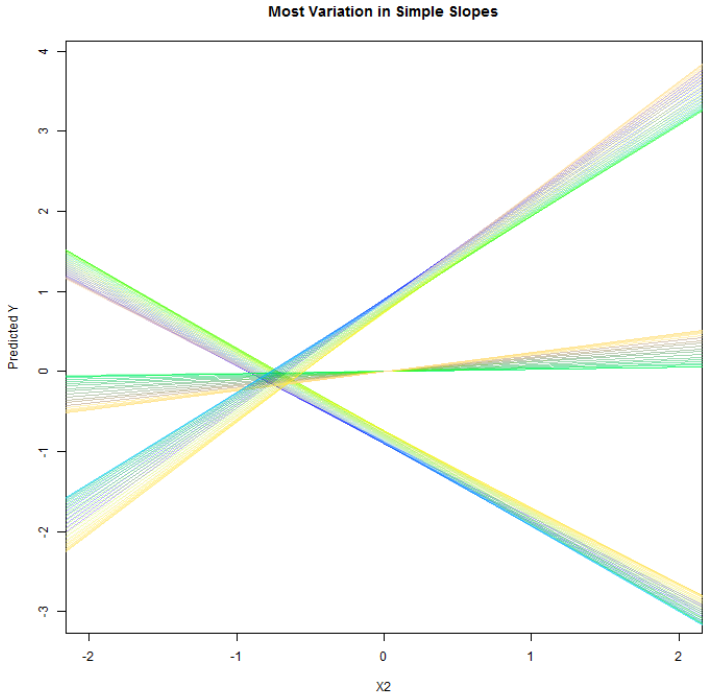

Figure 9.37: Simple Slopes from n = 40, $\rho_{X_1X_2} = 0.4$, $R^2 = 0.7$, $\frac{b_1}{b_2} = 3$

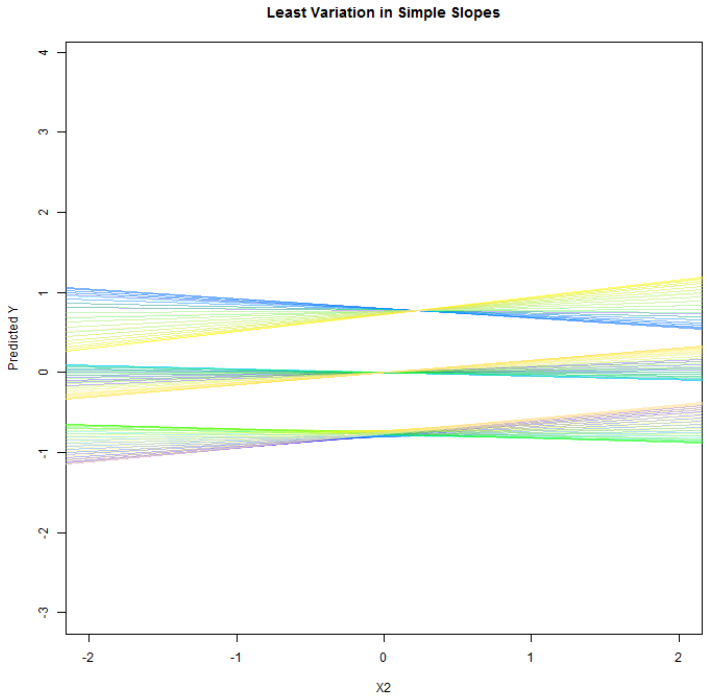

Figure 9.38: Simple Slopes from n = 40, $\rho_{X_1X_2} = 0.4$, $R^2 = 0.7$, $\frac{b_1}{b_2} = 3$

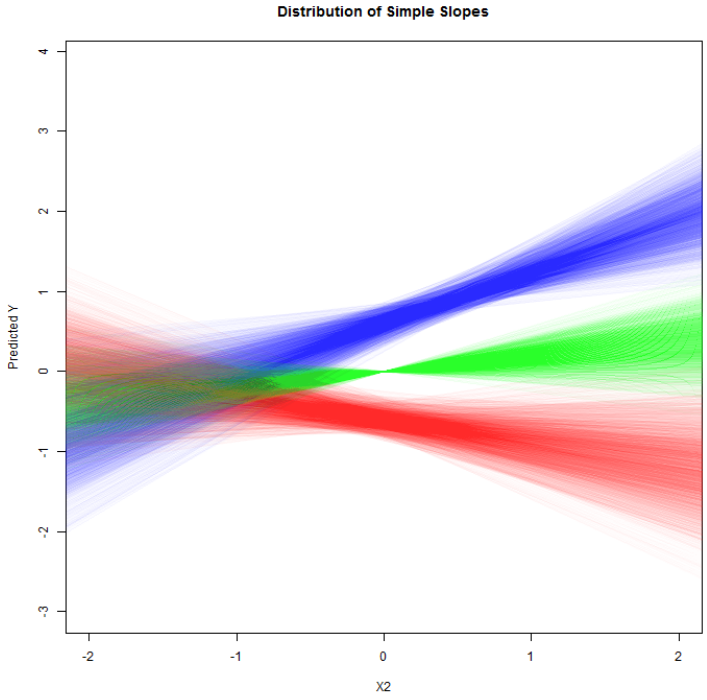

Figure 9.39: Simple Slopes from n = 40, $\rho_{X_1X_2} = 0.4$, $R^2 = 0.7$, $\frac{b_1}{b_2} = 3$

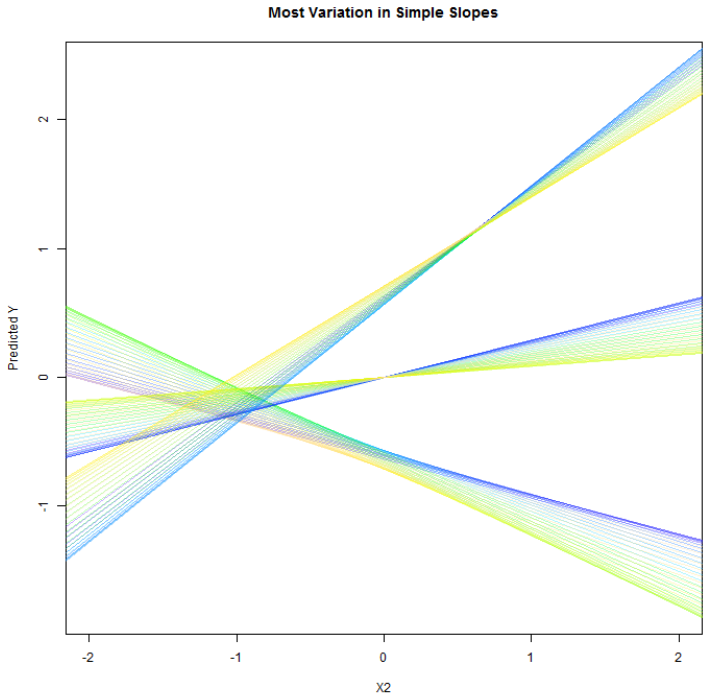

Figure 9.40: Simple Slopes from n = 400, $\rho_{X_1X_2} = 0.4$, $R^2 = 0.7$, $\frac{b_1}{b_2} = 3$

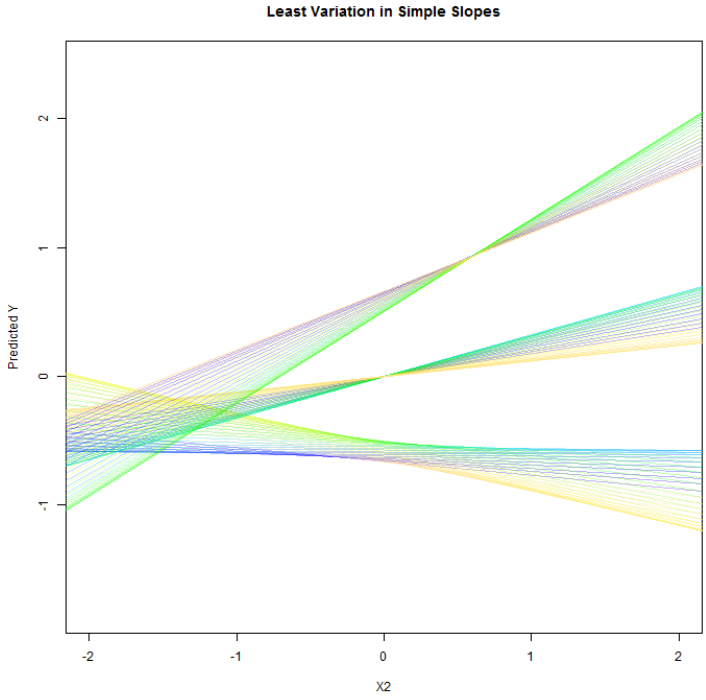

Figure 9.41: Simple Slopes from n = 400, $\rho_{X_1X_2} = 0.4$, $R^2 = 0.7$, $\frac{b_1}{b_2} = 3$

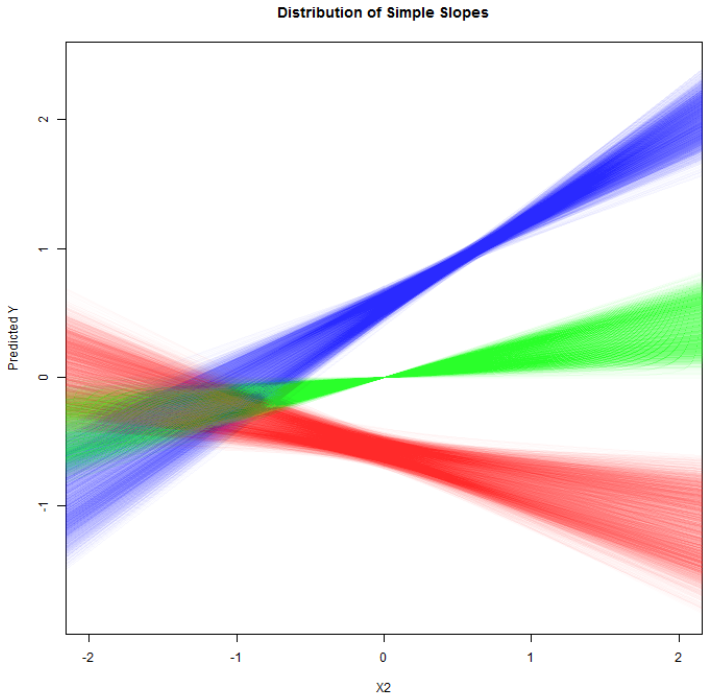

Figure 9.42: Simple Slopes from n = 400, $\rho_{X_1X_2} = 0.4$, $R^2 = 0.7$, $\frac{b_1}{b_2} = 3$

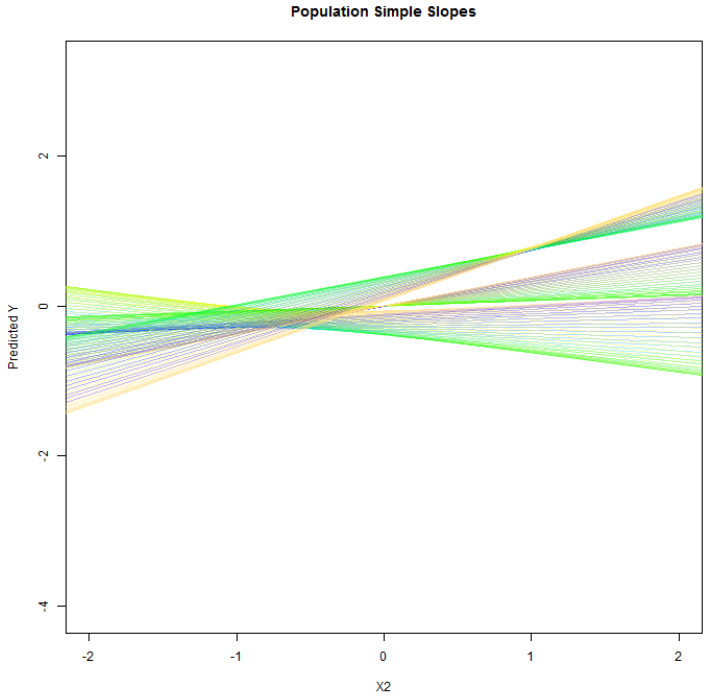

Figure 9.43: Simple Slopes from $\rho_{X_1X_2} = 0.8$, $R^2 = 0.3$, $\frac{b_1}{b_2} = 1$

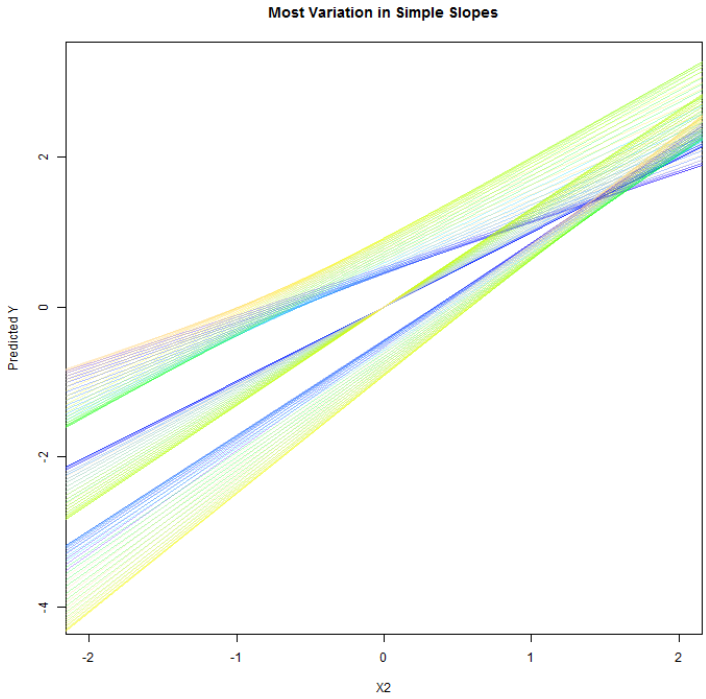

Figure 9.44: Simple Slopes from n = 40, $\rho_{X_1X_2} = 0.8$, $R^2 = 0.3$, $\frac{b_1}{b_2} = 1$

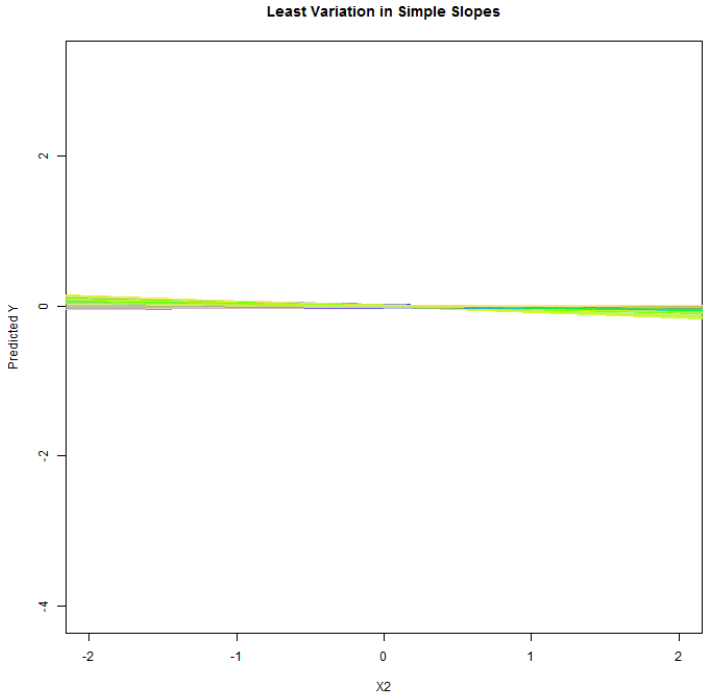

Figure 9.45: Simple Slopes from n = 40, $\rho_{X_1X_2} = 0.8$, $R^2 = 0.3$, $\frac{b_1}{b_2} = 1$

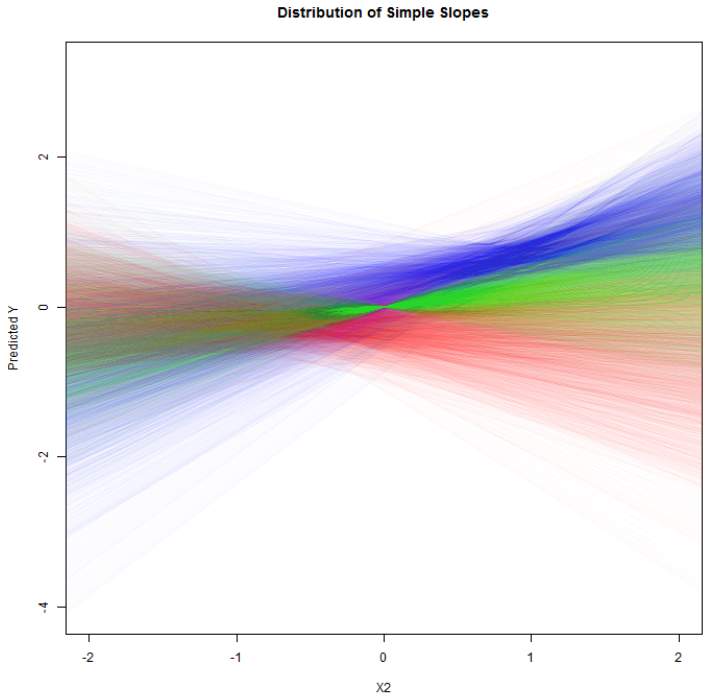

Figure 9.46: Simple Slopes from n = 40, $\rho_{X_1X_2} = 0.8$, $R^2 = 0.3$, $\frac{b_1}{b_2} = 1$

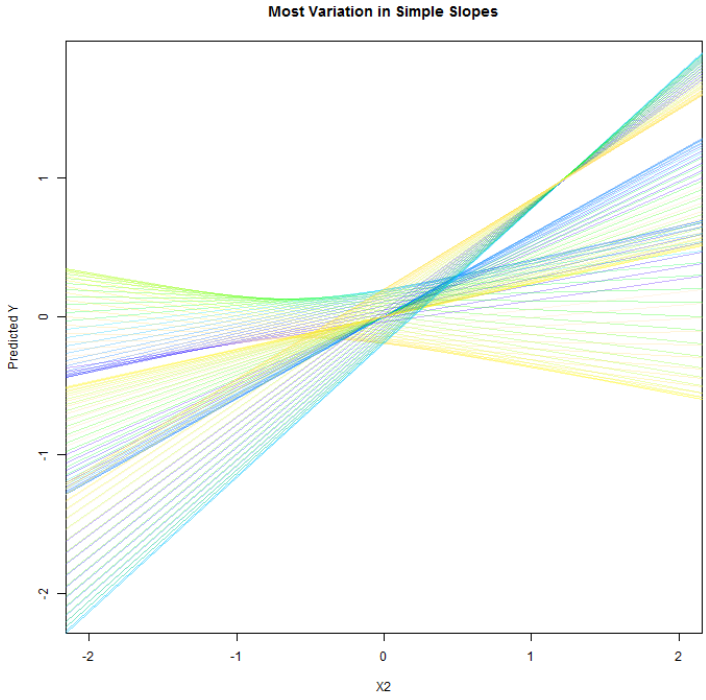

Figure 9.47: Simple Slopes from n = 400, $\rho_{X_1X_2} = 0.8$, $R^2 = 0.3$, $\frac{b_1}{b_2} = 1$

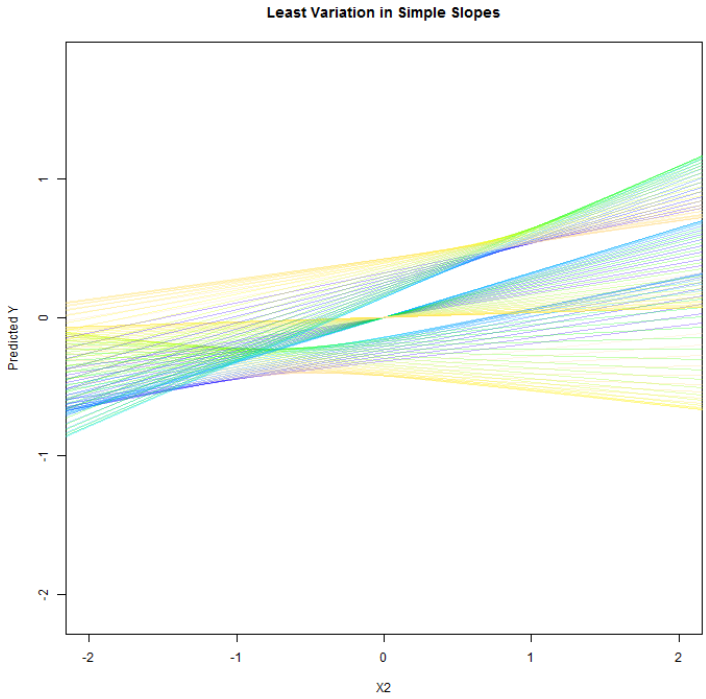

Figure 9.48: Simple Slopes from n = 400, $\rho_{X_1X_2} = 0.8$, $R^2 = 0.3$, $\frac{b_1}{b_2} = 1$

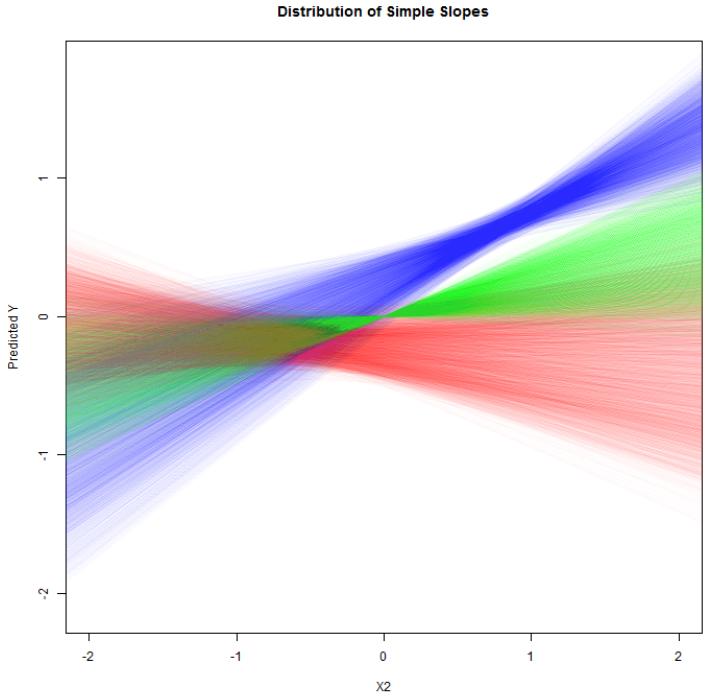

Figure 9.49: Simple Slopes from n = 400, $\rho_{X_1X_2} = 0.8$, $R^2 = 0.3$, $\frac{b_1}{b_2} = 1$

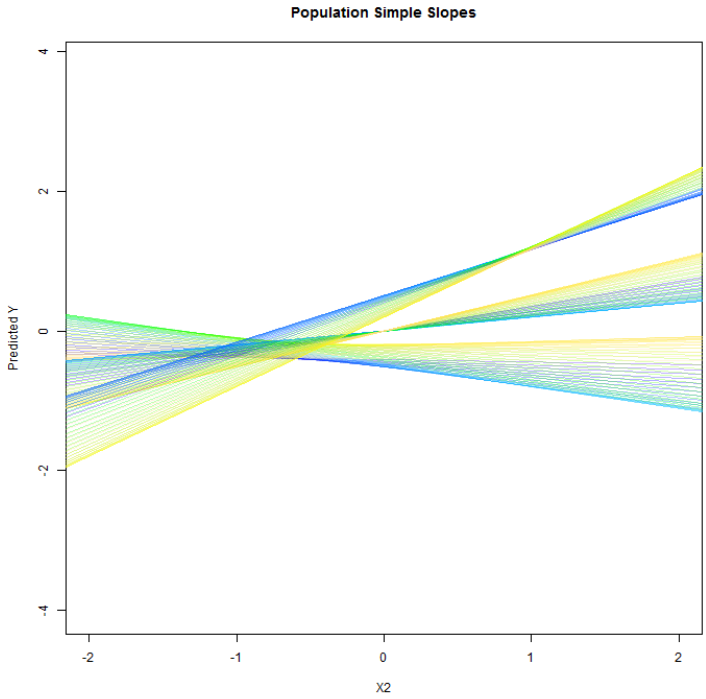

Figure 9.50: Simple Slopes from $\rho_{X_1X_2} = 0.8$, $R^2 = 0.7$, $\frac{b_1}{b_2} = 1$

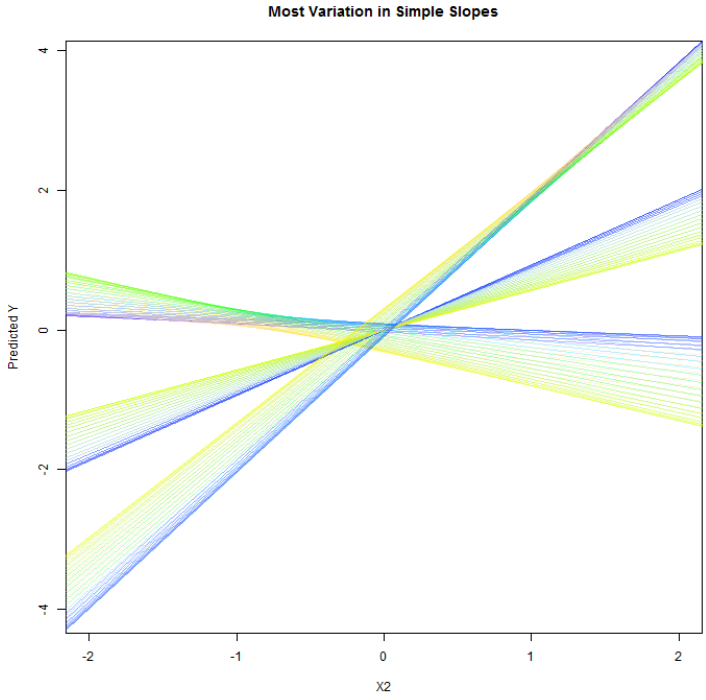

Figure 9.51: Simple Slopes from n = 40, $\rho_{X_1X_2} = 0.8$, $R^2 = 0.7$, $\frac{b_1}{b_2} = 1$

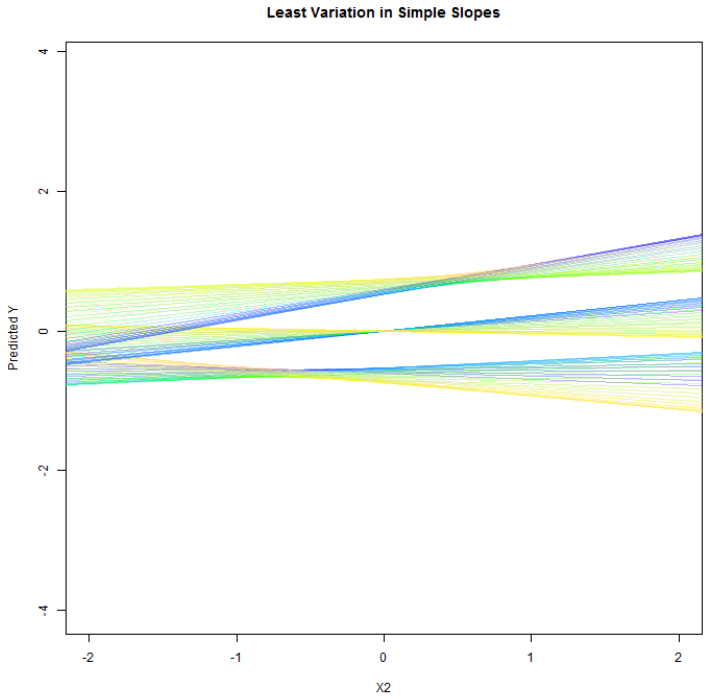

Figure 9.52: Simple Slopes from n = 40, $\rho_{X_1X_2} = 0.8$, $R^2 = 0.7$, $\frac{b_1}{b_2} = 1$

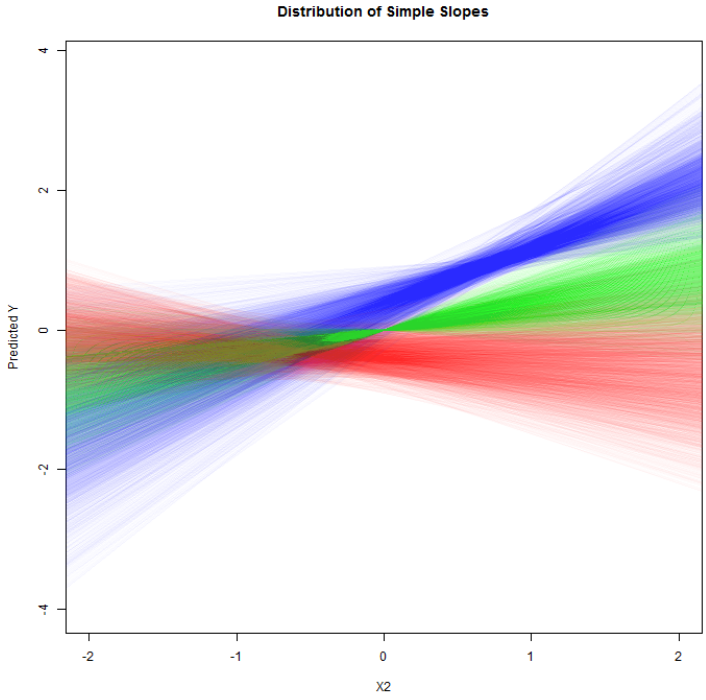

Figure 9.53: Simple Slopes from n =40, $\rho_{X_1X_2} = 0.8$, $R^2 = 0.7$, $\frac{b_1}{b_2} = 1$

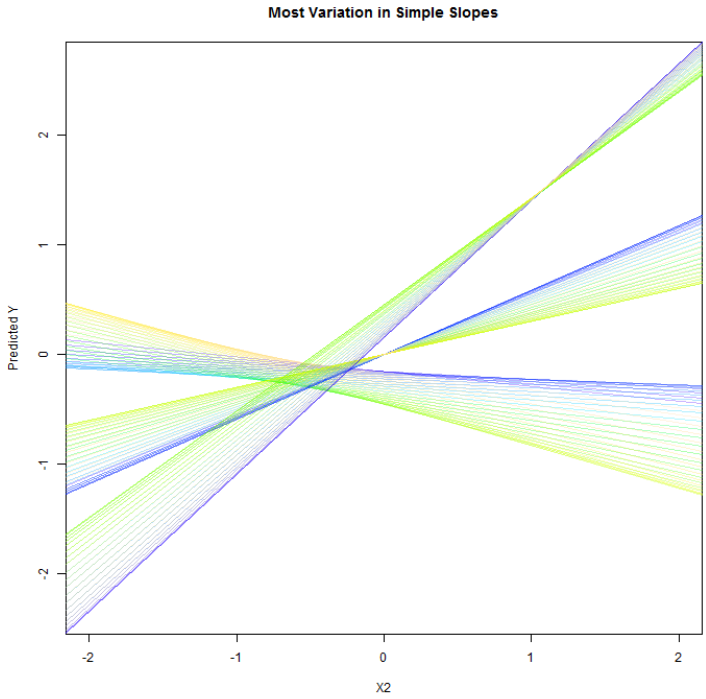

Figure 9.54: Simple Slopes from n = 400, $\rho_{X_1X_2} = 0.8$, $R^2 = 0.7$, $\frac{b_1}{b_2} = 1$

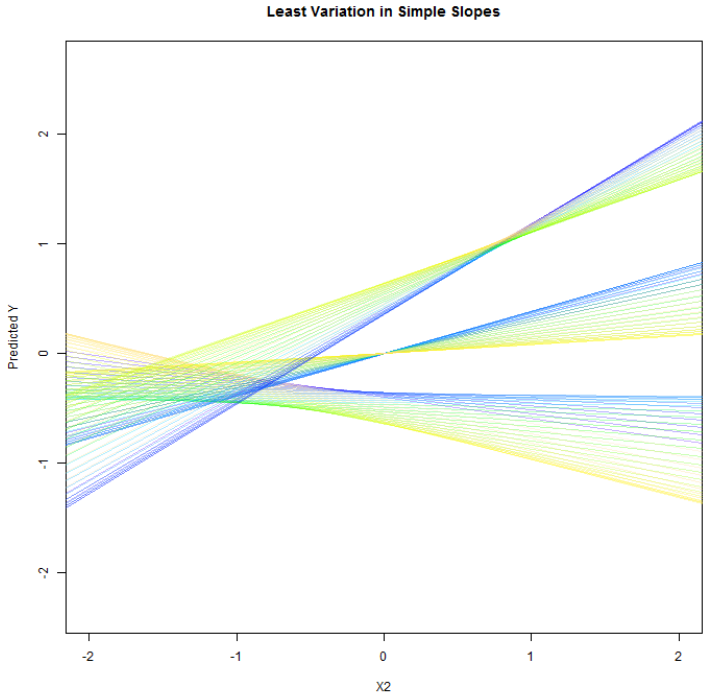

Figure 9.55: Simple Slopes from n = 400, $\rho_{X_1X_2} = 0.8$, $R^2 = 0.7$, $\frac{b_1}{b_2} = 1$

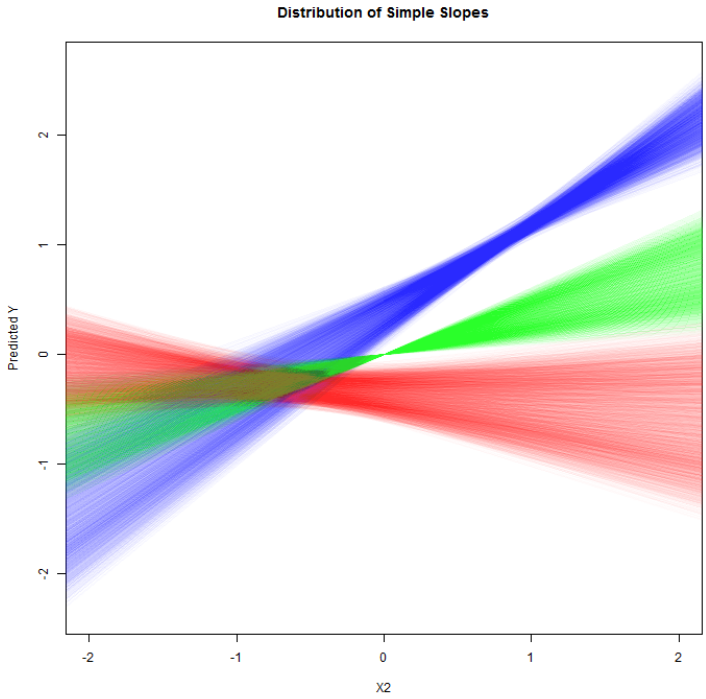

Figure 9.56: Simple Slopes from n = 400, $\rho_{X_1X_2} = 0.8$, $R^2 = 0.7$, $\frac{b_1}{b_2} = 1$

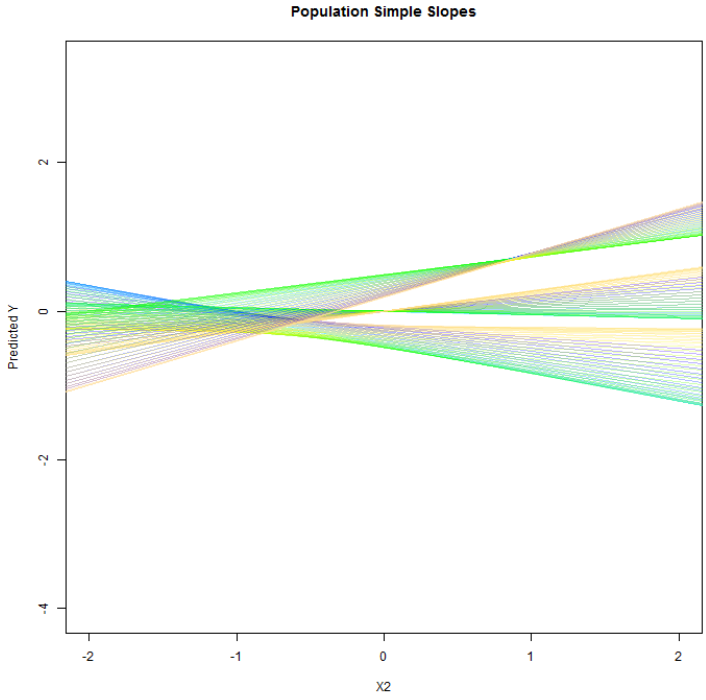

Figure 9.57: Simple Slopes from $\rho_{X_1X_2} = 0.8$, $R^2 = 0.3$, $\frac{b_1}{b_2} = 3$

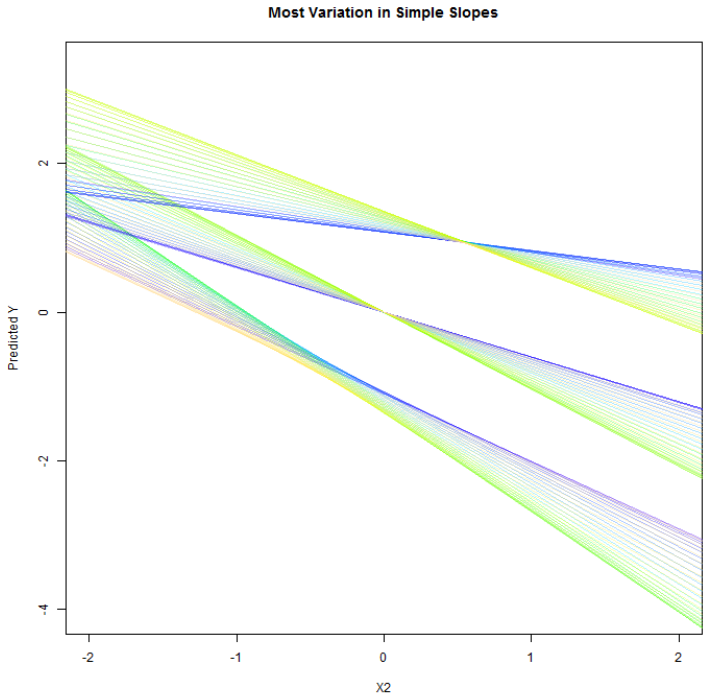

Figure 9.58: Simple Slopes from n = 40, $\rho_{X_1X_2} = 0.8$, $R^2 = 0.3$, $\frac{b_1}{b_2} = 3$

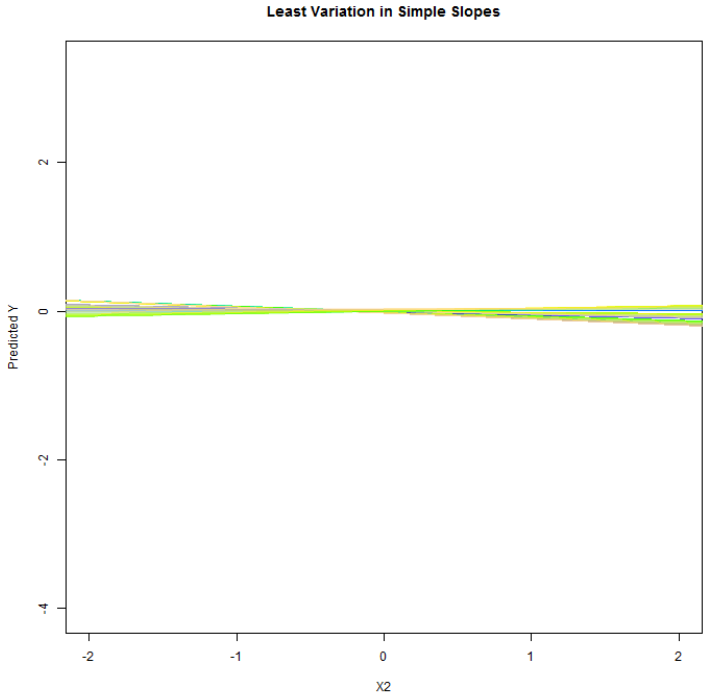

Figure 9.59: Simple Slopes from n = 40, $\rho_{X_1X_2} = 0.8$, $R^2 = 0.3$, $\frac{b_1}{b_2} = 3$

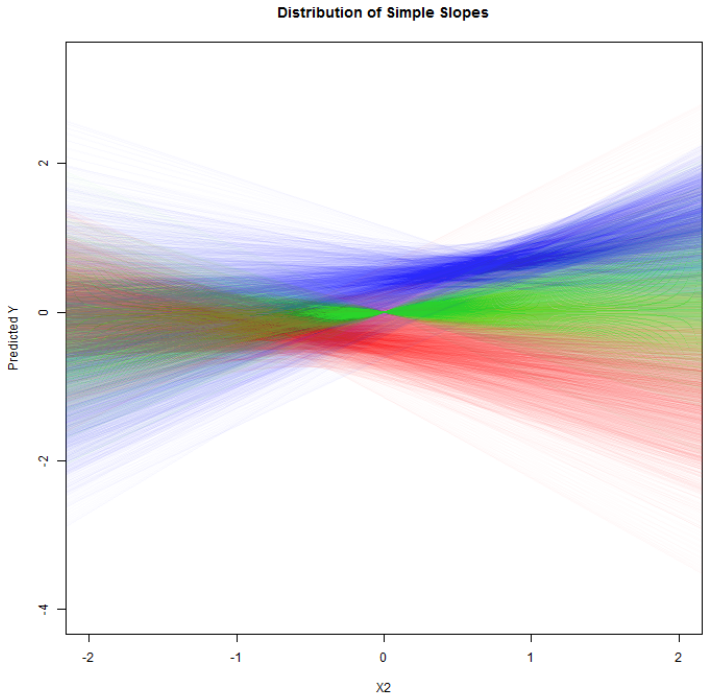

Figure 9.60: Simple Slopes from n = 40, $\rho_{X_1X_2} = 0.8$, $R^2 = 0.3$, $\frac{b_1}{b_2} = 3$

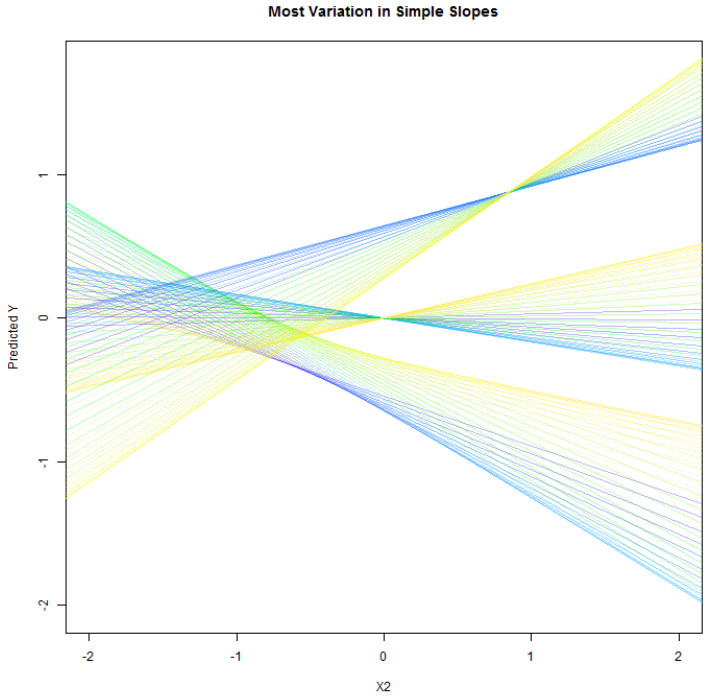

Figure 9.61: Simple Slopes from n = 400, $\rho_{X_1X_2} = 0.8$, $R^2 = 0.3$, $\frac{b_1}{b_2} = 3$

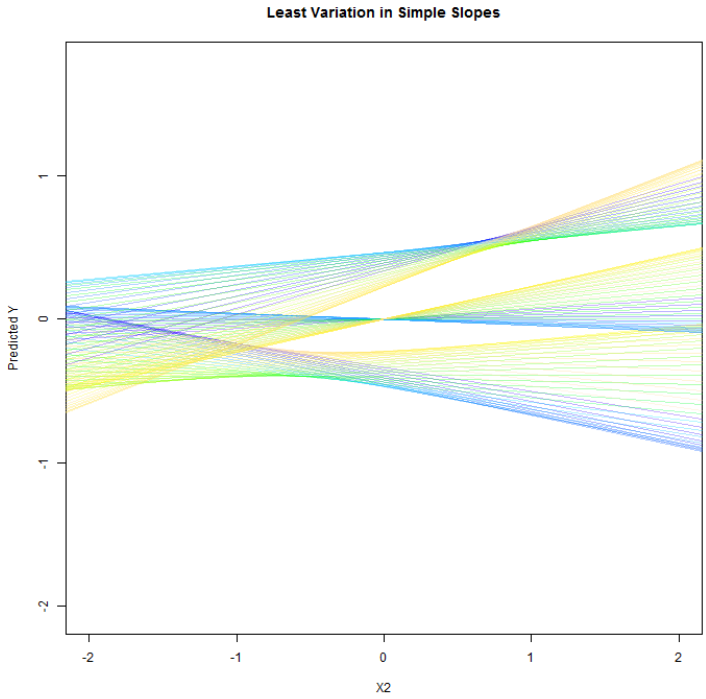

Figure 9.62: Simple Slopes from n = 400, $\rho_{X_1X_2} = 0.8$, $R^2 = 0.3$, $\frac{b_1}{b_2} = 3$

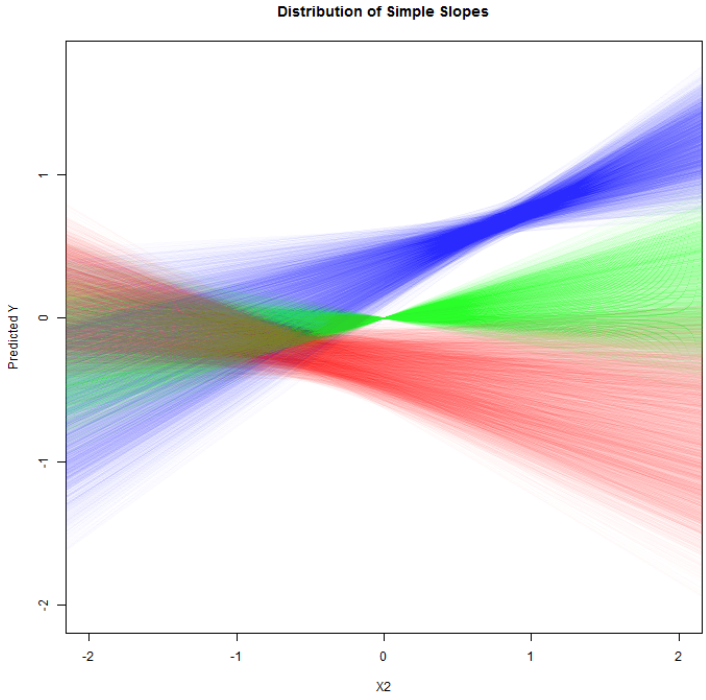

Figure 9.63: Simple Slopes from n = 400, $\rho_{X_1X_2} = 0.8$, $R^2 = 0.3$, $\frac{b_1}{b_2} = 3$

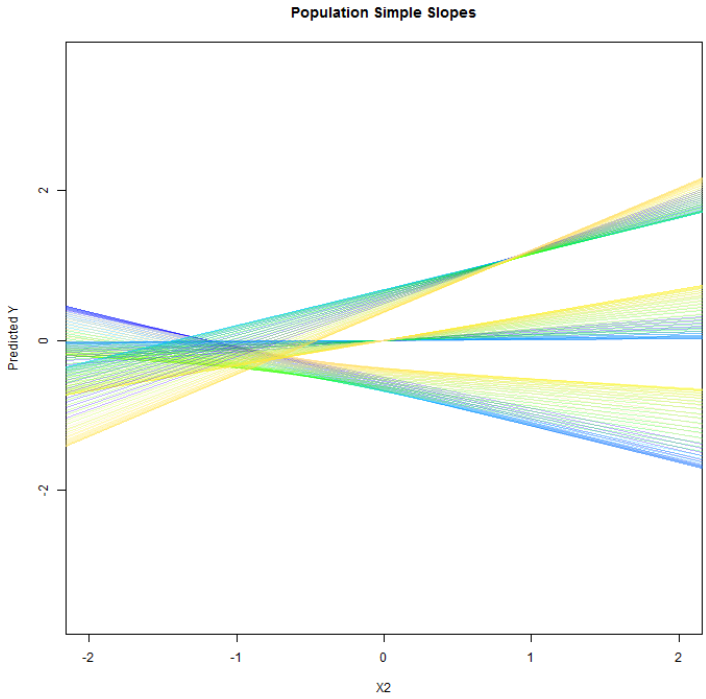

Figure 9.64: Simple Slopes from $\rho_{X_1X_2} = 0.8$, $R^2 = 0.7$, $\frac{b_1}{b_2} = 3$

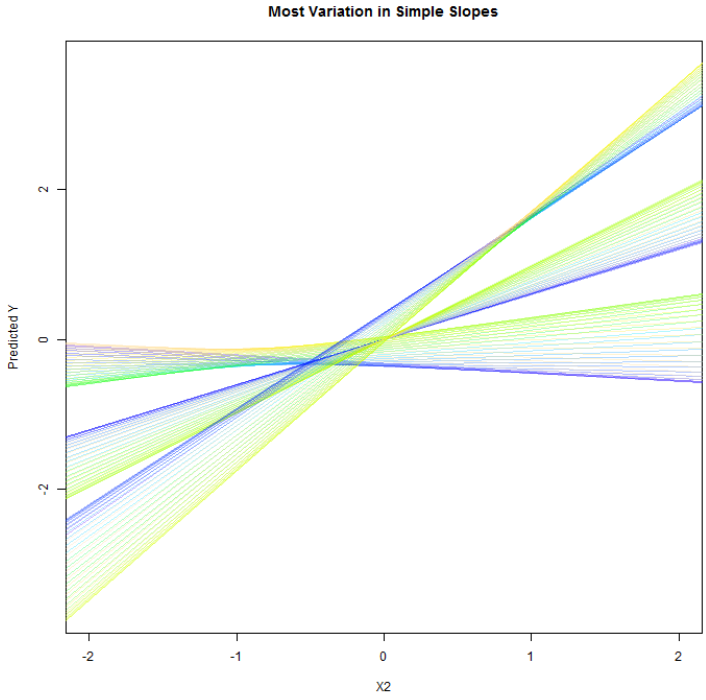

Figure 9.65: Simple Slopes from n = 40, $\rho_{X_1X_2} = 0.8$, $R^2 = 0.7$, $\frac{b_1}{b_2} = 3$

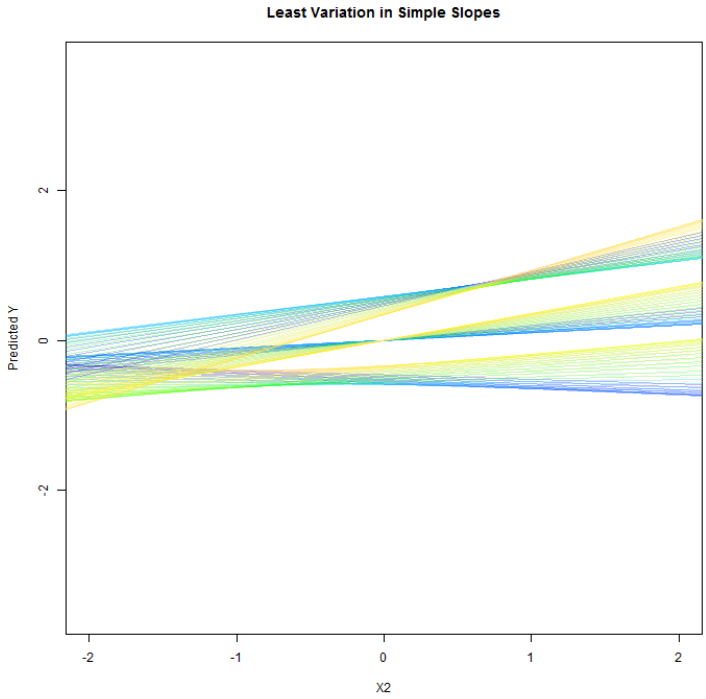

Figure 9.66: Simple Slopes from n = 40, $\rho_{X_1X_2} = 0.8$, $R^2 = 0.7$, $\frac{b_1}{b_2} = 3$

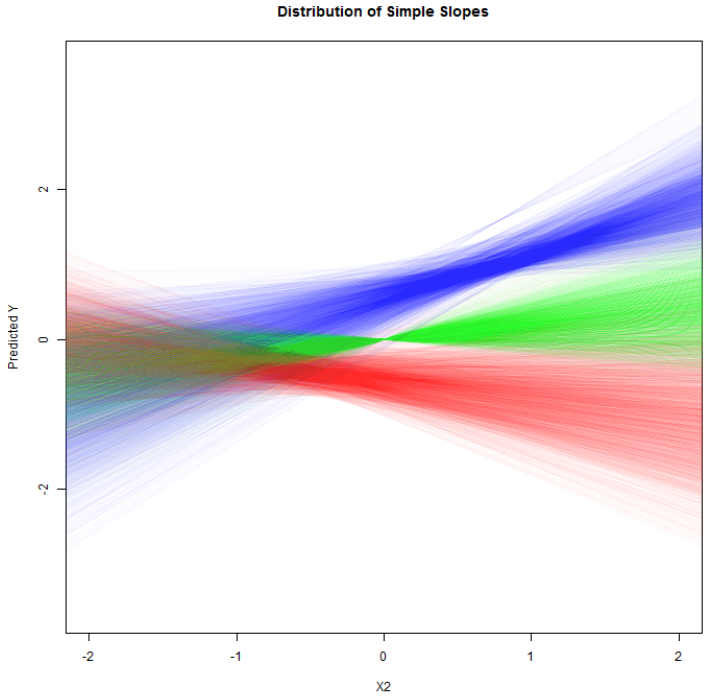

Figure 9.67: Simple Slopes from n = 40, $\rho_{X_1X_2} = 0.8$, $R^2 = 0.7$, $\frac{b_1}{b_2} = 3$

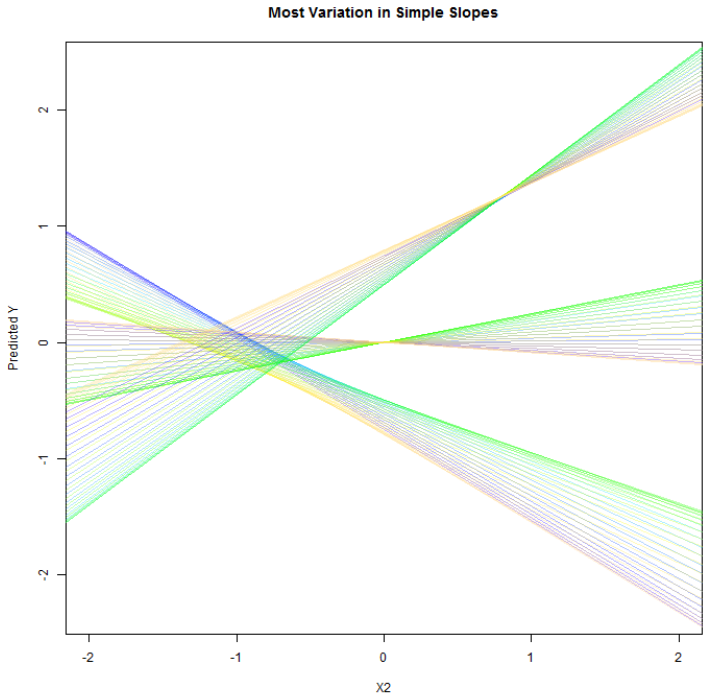

Figure 9.68: Simple Slopes from n = 400, $\rho_{X_1X_2} = 0.8$, $R^2 = 0.7$, $\frac{b_1}{b_2} = 3$

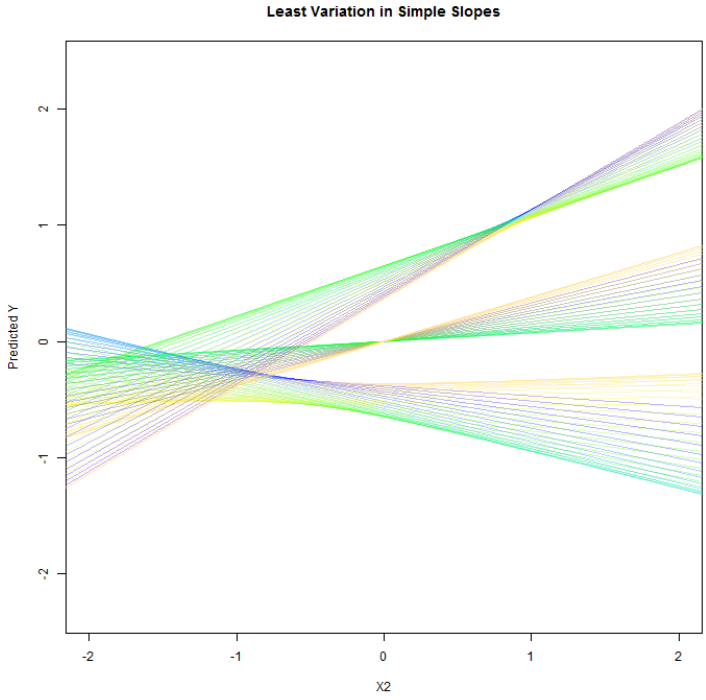

Figure 9.69: Simple Slopes from n = 400, $\rho_{X_1X_2} = 0.8$, $R^2 = 0.7$, $\frac{b_1}{b_2} = 3$

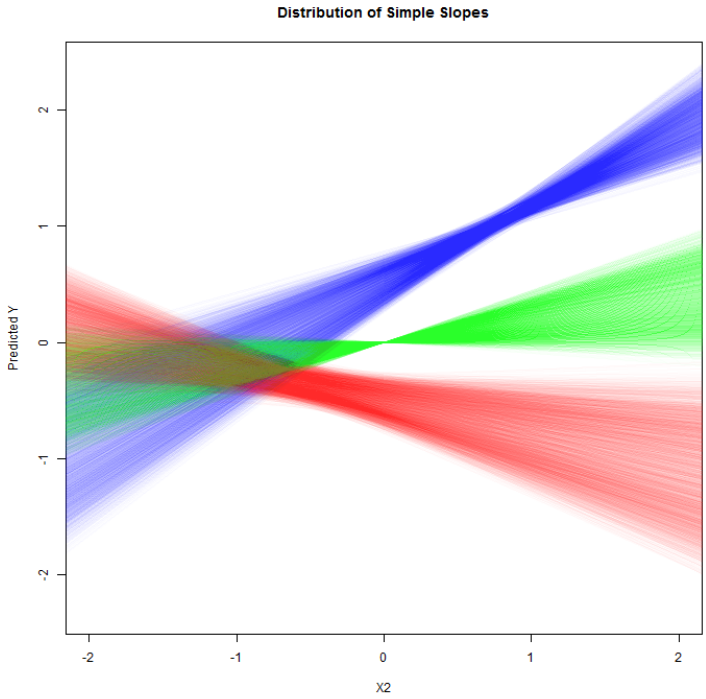

Figure 9.70: Simple Slopes from n = 400, $\rho_{X_1X_2} = 0.8$, $R^2 = 0.7$, $\frac{b_1}{b_2} = 3$

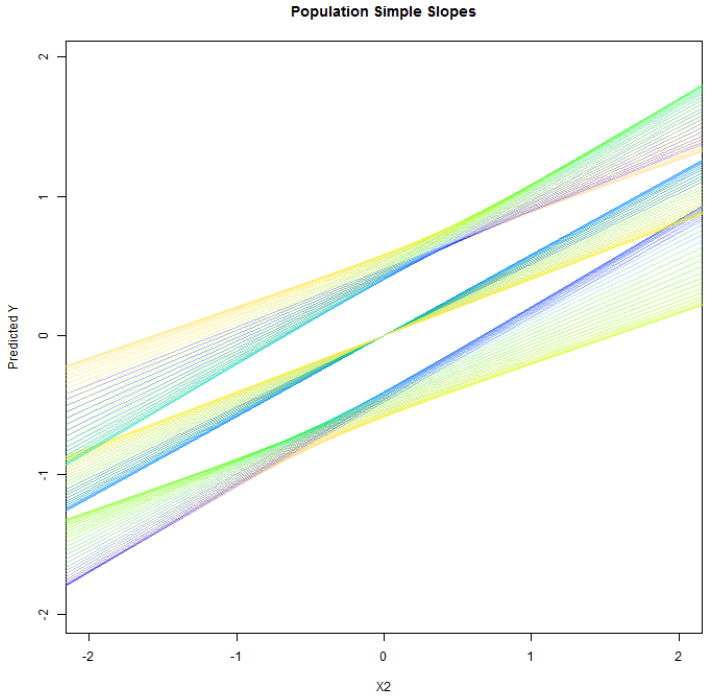

Figure 9.71: Simple Slopes from $\rho_{X_1X_2} = 0.4$, $R^2 = 0.7$, $\frac{b_1}{b_2} = 1$

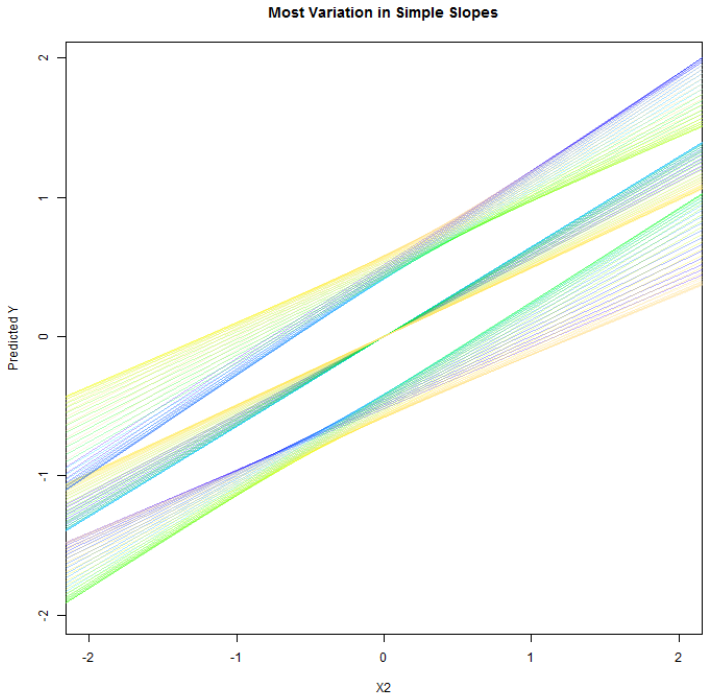

Figure 9.72: Simple Slopes from n = 400, $\rho_{X_1X_2} = 0.4$, $R^2 = 0.7$, $\frac{b_1}{b_2} = 1$

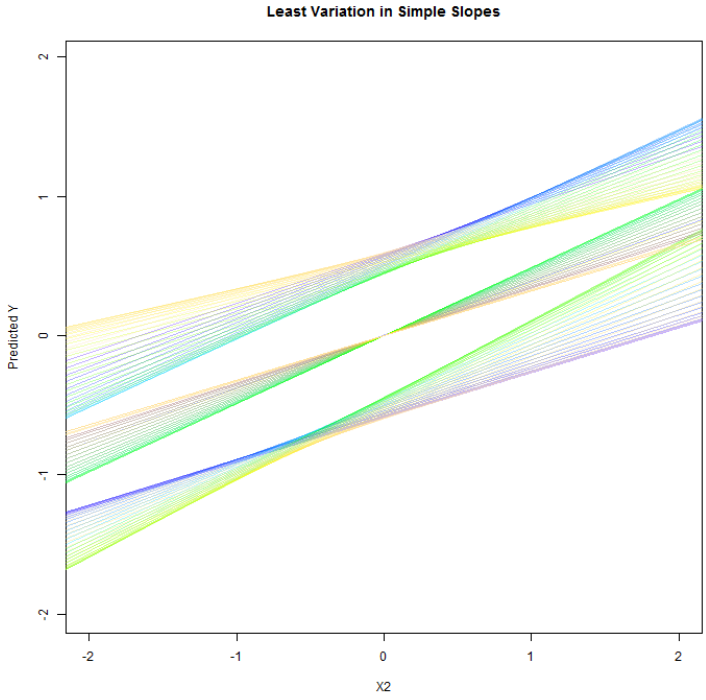

Figure 9.73: Simple Slopes from n = 400, $\rho_{X_1X_2} = 0.4$, $R^2 = 0.7$, $\frac{b_1}{b_2} = 1$

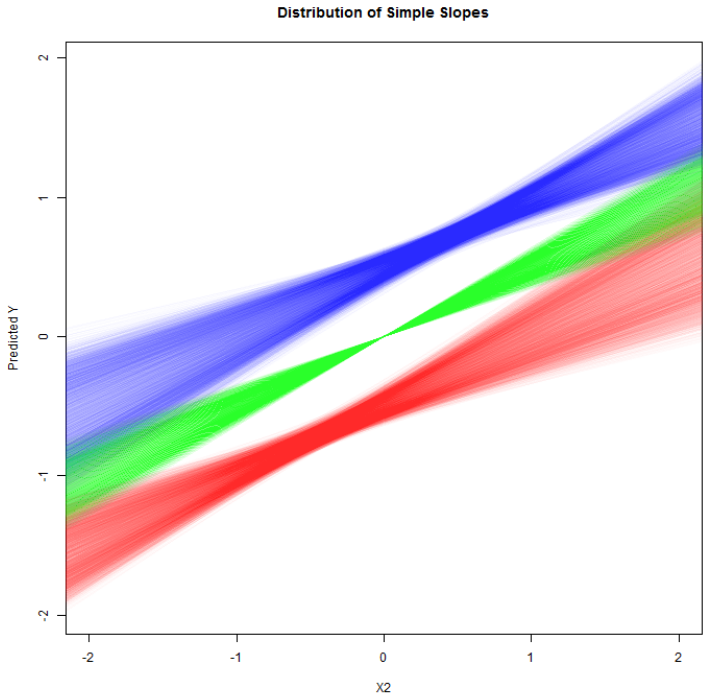

Figure 9.74: Simple Slopes from n = 400, $\rho_{X_1X_2} = 0.4$, $R^2 = 0.7$, $\frac{b_1}{b_2} = 1$

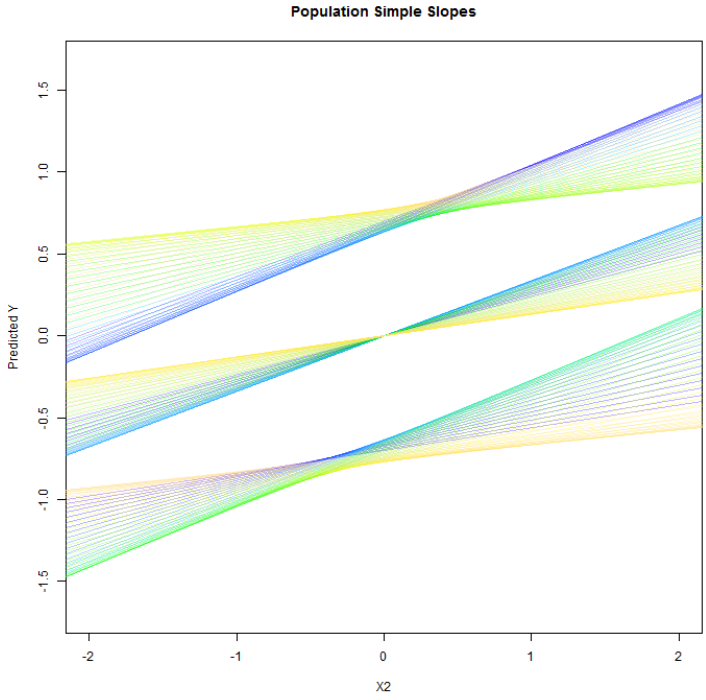

Figure 9.75: Simple Slopes from $\rho_{X_1X_2} = 0.4$, $R^2 = 0.7$, $\frac{b_1}{b_2} = 3$

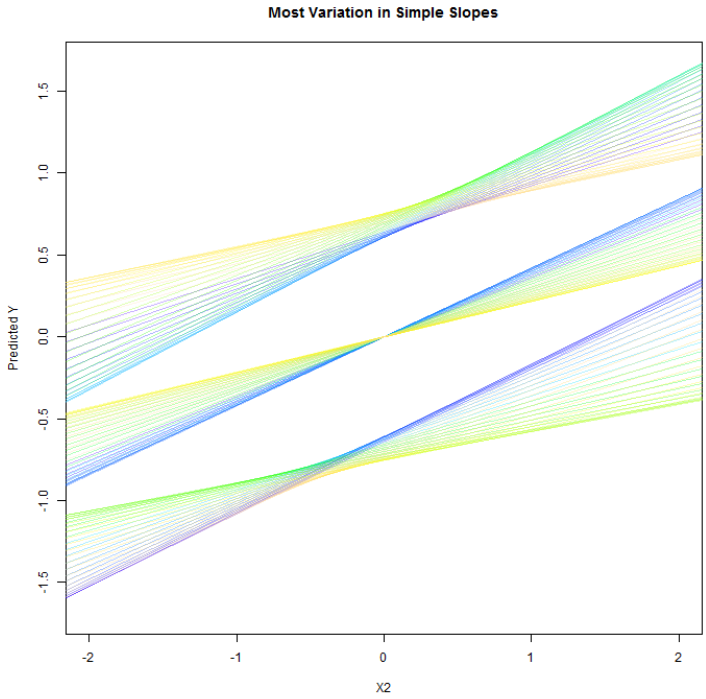

Figure 9.76: Simple Slopes from n = 400, $\rho_{X_1X_2} = 0.4$, $R^2 = 0.7$, $\frac{b_1}{b_2} = 3$

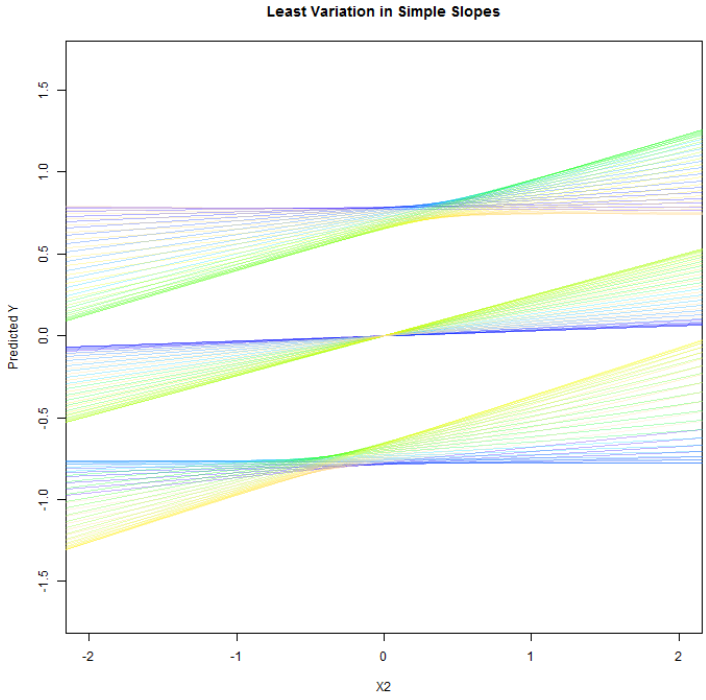

Figure 9.77: Simple Slopes from n = 400, $\rho_{X_1X_2} = 0.4$, $R^2 = 0.7$, $\frac{b_1}{b_2} = 3$

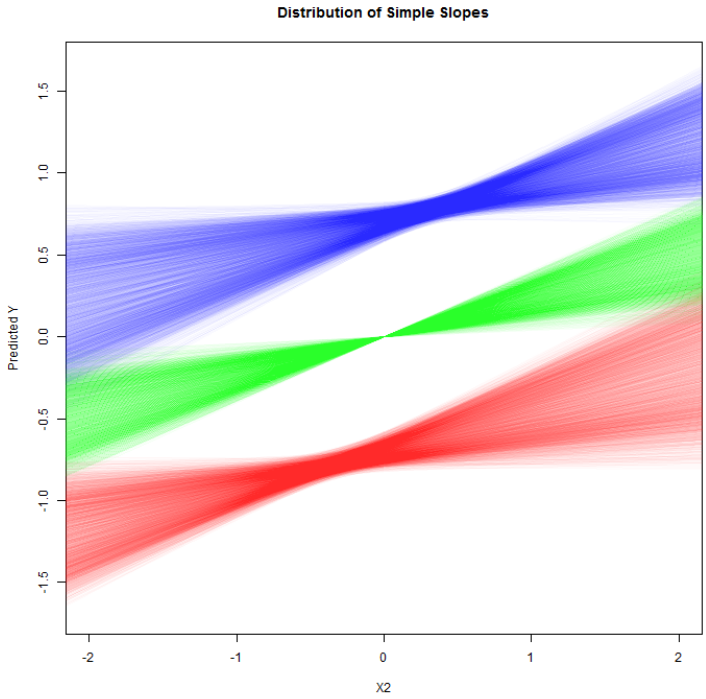

Figure 9.78: Simple Slopes from n = 400, $\rho_{X_1X_2} = 0.4$, $R^2 = 0.7$, $\frac{b_1}{b_2} = 3$

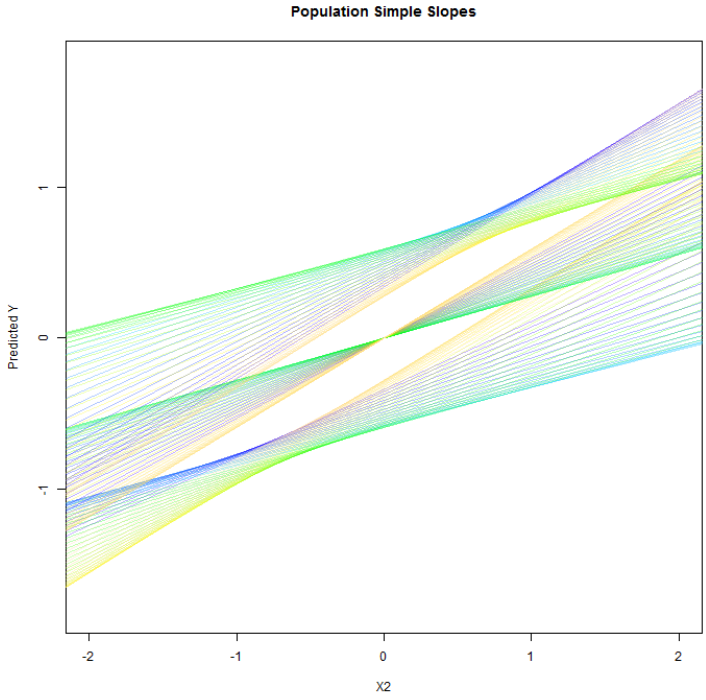

Figure 9.79: Simple Slopes from n = 400, $\rho_{X_1X_2} = 0.8$, $R^2 = 0.7$, $\frac{b_1}{b_2} = 1$

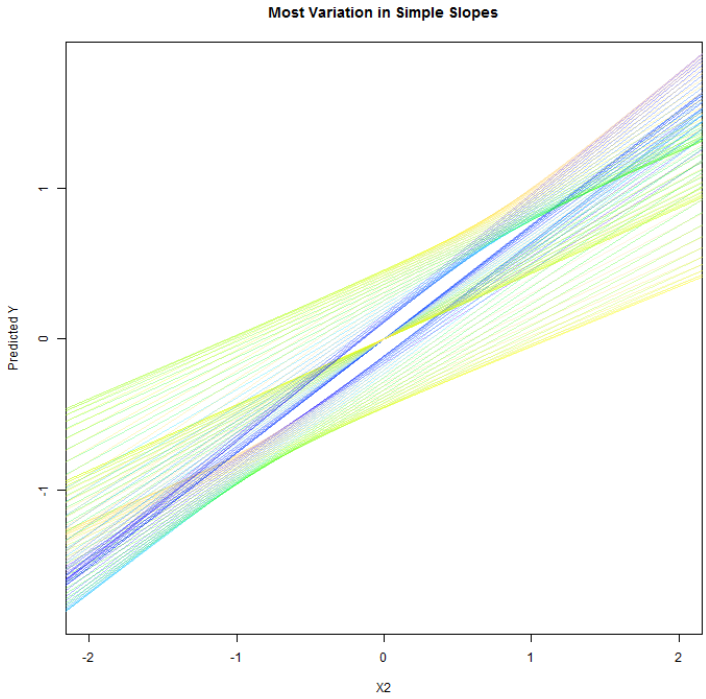

Figure 9.80: Simple Slopes from $\rho_{X_1X_2} = 0.8$, $R^2 = 0.7$, $\frac{b_1}{b_2} = 1$

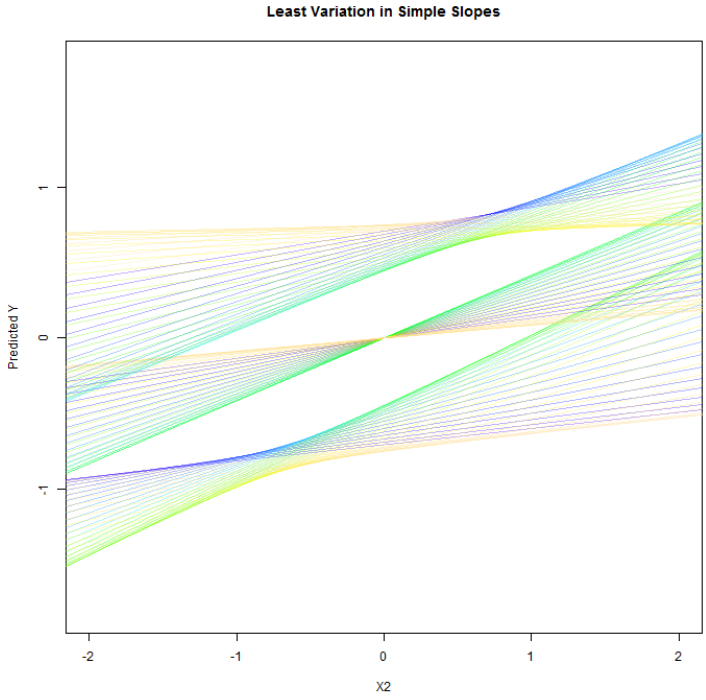

Figure 9.81: Simple Slopes from n = 400, $\rho_{X_1X_2} = 0.8$, $R^2 = 0.7$, $\frac{b_1}{b_2} = 1$

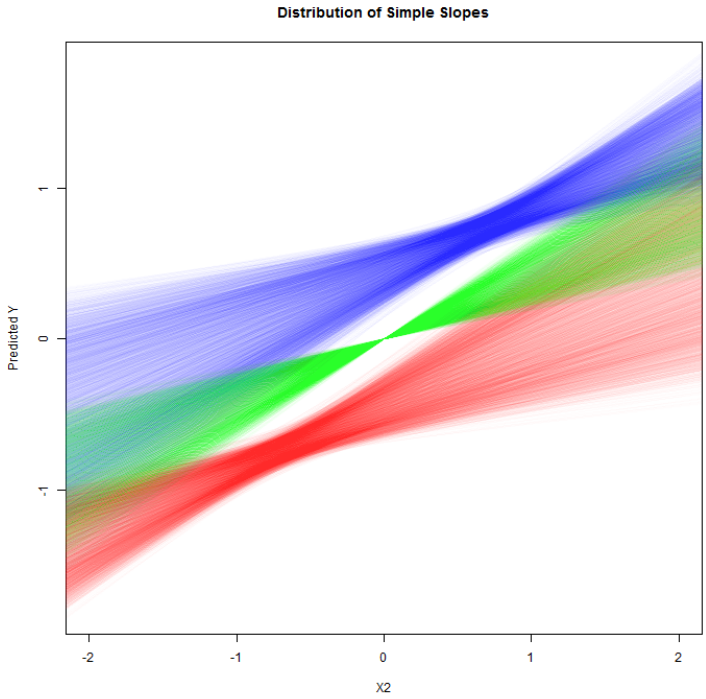

Figure 9.82: Simple Slopes from n = 400, $\rho_{X_1X_2} = 0.8$, $R^2 = 0.7$, $\frac{b_1}{b_2} = 1$

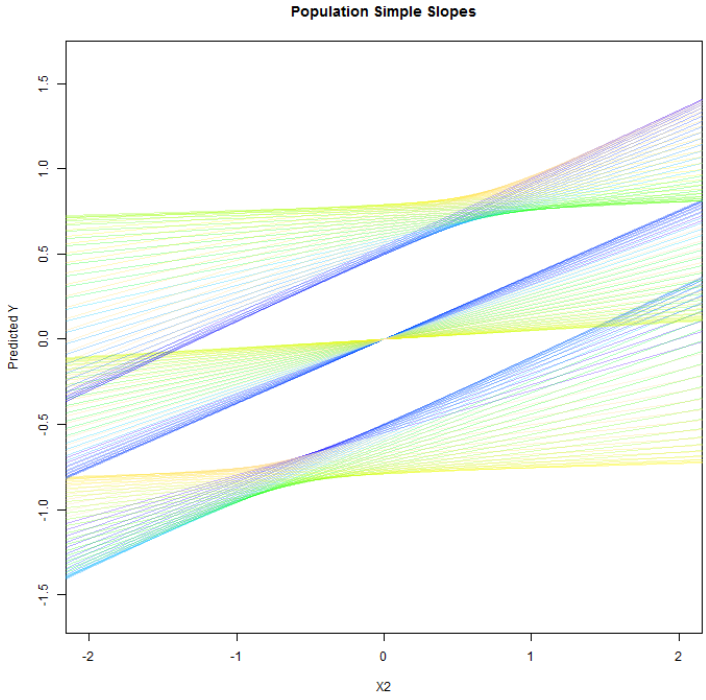

Figure 9.83: Simple Slopes from $\rho_{X_1X_2} = 0.8$, $R^2 = 0.7$, $\frac{b_1}{b_2} = 3$

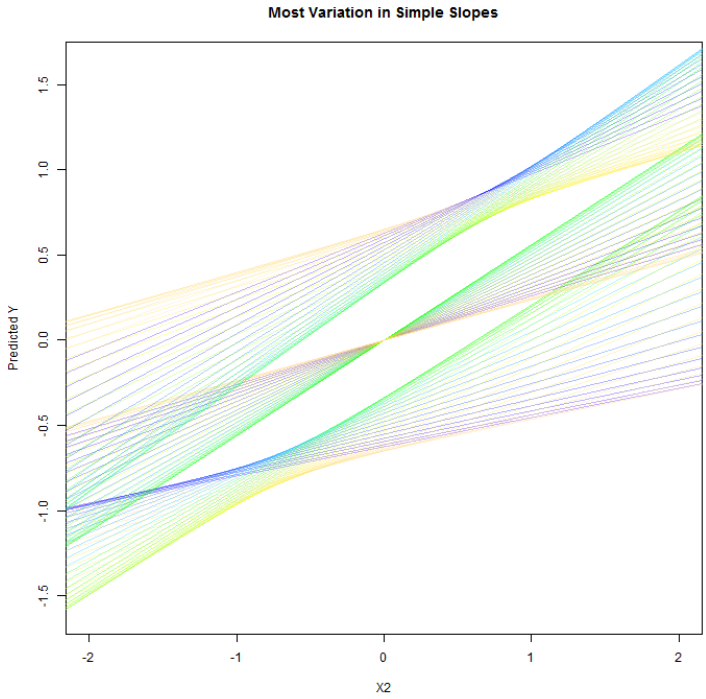

Figure 9.84: Simple Slopes from n = 400, $\rho_{X_1X_2} = 0.8$, $R^2 = 0.7$, $\frac{b_1}{b_2} = 3$

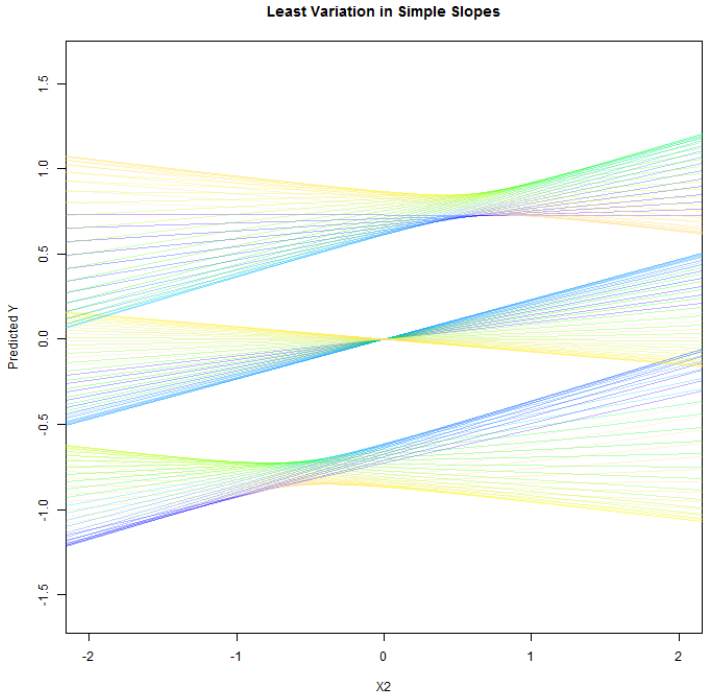

Figure 9.85: Simple Slopes from n = 400, $\rho_{X_1X_2} = 0.8$, $R^2 = 0.7$, $\frac{b_1}{b_2} = 3$

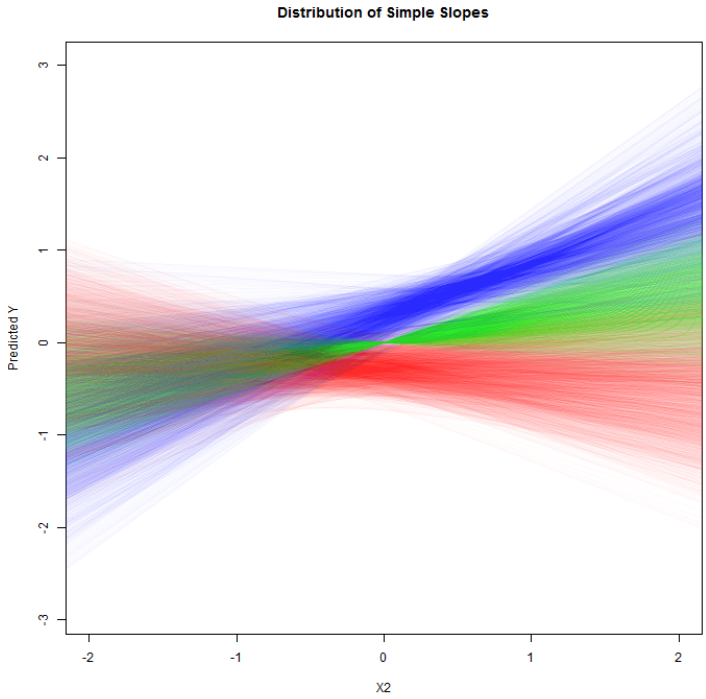

Figure 9.86: Simple Slopes from n = 400, $\rho_{X_1X_2} = 0.8$, $R^2 = 0.7$, $\frac{b_1}{b_2} = 3$

References

Development Core Team. (2011). R: A language and environment for statistical computing [Computer software manual]. Vienna, Austria. Retrieved from `http://www.R-project.org` (ISBN 3-900051-07-0)

Cohen, C. P. W. S. G., J., & Aiken, L. S. (2002). *Applied multiple regression/ correlation analysis for the behavioral sciences, third edition.* Routledge Academic.

Dana, J., & Dawes, R. M. (2004). The superiority of simple alternatives to regression for social science predictions. *Journal of Educational and Behavioral Statistics*, *29*, 317-331.

Dawes, R. M. (1979). The robust beauty of improper linear models in decision making. *American Psychologist*, *34*, 571-582.

Einhorn, & Hogarth. (1975). Unit weighting schemes for decision making. *Organizational Behavior and Human Performance*, *13*, 171-192.

Green, B. F. (1977). Parameter sensitivity in multivariate methods. *Multivariate Behavioral Research*, *12*, 263-287.

Kuncel, H. S., N.R., & Ones, D. S. (2001). A comprehensive meta-analysis of the predictive validity of the graduate record examinations: Implications for graduate student selection and performance. *Psychological Bulletin*, *127*, 165-181.

MacCallum, L. T., R. C., & Browne, M. W. (n.d.). *Fungible parameter estimates in latent curve models.*

Obenchain, R. (1981). Maximum likelihood ridge regression and the shrinkage pattern alternatives. *I.M.S. Bulletin*, *10*, 23-81.

Waller, N. G. (2008). Fungible weights in multiple regression. *Psychometrika*, *73*, 691-703.

Wallers, N. G., & Jones, J. A. (2009). Locating the extrema of fungible regression weights. *Psychometrika*, *74*, 589-602.